

# **SYNTHESIS CHARACTERIZATION AND THIRD-ORDER NONLINEAR OPTICAL STUDY OF SOME TRANSITION METAL AND BORON COMPLEXES**

Thesis

Submitted in partial fulfilment of the requirements for the degree of

**DOCTOR OF PHILOSOPHY**

by

**RUDRESHA B. J.**



**DEPARTMENT OF CHEMISTRY  
NATIONAL INSTITUTE OF TECHNOLOGY  
KARNATAKA,  
SURATHKAL, MANGALORE-575025  
December, 2012**

## **DECLARATION**

*by the Ph.D. Research Scholar*

I hereby declare that the Research Thesis entitled “**Synthesis, Characterization and Third-order Nonlinear Optical Study of Some Transition Metal and Boron Complexes**” which is being submitted to the *National Institute of Technology Karnataka, Surathkal* in partial fulfilment of the requirements for the award of the Degree of *Doctor of Philosophy* in **Chemistry** is a *bonafide report of the research work carried out by me*. The material contained in this Research Thesis has not been submitted to any University or Institution for the award of any degree.

**Rudresha B.J.**

(Reg. No: 081025CY08F02)

Department of Chemistry

**Place:** NITK, Surathkal

**Date:**

## CERTIFICATE

This is to *certify* that the Research Thesis entitled “**Synthesis Characterization and Third-order Nonlinear Optical Study of Some Transition Metal and Boron Complexes**” submitted by **Mr. Rudresha B.J.** (Register Number: 081025CY08F02) as the record of the research work carried out by him is accepted as the *Research Thesis Submission* in partial fulfilment of the requirements for the award of degree of **Doctor of Philosophy**.

Research Guide

Dr. B. Ramachandra Bhat

Date:

Chairman-DRPC

Date:

## ACKNOWLEDGEMENTS

First and foremost I offer my sincerest gratitude to my research supervisor, Dr. B. Ramachandra Bhat, Associate Professor, Department of Chemistry, NITK, for his consistent supervision, guidance, patience, support and encouragement throughout this research work, whilst allowing me the room to work in my own way. It was a valuable experience to learn many aspects from him both as a teacher and a human being. I admire among his other qualities, his kindness and balanced approach towards success and failure; his scientific outlook with his personal dignity makes him a unique advisor. One simply could not wish for a better or friendlier supervisor. I am extremely grateful to him for all the help he rendered during my research period.

I sincerely thank the Department of Chemistry, NITK Surathkal and also the institute for granting me the institute fellowship.

I would like to thank Prof. A. Chittaranjan Hegde, Head, Department of Chemistry and Chairman DRPAC and Members of the RPAC Committee Prof. M. Shankarnarayana Bhat and Prof. N. K. Udaya Shankar, for spending their precious time to attend my seminars, providing valuable suggestions and having fruitful discussions.

I thank Prof. A. Nithyananda Shetty, Prof. A. Vasudeva Adhikari, Dr. D. Krishna Bhat, Dr. Arun M. Isloor, Dr. D. Udayakumar and Dr. Darshak R. Trivedi, Department of Chemistry, NITK, Surathkal for their good wishes and moral support.

I thank Prof. G. Umesh, Department of Physics, NITK, Surathkal, Prof. Reji Philip, Raman Research Institute, Bangalore and John Kiran A., Division of Energy Systems Research, Ajou University, South Korea for providing facility during NLO measurements.

I am thankful to the authorities of NMR Research Centre, Indian Institute of Science, Bangalore for the NMR analysis.

I am very thankful to my fellow researchers for helping me in various stages of this research work. A special thanks to Dr. Dileep, Ms. Sandya Rani, Dr. Ravindra, Dr. Ramasubramanian, Mr. Sampath, Mr. Aravinda, Ms. Aparna and Ms. Pooja for their good support and cooperation.

I am thankful to fellow research students in the department for their kind help. I would like to thank Manjunath K. B., Nagaraj K. K., Vikas Shelar M. Department of Physics for their help in various activities during my research works.

I thank the non-teaching staff members of Chemistry Department, Mrs. Kasturi Rohidas, Mr. Prashanth, Mr. Pradeep, Mr. Ashoka, Mr. Harish, Mrs. Sharmila and Ms. Deepa for their help in the department.

My acknowledgement will not be complete without remembering the good wishes, encouragement and wholehearted support from my family members and friends. I extend my gratitude to all those who sincerely expressed and extended their cooperation, encouragement, support, love and affection.

**RUDRESHA B. J.**

## ABSTRACT

This research thesis entitled “**Synthesis, Characterization and Third-order Nonlinear Optical Study of Some Transition metal and Boron Complexes**” deals with the detailed information on synthesis of five different series of transition metal and boron coordination complexes for third-order nonlinear optical (NLO) study. Third-order NLO properties of all the synthesized complexes were measured using the open aperture Z-scan technique. The thesis divided into seven chapters viz Chapter 1 gives an overview of the introduction and historical background of nonlinear optics, theoretical aspects of light-matter interaction in nonlinear regime and different NLO processes and NLO materials. Chapter 2 deals with the literature review on NLO study of transition metals and boron coordination complexes and also the scope and objectives of the present work. Chapter 3 describes the synthesis, characterization and third-order NLO studies of diimine (1,10-phenanthroline and 2,2'-bipyridine) based Zn(II), Cd(II) and Hg(II) complexes with 1D dipolar NLO-phores. Chapter 4 explains the ultrafast and nonresonant NLO characteristics of two metal complexes (N-(2-pyridyl)-N'-(salicylidene) hydrazine triphenylphosphine Co(II) ([CoLPPh<sub>3</sub>]), N-(2-pyridyl)-N'-(salicylidene)hydrazine triphenylphosphine Pd(I) ([PdLPPh<sub>3</sub>])), incorporated into PMMA film was studied using time-resolved differential optical Kerr gate (DOKG) and Z-scan experiments. The synthesis, characterization and the third-order NLO properties of three new Cu(I) complexes with two electron withdrawing ligands has been discussed in chapter 5. Chapter 6 describes, the formation of “push-pull” boron fluoride complexes derived from chalcones. The NLO results show that these complexes exhibiting “effective” 2PA property. Chapter 7 deals synthesis and NLO property of substituted N,N'-p-phenylenebis(salicylideneimine) ligands as well as their coordinatively saturated boron fluoride complexes. Chapter 8 provides the summary of the work presented in this thesis along with the conclusions.

**Keywords:** Nonlinear optics, Coordination complexes, Two photon absorption, Boron complexes.

## CONTENTS

CHAPTER 1 .....	1
INTRODUCTION.....	1
1.1 HISTORICAL BACKGROUND.....	1
1.2 INTRODUCTION TO NONLINEAR OPTICS .....	1
1.3 NONLINEAR OPTICAL PROCESS .....	3
1.3.1 Two-photon Absorption (2PA) and Three-Photon Absorption (3PA) process .....	3
1.3.2 Excited state absorption.....	4
1.3.3 Two-photon absorption (2PA) in coordination complexes .....	6
1.3.4 Saturable absorption .....	8
1.3.5 Optical limiting.....	8
1.4 EXPERIMENTAL TECHNIQUES FOR THE DETERMINATION OF NLO PROPERTIES .....	9
1.4.1 Hyper-Rayleigh Scattering (HRS) Technique .....	10
1.4.2 Z-Scan technique .....	10
1.4.3 Degenerate Four-Wave Mixing Technique .....	13
1.4.4 Optical Kerr Gate and Pump–Probe Measurements.....	14
1.5 NONLINEAR OPTICAL MATERIALS.....	15
1.5.1 Coordination complexes as NLO materials.....	16
CHAPTER 2 .....	19
A BRIEF OVERVIEW OF THE PREVIOUS WORK.....	19
2.1 INTRODUCTION.....	19
2.2 TRANSITION METAL COMPLEXES AS NLO MATERIALS .....	21
2.3 BORON COMPLEXES AS NLO MATERIALS.....	29
2.4 SCOPE AND OBJECTIVES OF THE WORK .....	30
CHAPTER 3 .....	33
SYNTHESIS, CHARACTERIZATION AND THIRD-ORDER NONLINEAR OPTICAL STUDIES OF Zn(II), Cd(II) AND Hg(II) COMPLEXES.....	33
<b>3.1 INTRODUCTION</b> .....	33
3.2 EXPERIMENTAL .....	34
3.2.1 Materials .....	34

3.2.2 Analysis and measurements.....	34
3.2.3 Synthesis of metal complexes.....	35
3.2.4 UV-visible spectra of complexes.....	44
3.3 RESULTS AND DISCUSSION .....	48
3.3.1 Spectral analysis .....	48
3.3.2 Linear optical study .....	49
3.3.3 Nonlinear Optical Study .....	49
CHAPTER 4 .....	55
SYNTHESIS AND THIRD-ORDER NONLINEAR OPTICAL STUDIES OF Co(II) AND Pd(I) COMPLEXES .....	55
4.1 INTRODUCTION.....	55
4.2 EXPERIMENTAL .....	56
4.2.1 Materials .....	56
4.2.2 Synthesis of ligand N-(2-pyridyl)-N'-(salicylidene) hydrazine (L <sub>2</sub> ).....	57
4.2.3 Synthesis of [CoL <sub>2</sub> PPh <sub>3</sub> Cl] (7C) and [PdL <sub>2</sub> PPh <sub>3</sub> ] (8C) complexes.....	57
4.2.4 Nonlinear optical measurements .....	58
4.3 RESULTS AND DISCUSSION .....	59
4.3.1 Linear optical studies.....	59
4.3 NONLINEAR OPTICAL STUDIES .....	60
4.3.1 Differential Optical Kerr Gate study .....	60
4.3.2 Open aperture Z-scan study .....	63
CHAPTER 5 .....	65
SYNTHESIS, CHARACTERISATION AND THIRD-ORDER NLO STUDIES OF Cu(I) COMPLEXES .....	65
5.1 INTRODUCTION.....	65
5.2 EXPERIMENTAL .....	66
5.2.1 Materials .....	66
5.2.2 Analysis and measurements.....	66
5.2.3 Z-scan measurement .....	66
5.2.4 Synthesis of the complexes.....	67
5.3 RESULTS AND DISCUSSION .....	72
5.3.1 Spectral analysis of complexes.....	72

5.3.2 Linear optical study .....	73
5.3.3 Nonlinear optical studies .....	74
CHAPTER 6 .....	79
SYNTHESIS, CHARACTERIZATION AND THIRD-ORDER NONLINEAR OPTICAL STUDIES OF BORON CHALCONE COMPLEXES .....	79
6.1 INTRODUCTION.....	79
6.2 EXPERIMENTAL .....	80
6.2.1 Materials .....	80
6.2.2 Analysis and measurements.....	80
6.2.3 Z-scan measurement .....	80
6.3 SYNTHESIS OF BORON CHALCONE COMPLEXES.....	81
6.3.1 General procedure for synthesis of ligands (L <sub>4</sub> -L <sub>8</sub> ).....	81
6.3.2 General method for the synthesis of boron chalcone complexes (12C-16C) .....	88
6.4 LINEAR OPTICAL STUDY .....	96
6.5 RESULTS AND DISCUSSION .....	102
6.5.1 Spectral analysis .....	102
6.5.2 Nonlinear optical studies .....	102
CHAPTER 7 .....	107
SYNTHESIS, CHARACTERIZATION AND THIRD-ORDER NONLINEAR OPTICAL STUDIES OF BORON SCHIFF BASE COMPLEXES .....	107
7.1 INTRODUCTION.....	107
7.2 EXPERIMENTAL .....	108
7.2.1 Materials .....	108
7.2.2 Analysis and measurements.....	108
7.2.3 Z-scan measurement .....	108
7.2.4 General procedure for synthesis of ligands (L <sub>9</sub> -L <sub>11</sub> ) .....	109
7.2.5 General procedure for synthesis of Boron Schiff base complexes (17C-19C) .....	111
7.2.6 Linear optical study .....	115
7.3 RESULTS AND DISCUSSION .....	118
7.3.1 Spectral analysis .....	118
7.3.2 Nonlinear optical studies .....	119

CHAPTER 8 .....	123
SUMMARY AND CONCLUSIONS .....	123
REFERENCES.....	127
LIST OF JOURNAL PUBLICATIONS .....	147
CURRICULUM VITAE .....	149

# CHAPTER 1

## INTRODUCTION

### *Abstract*

*This chapter includes general introduction to nonlinear optics and nonlinear optical process. It also covers a brief account on the experimental techniques and deals with the nonlinear optical materials.*

### **1.1 HISTORICAL BACKGROUND**

The word “laser” is an acronym which stands for light amplification by stimulated emission of radiation. The first operating laser was developed in 1960 by Maiman using crystal of ruby. One year later, Franken et al. (1961) demonstrated the frequency doubling of light from a ruby laser by a quartz crystal. This frequency doubling phenomenon is termed second harmonic generation. These milestone discoveries opened up two fields of research: laser science in one direction and nonlinear optics in the other (Robert 1992).

### **1.2 INTRODUCTION TO NONLINEAR OPTICS**

Nonlinear optics is the study of phenomena that occur as a consequence of the modification of the optical properties of a material system by the presence of light. Typically, only laser light is sufficiently intense to modify the optical properties of a material system. In order to describe more precisely an optical non-linearity, let us consider how the dipole moment per unit volume, or polarization  $P(t)$ , of a material system depends upon the strength  $E(t)$  of the applied optical field. In the case of conventional (i.e., linear) optics, the induced polarization depends linearly upon the electric field strength in a manner that can often be described by the relationship,

$$P(t) = \chi^{(1)} E(t) \quad \text{----- (1.1)}$$

where the constant of proportionality  $\chi^{(1)}$  is known as the linear susceptibility. In nonlinear optics, the nonlinear optical response can often be described by generalizing eq. (1.1) by expressing the polarization  $P(t)$  as a power series in the field strength  $E(t)$  as,

$$P(t) = \varepsilon_0 \left[ \chi^{(1)} E(t) + \chi^{(2)} E^2(t) + \chi^{(3)} E^3(t) + \dots \right] \text{-----} \quad (1.2)$$

$$\equiv P(t) + P^2(t) + P^3(t) + \dots$$

The quantities  $\chi^{(2)}$  and  $\chi^{(3)}$  are known as the second and third-order nonlinear optical susceptibilities, respectively. For simplicity, the fields  $P(t)$  and  $E(t)$  to be scalar quantities in writing equations (1.1) and (1.2). In equation (1.1) and (1.2) assumed that the polarization at time 't' depends only on the instantaneous value of the electric field strength. The assumption that the medium responds instantaneously also implies (through the Kramers-Kronig relations) that the medium must be lossless and dispersionless. In general the nonlinear susceptibilities depend on the frequencies of the applied fields.

By considering  $P^{(2)}(t) = \chi^{(2)} E^2(t)$  as the second-order nonlinear polarization and to  $P^{(3)}(t) = \chi^{(3)} E^3(t)$  as the third-order nonlinear polarization. Physical processes that occur as a result of the second-order polarization  $P^{(2)}(t)$  tend to be distinct from those that occur as a result of the third-order polarization  $P^{(3)}(t)$ . Second-order nonlinear optical interactions can occur only in non centrosymmetric crystals—that is, in crystals that do not display inversion symmetry. Since liquids, gases, amorphous solids (such as glass) and even many crystals display inversion symmetry,  $\chi^{(2)}$  vanishes identically for such media and consequently such materials cannot produce second-order nonlinear optical interactions. On the other hand, third-order nonlinear optical interactions (i.e.  $\chi^{(3)}$ , those described by susceptibility) can occur for both centrosymmetric and noncentrosymmetric media. One might expect that the lowest-order correction term  $P^{(2)}$ , would be comparable to the linear response  $P^{(1)}$  when the amplitude of the applied field  $E$  is of the order of the characteristic atomic electric field strength  $E_{at} = \frac{e}{4\pi\varepsilon_0 a_0^2}$ , where  $e$  is the charge of the electron and  $a_0 = \frac{4\pi\varepsilon_0 \hbar^2}{me^2}$ , is the Bohr radius of the hydrogen atom (here  $h$  is Planck's constant, and  $m$  is the mass of the electron). Numerically, it is found to be  $E_{at} = 5.14 \times 10^{11} \text{V/m}$ . Under conditions of no resonant excitation the second order

susceptibility  $\chi^{(2)}$  will be of the order of  $\chi^{(1)}/E_{\text{at}}$ . For condensed matter  $\chi^{(1)}$  is of the order of unity, and hence expect that  $\chi^{(2)}$  will be of the order of  $1/E_{\text{at}}$ , or that,

$$\chi^{(2)} = 1.94 \times 10^{-12} \text{ m/V} \quad \text{-----} \quad (1.3)$$

Similarly, expected that  $\chi^{(3)}$  to be of the order of  $\chi^{(1)}/E_{\text{at}}^2$ , which for condensed matter is of the order of

$$\chi^{(3)} = 3.78 \times 10^{-24} \text{ m}^2/\text{V}^2 \quad \text{-----} \quad (1.4)$$

The most usual procedure for describing nonlinear optical phenomena is based on expressing the polarization  $P(t)$  in terms of the applied electric field strength  $E(t)$ . The reason why the polarization plays a key role in the description of nonlinear optical phenomena is that a time-varying polarization can act as the source of new components of the electromagnetic field (Robert 1992).

### 1.3 NONLINEAR OPTICAL PROCESS

#### 1.3.1 Two-photon Absorption (2PA) and Three-Photon Absorption (3PA) process

Two photon absorption (2PA) is the simultaneous absorption of two photons of identical or different frequencies in order to excite a molecule from one state (usually the ground state) to a higher energy electronic state. The energy difference between the involved lower and upper states of the molecule is equal to the sum of the energies of the two photons. The possible situation of two photon absorption is illustrated in Figure 1a. In the first step, a photon from the same optical field oscillating at frequency  $h\omega$  is absorbed to make the transition to reach a virtual state. In the next step, another photon of same energy is absorbed from the oscillating field to jump into the real excited state. In both cases, the intermediate (or virtual) state is not real (i.e., does not involve a real stationary state of the system). Hence the system must absorb the two photons simultaneously. This makes the process sensitive to the instantaneous optical intensity.

Although the transition does not involve a real intermediate state, often there are impurities present that will produce a small amount of linear absorption. It should be understood that this absorption does not contribute to the transition to the final state of

the process but only serves as an additional loss mechanism. Two-step absorption involving a single photon pumped intermediate state is described as excited state absorption. It may be a second-order process, several orders of magnitude weaker than linear absorption.

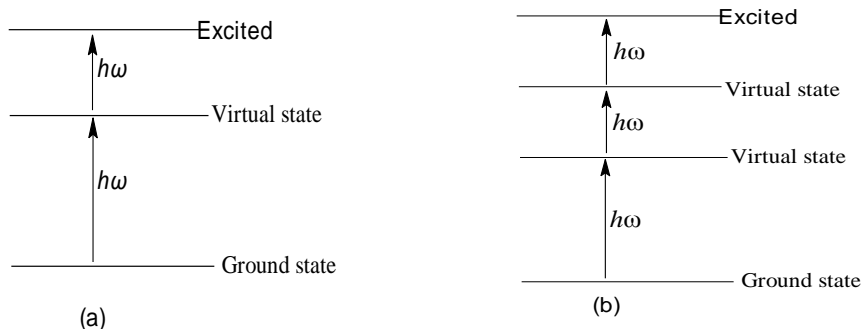


Figure 1 (a) Two-photon absorption (2PA) and (b) Three-photon absorption (3PA) processes.

Three-photon absorption (3PA) involves a transition from the ground state of a system to a higher-lying state by the simultaneous absorption of three photons (of energy,  $3h\omega$ ) from an incident radiation field. The schematic representation of this process is given in Figure 1b. When the input intensity increases, multi photon absorption processes, characterized by the simultaneous absorption of three or more photons, can occur in the system.

### 1.3.2 Excited state absorption

When the incident intensity is well above the saturation intensity, then the excited state becomes significantly populated. In systems, such as polyatomic molecules and semiconductors, there is a high density of states near the state involved in the excitation. The excited electrons can rapidly make a transition to one of these states before it eventually transits back to the ground state.

There are also a number of higher lying states that may be radiatively coupled to these intermediate states and for which the energy difference are in near resonance with the incident photon energy. Therefore, before the electron completely relaxes to the ground state, it may experience absorption that promotes it to a higher-lying state. This process is called excited state absorption (ESA). It is apparent when the incident intensity is sufficient to deplete the ground state significantly.

The mechanism of various types of absorption processes can be represented in an energy diagram as shown in Figure 1.2. The diagram shows different energy levels of a molecule, the singlet ground state  $S_0$ , the excited singlet states  $S_1$  and  $S_2$ , as well as triplet excited states  $T_1$  and  $T_2$ . It also displays the different transitions between the energy levels.

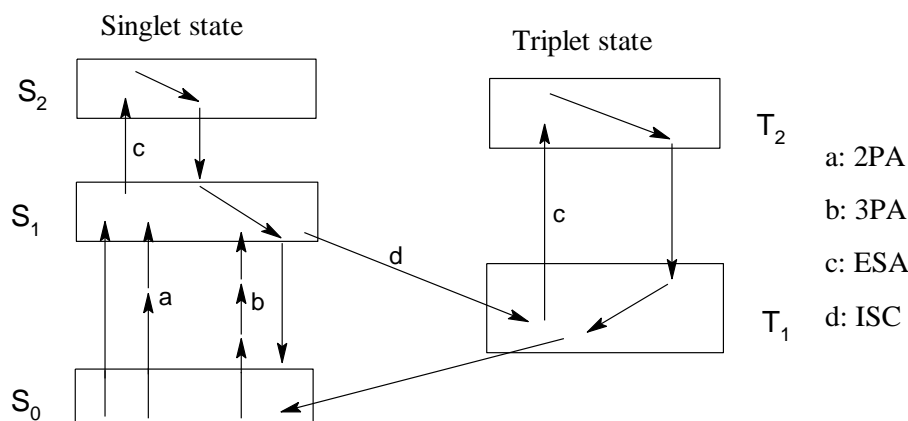


Figure 1.2 Energy level diagram showing 2PA, 3PA, ESA and ISC

The transition from the ground  $S_0$  to a higher singlet state by the absorption of a single photon gives rise to linear absorption. When the photons of the same or the different energy are simultaneously absorbed from the ground to higher excited state ( $S_0$  to  $S_1$ ), it is denoted as two photon absorption (2PA), which occurs at high light intensities. When the excited state absorption (ESA) occurs, molecules are excited from an already excited state to a higher excited state ( $S_1$  to  $S_2$  and/or  $T_1$  to  $T_2$ ). For this to happen the population of the excited states ( $S_1$  and/or  $T_1$ ) needs to be high so that the probability of photon absorption from that state is high. Therefore high intensity light is needed to pump up the molecules to the excited states before a substantial amount of ESA starts to take place. Also, it is important that life times of excited states are long enough so that a population of excited states can be obtained. The life times of the triplet states are longer than the singlet states and therefore ESA could be enhanced if the molecules could undergo intersystem crossing (ISC) to the triplet states. More ISC could be achieved by including heavy atoms which introduces a strong spin orbit coupling between the states. If more absorption occurs from the excited state than from the ground state, it is usually referred to as reverse saturable absorption (RSA).

### 1.3.3 Two-photon absorption (2PA) in coordination complexes

Two-photon absorption (2PA) in molecule has received considerable attention in recent years, owing to a number of potential applications (Bhawalkar et al 1996, He et al. 1995 and Zhao et al. 1995) in several areas of bio-photonics and material science, such as two-photon up-conversion lasing (Bhawalkar et al 1996, He et al. 1995 and Zhao et al. 1995) optical power limiting (Fleitz et al, 1998, He et al. 1995 and Ehrlich et al. 1997), photodynamic therapy (Bhawalkar et al 1997), and three-dimensional (3D) micro fabrication (Maruo et al. 1997, Cumpston et al. 1999 and Kawata et al. 2001). The push-pull dipolar molecules, in the earlier studies, have been the active research point, because this kind of molecules generally has large 2PA cross-sections (Albota et al. 1998, Reinhardt et al 1998, Ventelon et al. 2001, Bhawalkar et al. 1996, Painelli et al. 2001 and Kogej et al. 1998).

However, these dipoles may present many problems from a material standpoint (Peticolas 1967). The dipole-dipole electrostatic interactions that often results in an antiparallel molecular arrangement leads subsequent cancellation of the nonlinear response at bulk materials. In addition, the optimized molecular structures for this kind of molecules often lead to red-shift of linear absorption, damaging the transparency of materials. In order to overcome these difficulties, the enlarged potential for nonlinear optics of octupolar molecules (Ledoux et al. 1990 and Burland 1994) has sparked intense research in design of excellent 2PA materials. Compared with the 1D dipolar 2PA chromophores, octupolar molecules possess more round-off shapes, which ease their packing in a single crystalline lattice as opposed to less favourable elongated dipolar rod like molecules, the absence of dipole moments in excited as well as ground state makes octupolar molecules more suitable in various optical applications (Vance and Hupp 1999, Voigt-Martin et al. 1996 and Bredas et al. 1992).

More importantly, octupolar compounds resolve the inherent conflict between the transparency and nonlinearity existing in traditional dipolar molecules. The results of experiments and theoretical calculations reveal that the 2PA cross-section value increases on proceeding from dipolar to octupolar molecules and also with increasing donor and acceptor strength (Cho et al. 2002, Hurst et al. 2002, Cho et al. 2001, Chung et al. 1999 and Zhou et al. 2005). Most octupolar systems developed to date

are organic molecules. They have been designed by chemical functionalization of a central core and can be roughly classified into three main classes:

1. 2D or 3D molecules of global  $D_{3h}$  and  $C_3$  symmetry obtained by 1,3,5-functionalization of a central aromatic core (phenyl, or triazine) (Cho et al. 2001).
2.  $D_{3h}$  or slightlytwisted  $D_3$  propeller-like molecules, such as functionalized trivalent carbocation, boron, aluminum or nitrogen atoms (Chung et al. 1999).
3. 3D tetrahedral molecules, such as tetra substituted carbon or phosphonium derivatives (Zhou et al. 2005). Other examples of octupolar structures, such as paracyclophane, truxenone, sumanene and triphenylene derivatives, have also been described recently (Bartholomew et al. 2004 and Zhang et al. 2005).

Coordination chemistry has been proved to be another powerful tool to build up octupolar arrangements. Metal ions can assemble organic ligands in a variety of multipolar arrangements which show interesting electronic and optical properties tunable by virtue of the coordinated metal center. In the UV–Vis region of spectrum of metal complexes, there are often two different transitions, i.e., a strong intra-ligand charge-transfer (ILCT) transition and a low-energy metal to ligand charge-transfer transition (MLCT), which are often associated with large 2PA cross-section. High damage threshold and fast response time that metal complexes have in comparison to organic compounds are important from the perspective of application. A wide range of metals with different oxidation states and ligands necessarily make metal complexes active research point in design of 2PA material. Some reports are available describing the effect of metal ions on 2PA-active organic molecules. Metal cation Mg(II) was shown to lower the 2PA cross-section values by 50% in an azo-crown ether connected to distyrylbenzenes in the donor- $\pi$ -acceptor- $\pi$ -donor format (Pond et al. 2004). Upon binding with Ni(II) ion, the 2PA cross-sections of 1,10-phenanthrolinebased  $\pi$ -conjugated 2PA chromophores increase from 165 GM (1 GM =  $10^{-50}$  cm<sup>4</sup>/photon) to 578 GM (Zheng et al. 2005). Recently, Das et al. (2006) pointed out complexation of the bis-cinnamaldimine with metal cation can enhance electron-withdrawing character of the central diimine, making the complexes potential candidates for third-order nonlinear responses.

### 1.3.4 Saturable absorption

Many material systems have the property that their absorption coefficient decreases, when measured using high laser intensity. Often the dependence of the measured absorption coefficient  $\alpha$  on the intensity  $I$  of the incident laser radiation is given by the expression,

$$\alpha = \frac{\alpha_0}{1 + I/I_s} \dots\dots\dots (1.5)$$

Where  $\alpha_0$  is the low-intensity absorption coefficient, and  $I_s$  is a parameter known as the saturation intensity. When the absorption cross section of the excited state is smaller than that of ground state, the transmission of the system will be increased once the system is highly excited. This process is called as saturable absorption. One consequence of saturable absorption is optical bistability. Certain nonlinear optical systems can possess more than one output state for a given input state. The term optical bistability refers to the situation in which two different output intensities are possible for a given input intensity, and the more general term optical multistability is used to describe the circumstance in which two or more stable output states are possible. Interest in saturable absorption originates from its potential usefulness as a switch, for its use in optical communication and in optical computing. All of the nonlinear phenomena discussed above can be used for optical limiting configurations. The optical limiting devices that have been reported in the literature are many and varied, but they all rely on a material (or materials) that exhibit at least one nonlinear optical mechanism. The origins of such nonlinearities vary widely. Often materials may exhibit multiple nonlinear properties.

### 1.3.5 Optical limiting

Optical limiters display a decreasing transmittance as a function of intensity or fluence of the laser. The greatest amount of attention in optical limiters in recent years has been for optical sensor protection from intense laser light. Several physical mechanisms have been exploited for optical limiting, including the nonlinear refractive index. Primarily these are based on the various nonlinear absorption processes in the limiting materials. For low incident intensity or fluence, the device has a linear transmittance. For some materials, e.g., two-photon absorbers, this

transmittance may be near 100%, and the input-output curve would have a slope of 45°. On the other hand, RSA materials require a certain amount of linear absorption, and thus the input-output slope in the linear regime would be <45°. At some critical intensity or threshold in an ideal limiter, the transmittance changes suddenly and exhibits an inverse intensity or fluence dependence. Thus the output is clamped at some value that would actually be less than the amount required to damage the sensor. This critical point is called the threshold of the device, while the clamped output is called the limiting value of intensity or fluence. An optical limiter must provide protection over a wide range of incident intensity or fluence. Thus if the input-output slope is nonzero, at some input above the threshold the device will fail to provide protection. In some cases, the material itself may be damaged if its damage threshold is below this point, or the intensity/fluence dependent transmittance may approach a constant asymptote so that the input-output slope again increases. Any one of these situations will define a maximum input for which the device will provide effective limiting. The ratio of this input value to the threshold is called the dynamic range of the limiter.

Therefore, two desirable attributes of an optical limiter are low threshold and wide dynamic range. In addition, since the device is usually passive and must respond to pulses of arbitrary duration, a fast optical response is required. Also, as optical sensors usually have wide spectral pass bands, the device should have a broadband response. Other requirements may include high linear transmittance, optical clarity, color neutrality, and robustness (i.e., resistance to damage and degradation due to humidity, temperature swings, etc.). These necessities place severe restrictions on materials. Consequently, development of good optical limiter materials is an active research area in recent years.

#### **1.4 EXPERIMENTAL TECHNIQUES FOR THE DETERMINATION OF NLO PROPERTIES**

A number of techniques have been used for the measurement of second and third-order NLO properties of coordination complexes, the most popular of which are described below (Joseph et al. 2008).

### 1.4.1 Hyper-Rayleigh Scattering (HRS) Technique

HRS is a technique that is widely used to measure molecular quadratic nonlinearities of transition metal complexes. The HRS technique involves detecting the incoherently scattered second-harmonic light generated from an isotropic solution. An isotropic solution is normally thought to be a random collection of molecules with no preferred orientation, and therefore having all tensor components of  $\chi^{(2)}$  equal to zero (an exception is a liquid containing chiral molecule); it is thus unable to generate a coherent second-harmonic beam. However, orientational fluctuations of unsymmetrical molecules in solution do result in local asymmetry and give rise to scattering of light at the second-harmonic frequency. The intensity of the second harmonic component of the scattered light depends on certain tensor components of the first hyperpolarizability of the solute molecules, and varies quadratically with the incident light intensity (Joseph et al. 2008).

### 1.4.2 Z-Scan technique

The Z-scan technique (Sheik-Bahae et al. 1990) is a very simple and convenient way of investigating self-focusing or self-defocusing phenomena as well as nonlinear absorption in a nonlinear material. Z-scan has been used for the measurement of the cubic NLO properties of the majority of transition metal complexes to date.

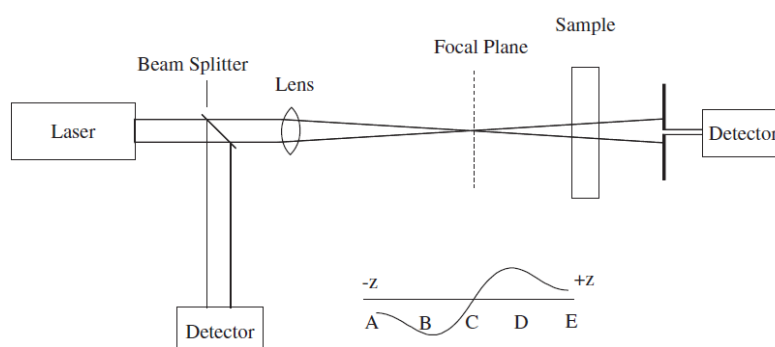


Figure 1.4 Schematic diagram of the Z-scan experiment.

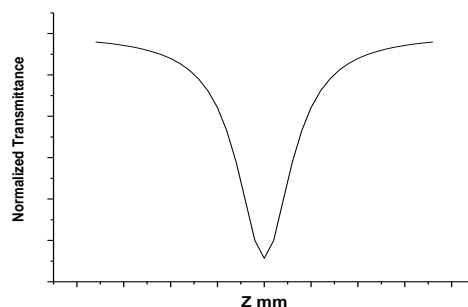


Figure 1.5 Typical open aperture Z-scan transmittance curves for a cubic nonlinearity.

A schematic diagram of a Z-scan experiment is shown in Figure 1.4. A laser beam with a well-defined geometry (usually Gaussian, but modifications of the experiment using a top-hat beam or a truncated Airy pattern beam are also in use) is focused with a lens, such that the focal plane is at  $z = 0$ , and forming a spot with the  $1/e^2$  intensity radius  $w_0$ . A thin sample (i.e. thinner than the Rayleigh length of the Gaussian beam defined as  $z_R = \omega_0^2 / \lambda$ ) is moved along the z-axis from  $-z$  to  $+z$ , usually scanning several Rayleigh lengths in both directions. As the sample travels, the light intensity that it experiences changes as  $I(z) = I_{\max} / [1 + (z/z_R)^2]$  thus, the scan is started at a low intensity, the highest intensity is reached at  $z = 0$  and then it decreases again. Due to the intensity changes, the beam passing through the sample is subject to a varying degree of focusing or defocusing by the virtual lens created by the sample nonlinearity (for positive values of the nonlinear refractive index  $n_2$ , the sample acts as a positive lens, and for  $n_2 < 0$  as a negative lens), and may also be modified in intensity if the sample acts as a nonlinear absorber. The intensity of the central part of the beam can be monitored as a function of the position of the sample by an aperture that is placed in the far field. Therefore, both distortion of the beam and the changes of its intensity due to changes in the absorption can be detected.

The sample is far from the focal plane at the start (A) (and the finish (E)) of the scan, and so the intensity of the beam is low, and lensing and modification of absorption are not observed. However, for higher intensities the sample acts as a thin lens due to the fact that the refractive index in the sample varies as  $n = n_0 + n_2 I(r, z)$ , where  $n_2$  is the nonlinear refractive index (related to  $\chi^{(3)}$ ) and  $I(r, z)$  is the intensity. For a positive value of  $n_2$ , as the sample approaches the focal plane (B), lensing results

in additional focusing of the beam and its increased size in the far field, and so the transmittance through the aperture is reduced. The focal plane (C) corresponds to the maximum intensity, but the presence of a lens at this plane does not influence the focused beam wave front and there is no change in transmittance. At point D lensing has an effect that is the reverse to that of (B), the size of the beam in the far field is decreased and the transmission through the aperture is increased. A characteristic S-shaped Z-scan curve (a valley followed by a maximum of transmittance) is obtained. This shape is reversed in the case of negative  $n_2$ .

The shape of the Z-scan curve is additionally modified if nonlinear transmission (absorption bleaching) or nonlinear absorption occurs. Due to the presence of the intensity-dependent absorption coefficient, which can often be expressed as  $\alpha = \alpha_0 + \beta_2 I(z)$ , the curves become unsymmetrical because of increased transmission or absorption close to the focal plane. The absorption changes can also be monitored by measuring the total intensity of the transmitted beam without the use of an aperture in an “open-aperture Z-scan” as shown in Figure 1.5. Materials with potential optical limiting properties are often studied using this technique. The sample nonlinearity as a function of concentration is determined. The concentration dependence is then used to derive the extrapolated nonlinear parameters of the pure solute and they can be expressed as the real and imaginary part of  $\chi^{(3)}(-\omega; \omega, -\omega, \omega)$ , the components of the complex hyperpolarizability  $\gamma(\omega; \omega, -\omega, \omega)$ , or the macroscopic parameters,  $n_2$  and  $\beta_2$ . In the nonlinear absorption case, an alternative way of expressing the molecular NLO parameters is by quoting the appropriate molecular absorption cross-sections, and referring to the absorption process responsible for the observed effects, for example, two-photon absorption cross-section or excited-state absorption cross-section.

There are numerous advantages in the use of the Z-scan technique for the determination of the third-order NLO properties: the sign and the magnitude of the nonlinear refractive index can be determined, both the real and the imaginary parts of  $\chi^{(3)}$  are obtained, and the single-beam configuration results in simplicity. The main difficulty is that Z-scan provides data that often lead to uncertainties about the origin of nonlinear effects. Thermal effects (changes in the refractive index and the

absorption coefficient due to local heating of the sample by the laser beam), photochemical changes, and other cumulative effects are difficult to distinguish from the (practically) instantaneous changes due to the electronic third-order nonlinearity. It is of crucial importance to use a short pulse laser system at a sufficiently low repetition rate that any long-lived changes in the sample can completely relax in the time interval between the consecutive laser pulses.

### 1.4.3 Degenerate Four-Wave Mixing Technique

Degenerate four-wave mixing (DFWM) is an elegant technique for investigating cubic nonlinearities in various materials that has been used to measure molecular cubic nonlinearities of transition metal complexes (Figure 1.6). The principle of DFWM is the interaction of three laser beams at the same frequency  $\omega$  to generate a fourth beam at the same frequency. One of the ways to understand the principle of DFWM is to consider it as a “transient grating” experiment. When two coherent laser beams are crossed at a certain angle within a material, they create an interference pattern of light intensity and, through the dependence of the refractive index of a third-order NLO material on the light intensity, a periodic modulation (a 3D grating) of the (complex) refractive index:

$$\Delta n(r) = n_2 I(r) = n_2 I_0 \sin(\Delta k r) \quad \text{-----} \quad (1.6)$$

Where  $\Delta k$  is the difference between the wave vectors of the two beams creating the grating. A third beam of light at the same frequency can then be diffracted at the grating, generating a fourth beam. To maximize the intensity of the fourth beam, it is necessary to fulfil the Bragg diffraction condition, which is equivalent to the phase matching condition, i.e.  $\sum_i k_i = 0$ , where  $k_i$  are the wave vectors of the four interacting waves. Under phase-matching conditions, the intensity of the diffracted wave is proportional to the product of all the input intensities and to the square of the absolute value of the complex third-order susceptibility and to the square of the interaction length:

$$I_4 \propto |\chi^{(3)}|^2 I_1 I_2 I_3 L^2 \quad \text{-----} \quad (1.7)$$

It is very important to carry out concentration dependence studies, so that contributions to the signal from the real and imaginary parts of the third-order

susceptibility can be distinguished. The concentration dependence of the DFWM signal is given by:

$$I_{DFWM} \propto |\chi^{(3)}|^2 \propto [N_{\text{solvent}} \gamma_{\text{solvent}} + N_{\text{solute}} \text{Re}(\gamma_{\text{solute}})]^2 + [N_{\text{solute}} \text{Im}(\gamma_{\text{solute}})]^2 \quad (1.8)$$

where it is assumed that the solvent contributes only to the real part of the solution susceptibility, whereas the solute can contribute to both the real (refractive) and the imaginary (absorptive) components. The concentration dependence is thus, in general, nonlinear, complicating the derivation of the molecular hyperpolarizability from the experimental data. Despite the experimental complexity, DFWM is very useful as a technique complementary to Z-scan, in that it can be used to verify that the origin of the observed nonlinearity is electronic.

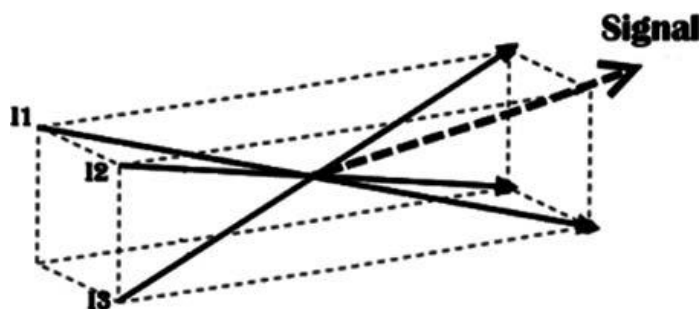


Figure 1.6 Four-wave mixing in the Boxcars geometry.

#### 1.4.4 Optical Kerr Gate and Pump–Probe Measurements

A variety of two-beam experiments have been devised to measure NLO properties, the principle being that a high-intensity beam, the “pump”, causes a change in the optical properties of a material and the change is then (usually after a variable delay) detected by the second beam, the “probe”. The pump and probe beams can be at different frequencies (for nondegenerate nonlinear effect studies) or at the same frequency, similar to the DFWM experiment. The simplest modification of a pump–probe experiment can be used to determine nonlinear absorption, which can be related to the imaginary part of  $\chi^{(3)}$ . Another modification is called the optical Kerr gate (OKG). In the OKG experiment (Figure 1.7), the pump is linearly polarized and its action on the material induces optical birefringence, that is, a change in the refractive index for directions parallel to the polarization and perpendicular to it (Sutherland 1996), the probe beam is also linearly polarized. As the probe passes

through the material, its polarization becomes elliptic and thus a part of its intensity will be transmitted through a crossed polarizer. The Kerr gate transmittance is proportional to the square of the induced birefringence, and this allows one to determine the appropriate effective  $\chi^{(3)}$ . However, the OKG experiment measures a specific combination of the tensor components ( $\chi^{(3)}_{xxyy} + \chi^{(3)}_{xyyx}$ ), and both the real and the imaginary parts of  $\chi^{(3)}$  contribute to the signal. Pump-probe experiments are of similar complexity to DFWM. Various modifications of the pump-probe principle allow one to resolve both the real and the imaginary parts of  $\chi^{(3)}$  and the temporal dependence of the response.

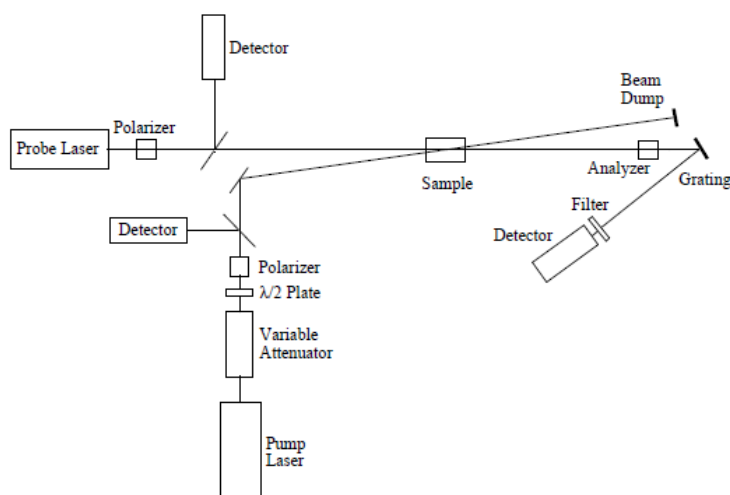


Figure 1.7 Schematic diagram of optical Kerr gate experiment.

## 1.5 NONLINEAR OPTICAL MATERIALS

Nonlinear optical (NLO) materials play a major role in nonlinear optics and in particular they have a great impact on information technology and industrial applications. Due to their varied important applications, the search for nonlinear optical (NLO) materials has continuously attracted attention since the discovery of NLO phenomena in 1961. The practically useful NLO materials thus far are mainly inorganic crystals, which include  $\text{KH}_2\text{PO}_4$  (KDP),  $\text{KTiOPO}_4$  (KTP),  $\text{LiNbO}_3$  (LN),  $\text{BaB}_2\text{O}_4$  (BBO), etc. Organic NLO materials, on the other hand, have developed rapidly in the last few decades (Nalwa and Miyata 1997) due to their higher nonlinearity, faster response and easier structural modification compared with inorganic materials. The Charge Transfer Theory has been proposed (Chemla et al.

1975) to describe successfully the relationship between structure and NLO properties in organic compounds. The concepts of molecular and crystal engineering have been developed (Chuang-Tian Chen and Guang Zhao Liu 1986) in the design of new NLO materials. However, organic NLO materials have encountered also some disadvantages, such as the difficulty to grow single crystals to large sizes, poor environmental stability and poor mechanical strength.

### **1.5.1 Coordination complexes as NLO materials.**

Organometallic compounds (defined here as those which contain at least one direct M–C bond between metal and organic ligands) and coordination compounds (in which the metal and the ligands are connected through M–O, M–N, M–S or M–P bonds) are compounds which combine the features of both inorganic and organic compounds. The study of the NLO properties of these complexes was first reported in the mid-1980s (Frazier and Harvey 1986). Since then, these studies have become gradually more popular due to their advantages over traditional inorganic or organic materials. For example, organometallic and coordination compounds offer a variety of molecular structures by changing the metals, ligands, coordination numbers and so on. This diversity of molecular structure gives one an opportunity to tune the electronic properties of the molecules and hence to tune the linear and nonlinear optical properties. The metal centre can also behave as either an electron donor or acceptor due to the rich oxidation–reduction properties of the transition metals. Therefore, it can be expected that some novel NLO materials may be found from organometallic or coordination compounds that may combine the features and advantages of both inorganic and organic compounds and hence may be superior to the existing inorganic and organic NLO materials (Jingui Qin et al. 1999).

There are three main types of interest in the study of NLO organometallic and coordination compounds thus far. The first interest is to find transparent SHG (second harmonic generation) materials to be used for frequency-doubling of a semiconductor laser. For this purpose, the material should exhibit a large SHG effect and optical transparency both at second-harmonic (SH) and fundamental wavelengths. Secondly, organometallic and coordination compounds may offer some excellent chromophores for synthesis of electro-optical (EO) polymers. In this case, a large value of the product of  $\beta\mu$  (where  $\beta$  is the first molecular hyperpolarisability and  $\mu$  is the dipole

moment) and reasonable thermal stability are required. The third purpose is to find new third order NLO materials. Normally, a large conjugated system is an important factor in achieving this third order effect (Jingui Qin et al. 1999).

Some excellent NLO studies of organometallic and coordination compounds have been reported (Marder 1992, Nalwa 1991 and Nalwa and Miyata 1997). These include some SHG crystals transparent in the visible region, compounds with both large values of  $\beta$  and  $\mu$  and materials with a strong third order NLO effect.

In the early period, scientists often utilised the principles of the Charge Transfer Theory, which was summarised originally from organic NLO materials, for designing NLO materials with organometallic and coordination compounds. Later, Cheng et al. (1990) measured (using the EFISH technique) and calculated the first molecular hyperpolarisability,  $\beta$ , of some types of organometallic compounds and they were studied the correlation between structure and  $\beta$ . Summarised their work on octahedral coordination compounds as SHG materials. All these studies are good examples of attempts to learn about the structure–property correlations in organometallic and coordination compound as NLO materials.

Organometallic chemistry and coordination chemistry are mature disciplines. Since these compounds exhibit features of both inorganic and organic compounds, they have been expected to be new candidates for electronic and optical materials. Therefore, the study of structure–property relationships is of great importance and will attract more attention from the experimental and theoretical chemists as well as the  
physicists.



## CHAPTER 2

### A BRIEF OVERVIEW OF THE PREVIOUS WORK

#### *Abstract*

*This chapter deals with detailed literature survey on nonlinear optical activity of coordination complexes. The scope and objectives of the present work have been discussed.*

#### **2.1 INTRODUCTION**

According to literature, many coordination complexes were put forth as promising candidates for NLO applications. Materials which exhibit highly nonlinear optical responses are currently of great scientific and technological interest. While inorganic solids such as  $\text{LiNbO}_3$  and  $\text{KH}_2\text{PO}_4$  have traditionally attracted the widest attention, (Kurtz 1972) it is now recognized that molecular-based materials possess many superior NLO characteristics: ultrafast response time, lower dielectric constants; better processability as thin film devices and enhanced non-resonant NLO responses relative to the traditional inorganic solids (Dalton et al. 1995). Over the years, there has been sustained interest in the search of nonlinear optical (NLO) materials due to their potential applications in a wide range such as optical signal processing, all-optical switching, optical computing and other NLO devices. These efforts have initially focused on purely inorganic or organic systems (Zyss 1994 and Prasad and Williams 1991). Recent interest has been engendered by studying organometallic and coordination compounds. Organometallic and coordination chemistry (transition metal chemistry) can offer a very large variety of molecular and bulk NLO structures in relation to the metal electronic configuration, oxidation state, spin state, etc. The central metal atom of a transition metal complex can readily coordinate to conjugated ligands and undergo  $d$ -orbital overlap facilitating effective electronic communication and CT transitions leading to large dipole moment changes between the excited states. New nonlinear optical materials of inorganic, organic and polymeric ones are essential to the development of optoelectronic technologies e.g. optical communications, high speed electro-optical information processing, high density data

storage, spatial light modulation and switch, have continued to be at the fore front of research activities since the mid-1980s.

There are a large number of articles already concerning the design and preparation of these new materials over the past three decades, however, only a few appropriate nonlinear materials required for the practical NLO devices, including optical limiting devices, are available till now. There has thus been a continuing pronounced interest in the search for novel NLO materials coupled with desirable physical properties and a low cost. Design and preparation of new nonlinear optical active materials required for the practical NLO devices are still a challenge for many scientists.

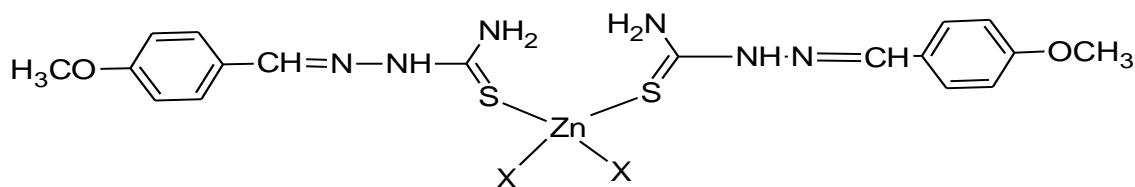
The development of new materials that exhibit nonlinear optical behaviour and have the potential for commercial device applications continues to be of primary interest in industrial and university laboratories. Thus, recognition of molecules with multi-dimensional (nD) charge-transfer characteristics in nonlinear optics have triggered various synthetic research activities. Some excellent NLO studies of organometallic and coordination compounds have been reported (Marder 1992, Nalwa et al. 1991 and Nalwa and Miyata 1997). These include some SHG crystals transparent in the visible region, compounds with both large values of  $\beta$  and  $\mu$  and materials with a strong third order NLO effect.

Since the report in 1987 by Green *et al.*, in which good second-harmonic generation (SHG) efficiency was revealed for a ferrocenyl derivative, attention has been paid to the study of metal complexes as potential second-order NLO materials. Various classes of metal complexes have thus been systematically studied for new and optimised second order NLO activity. Early and more recent review articles on NLO metal complexes show the breadth of the active research in this field. The metal-ligand interaction can be tuned by varying the metal atom, the oxidation state of the metal or the surrounding ligands. It should thus be possible to exploit the good electronic flexibility of organometallic and coordination compounds to develop new third order NLO materials. The design and synthesis of novel compounds with more perfect optical nonlinearities represent an active research field in modern chemistry and material science. This may be due to that the third-order NLO materials can be

used for a number of photonic applications, such as optical signal processing, optical communication, optical computing, optical limiting effect and etc.

## 2.2 TRANSITION METAL COMPLEXES AS NLO MATERIALS

Yu-Peng Tia et al. (2002) reported three zinc(II) halide complexes  $ZnL_2X_2$  ( $X = Cl, Br, I$ ;  $L = 4$ -methoxybenzaldehyde thiosemicarbazone) (Figure 2.1) have been synthesized and characterized by spectroscopic techniques. The complexes exhibit powder SHG efficiency approximately ten times higher than that of urea. The molecular hyperpolarizabilities are calculated to be  $-2.6 \times 10^{-30}$  esu for the free ligand  $L$ , and  $-4.6 \times 10^{-30}$ ,  $-6.2 \times 10^{-30}$ ,  $-10.1 \times 10^{-30}$  esu for the three zinc complexes, respectively.



$X = Cl, Br, I$

Figure 2.1 Chemical structures of  $ZnL_2X_2$

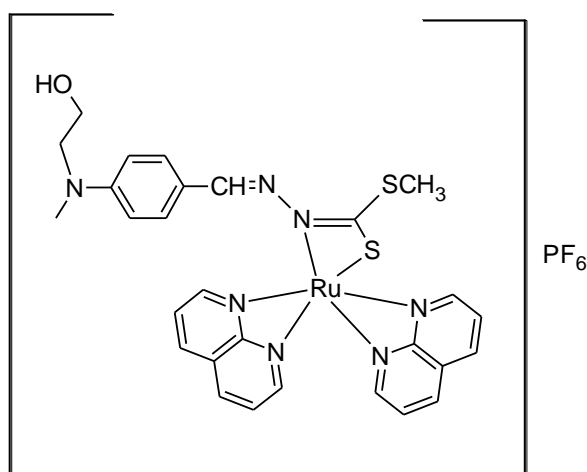


Figure 2.2 Chemical structures of  $[Ru(bpy)_2L]PF_6$  ( $bpy = 2,2'$ -bipyridine)

A new Schiff base 4-[N-hydroxyethyl-N-(methyl)amino]benzaldehyde S-methyl dithiocarbamate (HL, where H is a dissociable proton) and the ruthenium complex  $[Ru(bpy)_2L]PF_6$  ( $bpy = 2,2'$ -bipyridine) (Figure 2.2) have been synthesized by Yu-Peng Tian et al. (2005) and the complex shows intense MLCT transitions in the visible region. Fluorescent and electrochemical properties have been also studied. The complex in DMF solution exhibited a strong two photon absorption (t.p.a.) at 532 nm

nanosecond laser pulses. The t.p.a. coefficient  $\beta$ , t.p.a. cross-section  $\sigma$  and the third-order optical nonlinearity  $\chi^{(3)}$  of the complex and the ligand have been determined by the Z-scan technique (Figure 2.3).

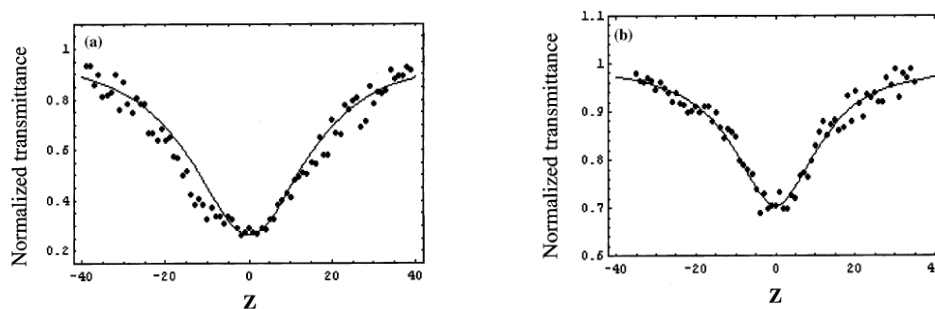


Figure 2.3 Open-aperture Z-scan data. Normalized transmittance of (a)  $[\text{Ru}(\text{bpy})_2\text{L}]\text{PF}_6$ , (b) HL. Scatter points are experimental data, and solid curves are theoretical fitting results.

Excited-state enhancement of the third-order nonlinear optical susceptibility of a square planar platinum complex, (2,2'-bipyridine)Pt(1,2-dicyano-1,2-ethylenedithiolate), was observed by Jinhai Si et al. (1996). When the sample was optically pumped by either a picosecond or a nanosecond pump beam of 355 nm wavelength.

Dhenaut et al. (1995) first reported the Second-order NLO properties of octupolar metal complexes like tris(bipyridine) (Figure 2.4) and tris(phenanthroline)ruthenium(II) complexes. These complexes possess  $D_3$  symmetry and exhibit intense multidirectional  $[d_p(\text{Ru}^{2+}) \rightarrow \pi^*(\text{bpy or phen})]$  MLCT excitations responsible for their relatively high second-order NLO response.

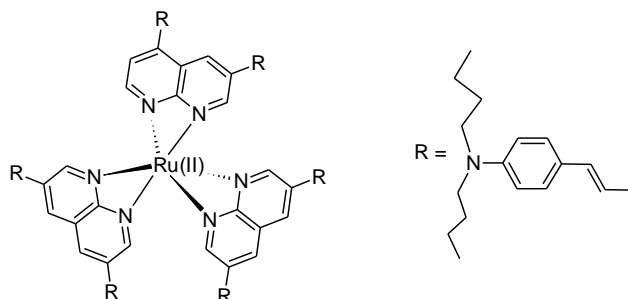
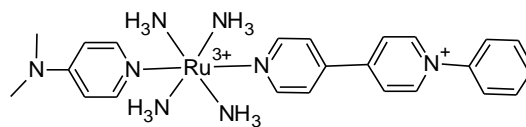


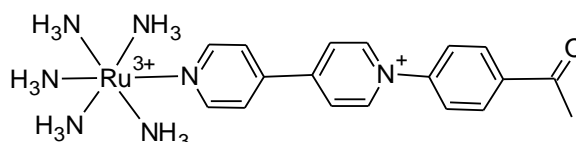
Figure 2.4 Chemical structures of tris(bipyridine) complex.

By using HRS measurements, Coe et al.(1997) have shown that dipolar ruthenium(II) ammine complexes of 4,4'-bipyridinium ligands (Figure 2.5) exhibit

very large, tunable  $\beta$  values, which are associated with intense, low energy MLCT excitations.



$$\beta = 794 \times 10^{-30} \text{ esu.}$$



$$\beta = 1112 \times 10^{-30} \text{ esu.}$$

Figure 2.5 Chemical structures of ruthenium (II) ammine complexes of 4,4'-bipyridinium ligands.

dmit organometallic complex,  $[(C_2H_5)_4N]_2[Cu(dmit)_2]$  ( $dmit^{2-} = 1, 3$ -dithiole-2-thione-4,5-dithiolate), abbreviated as EtCu (Figure 2.6) synthesized (Ren et al. 2008). Optical nonlinearities of this complex in acetone solution at 532 nm and 1064 nm were studied by the Z-scan technique with laser pulses of picosecond duration (Figure 2.7).

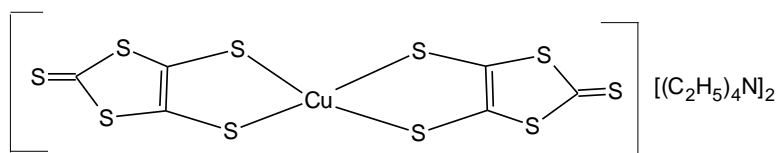


Figure 2.6 Chemical structures of  $[(C_2H_5)_4N]_2[Cu(dmit)_2]$ .

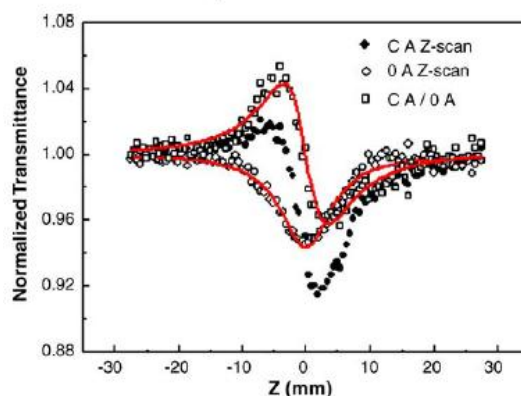


Figure 2.7 Normalized Z-scan transmittance curve of the sample solution S1 with concentration of  $2.0 \times 10^{-3} \text{ mol/L}$  measured at 1064 nm with the Z-scan. The solid lines are the theoretical fit to the experimental data.

The two-photon absorption at 1064 nm and the saturable absorption at 532 nm were observed. The Z-scan curves also revealed that EtCu sample solutions exhibited self-defocusing effects at both wavelengths.

Xiao-Zeng You (1997) synthesized following series of square planar complexes of Pd and Pt and measured their third order NLO response ( $\chi^{(3)}$ ) using DFWM technique.  $(n\text{-Bu}_4\text{N})_2[\text{Pd}(\text{S}_2\text{C}=\text{NC}_6\text{H}_4\text{NH}_2)_2]$  -  $\chi^{(3)}=6.4\times 10^{-12}$ ,  $(n\text{-Bu}_4\text{N})_2[\text{Pt}(\text{S}_2\text{C}=\text{NC}_6\text{H}_4\text{NH}_2)_2]$  -  $\chi^{(3)}=5.7\times 10^{-12}$ ,  $[\text{Pd}(\text{S}_2\text{CNHC}_6\text{H}_4\text{NH}_2)_2]$  -  $\chi^{(3)}=1.34\times 10^{-12}$ ,  $[\text{Pt}(\text{S}_2\text{CNHC}_6\text{H}_4\text{NH}_2)_2]$ -  $\chi^{(3)}=1.39\times 10^{-12}$ .

New metal-organic complex formulated as  $\{[\text{Co}(\text{bipy})_3][\text{Co}_2(\mu_2\text{-ox})_3]\}_n$  (bipy=2,2'-bipyridine; ox=oxalate) was synthesized and its third-order nonlinear optical properties of the complex was investigated (Yong Li et al. 2007) and they exhibit the reverse saturable absorption and self-defocusing performance with modulus of the hyperpolarizability ( $\gamma$ )  $5.75\times 10^{-30}$  esu in DMF solution.

Third-order optical nonlinearity of some salts, which consist of planar complex cation  $[\text{Cu}(\text{L})_2]^{2+}$  (L = 2,2'-bipyridine or phenanthroline) and planar complex anion  $[\text{M}(\text{mnt})_2]^{2-}$  (M = Ni, Co, Cu, or Pd; mnt = maleonitriledithiolate) were studied by DFWM technique (Chuluo Yang et al. 2001). It was found that these compounds exhibit large non-resonant nonlinearity at 1064 nm ( $\gamma$  in the order of  $10^{-31}$ - $10^{-30}$ ).

dmit organometallic complex,  $[(\text{C}_4\text{H}_9)_4\text{N}][\text{Co}(\text{dmit})_2]$  ( $\text{dmit}^{2-} = 1, 3\text{-dithiole-2-thione-4,5-dithiolate}$ ), abbreviated as BuCo and its third order optical nonlinearity of the acetone solution is characterized using the Z-scan technique with a 40-ps pulse width at 1064 nm (Ren Q et al. 2007). Z-scan curves show that BuCo sample solution possesses the negative nonlinear refraction, exhibiting a self-defocusing effect. In addition, the two-photon absorption has been observed in BuCo. The effective molecular second-order hyperpolarizability  $\gamma$  of the BuCo molecule was estimated to be as large as  $5.60\times 10^{-31}$  esu, suggesting BuCo is a potential material for optical device applications.

Third order optical nonlinearities of  $[(\text{CH}_3)_4\text{N}]\text{Au}(\text{dmit})_2$  ( $\text{dmit} = 4,5\text{-dithiolate-1,3-dithiole-2-thione}$ ) was studied at 532nm and 1064 nm using the Z-scan technique. The Z-scan spectra reveal a strong nonlinear absorption (reverse saturable

absorption) and a negative nonlinear refraction at 532 nm and  $\gamma$  of the molecule was found to be  $2.1 \times 10^{-31}$  esu. Nonlinear transmission measurements suggest that this material has potential applications in optical limiting (Sun et al. 2008).

Three Zn(II) complexes bearing 1,10-phenanthroline and one-dimensional (1D) push-pull NLO-phores with various acceptor strength as well as  $\pi$ -conjugation length have been synthesized in high yields for two-dimensional (2D) nonlinear optical response (Sanjib Das et al. 2006). The quadratic optical nonlinearity of the ligands and the complexes are measured by the HRS technique. The ligands show small second-order optical nonlinearity ( $\beta$ ) comparable to the standard, para-nitroaniline (pNA). However, upon complexation with Zn(II), each complex exhibits large  $\beta$  values showing the importance of metal ion in enhancing the optical nonlinear effect.

The synthesis and characterization of a series of new  $\pi$ -donor substituted vinyl bipyridines and their rhenium, zinc and mercury complexes {donor = 4-R<sub>2</sub>N=Me<sub>2</sub>N, n-Bu<sub>2</sub>N, (Me)(Oct<sup>n</sup>N); ( $\eta^5$ -C<sub>5</sub>H<sub>5</sub>)Fe ( $\eta^5$ -C<sub>5</sub>H<sub>4</sub>-)} with large nonlinear optical properties were reported by Bourgault M et al. (1993).

Hongliang Yang et al. (2005) reported dmit<sup>2-</sup> salt: bis(tetrabutylammonium)bis(1,3-dithiole-2-thione-4,5-dithiolato) cadmium (BCDT). The Optical Kerr Effect (OKE) signal of its acetone solution was measured by femtosecond optical Kerr gate technique. Using CS<sub>2</sub> OKE signal as reference signal measured under identical conditions, the third-order optical nonlinear susceptibility  $\chi^{(3)}$ , of the sample solution was obtained to be about  $1.08 \times 10^{-13}$  esu at the concentration of  $3.4 \times 10^{-4}$  M. The second-order hyperpolarizability for BCDT molecule was estimated to be as large as  $1.9 \times 10^{-31}$  esu. Its response time was about 239 fs, which is believed to be the contribution from the delocalized electrons.

Degenerate four wave mixing and nonlinear absorption studies of five binuclear ruthenium complexes (Figure 2.8) with different  $\pi$ -delocalized bridging ligands and mixed-valence metal centers at 532 nm were studied by Wenfang Sun et al. (2003). The resonant molecular second-order hyperpolarizabilities of all complexes are of the order of  $10^{-31}$ – $10^{-29}$  esu in picosecond regime, which originate from both the ground state and the excited state electronic processes. Nonlinear

absorption is found to be the dominant contributor to the third-order nonlinearities of the complexes.

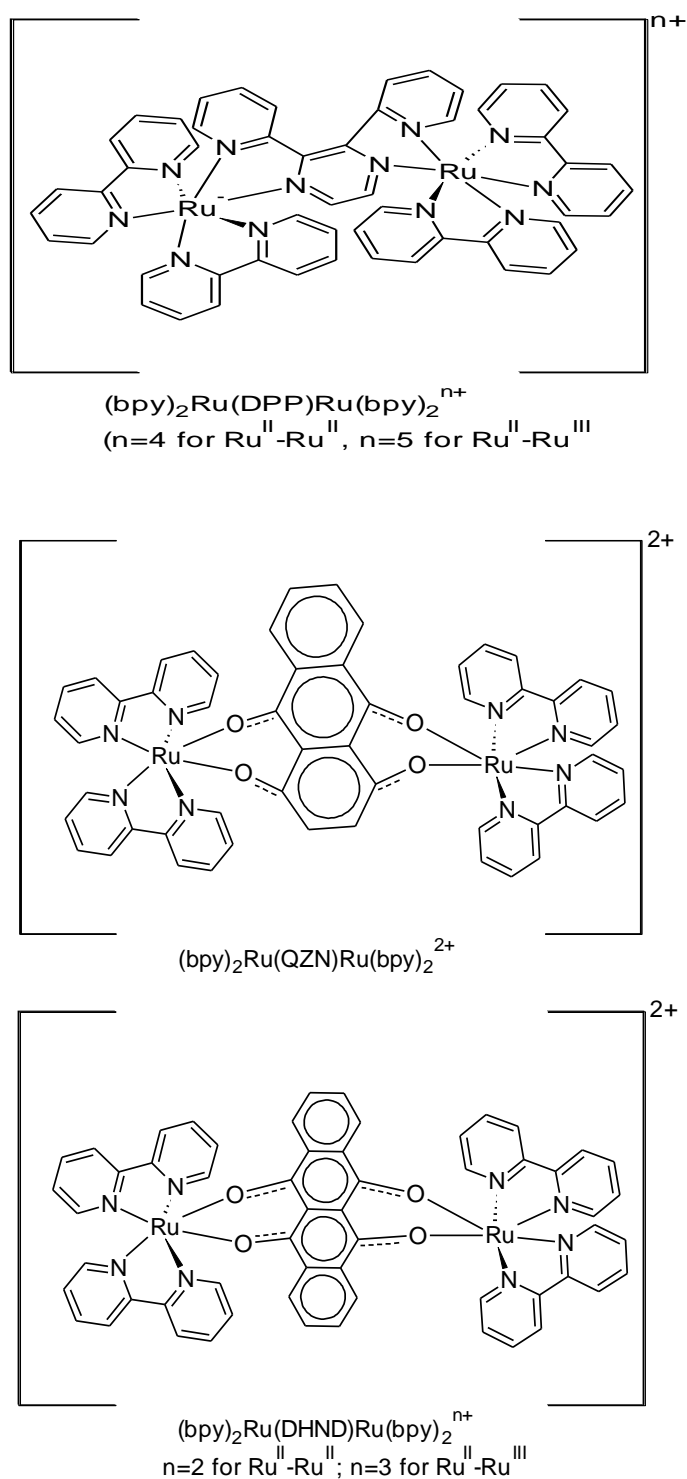


Figure 2.8 Chemical structures of tetrakis(2,2'-dipyridyl)diruthenium complexes.

However, nonlinear absorption of picosecond and nanosecond laser pulses exhibit different characteristics due to the relative contributions from singlet–singlet excited state and triplet–triplet excited state absorptions. The large resonant third order nonlinearity, fast time response and strong saturable absorption of picosecond laser pulses suggest that these complexes might be good candidates for laser mode-locking applications.

Third order nonlinearity of a ferrocene derivative of a 2-amino-1,2,3-triazoloquinone system [2-(yliminomethylferroceneyl)naphtho-1,2,3-triazole-4,9-dione] (Figure 2.9) in solution was reported by Rangel-Rojo et al. (2003).

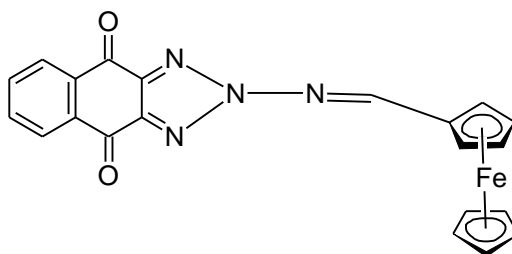


Figure 2.9 Chemical Structure of [2-(yliminomethylferroceneyl)naphtho-1,2,3-triazole-4,9 dione].

The pentanuclear cluster complex  $(\text{NEt}_4)_2[\text{MoS}_4(\text{CuBp})_4]$  was synthesized by Moayad Hossaini Sadr et al. (2006) in acetone as a new candidate for nonlinear optical activity and its  $\chi^{(3)}$  value was found to be  $-1.069 \times 10^{-12}$  esu.

Picosecond nonlinear optical response of a metal-dielectric composite made by implanting Cu ions in fused silica (Haglund et al. 1993). The third-order susceptibility  $\chi^{(3)}$  has an electronic component with a magnitude of the order of  $10^8$  esu and is enhanced for laser wavelengths near the surface plasmon resonance of the copper colloids.

Third-order nonlinear optical and optical limiting properties of 2,3,9,10,16,17,23,24-octakis-(heptyloxy)-phthalocyanine (PC1), 2,3,9,10,16,17,23,24-octakis-(heptyloxy)-phthalocyanine zinc(II) (PC2) (*symmetric*) and 2(3)-(butane-1,4-dioic acid)-9(10),16(17),23(24)-tri *tert*-butyl phthalocyanine zinc(II) (PC3) (*unsymmetrical*) (Figure 2.10) have been investigated using a continuous wave laser at 633 nm. Employed the Z-scan technique to evaluate the sign and magnitude of nonlinear refractive index and the nonlinear absorption coefficient.

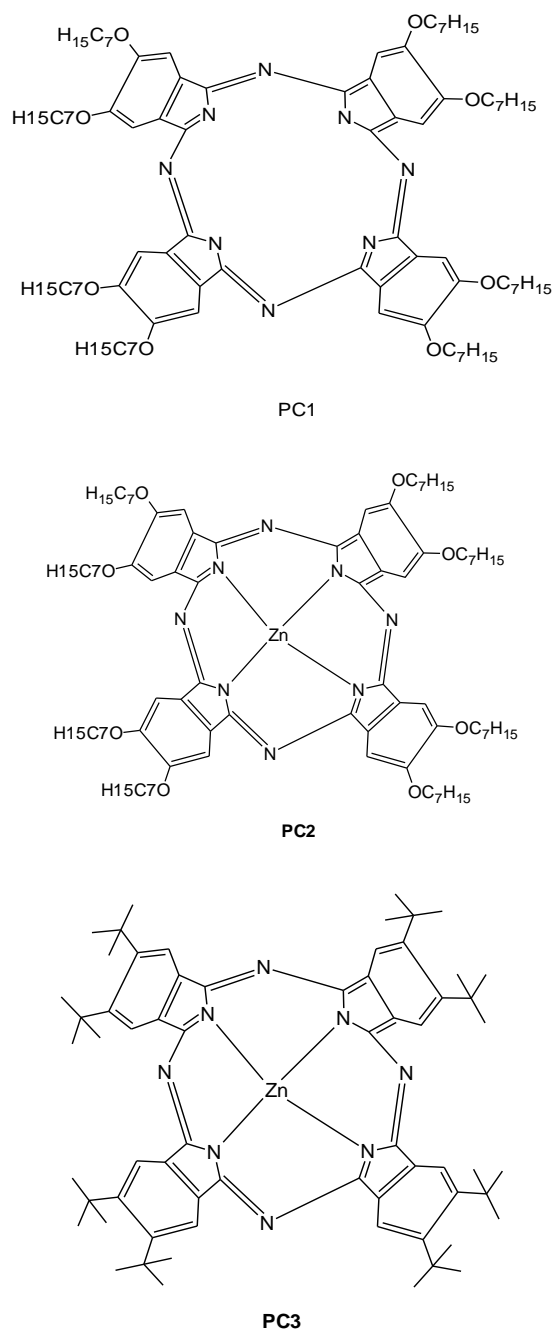


Figure 2.10 Chemical Structures of 2,3,9,10,16,17,23,24-octakis-(heptyloxy)-phthalocyanine (PC1), 2,3,9,10,16,17,23,24-octakis-(heptyloxy)-phthalocyanine zinc(II) (PC2) (*symmetric*) and 2(3)-(butane-1,4-dioic acid)-9(10),16(17),23(24)-tri *tert*-butyl phthalocyanine zinc(II) (PC3) (*unsymmetrical*).

Optical limiting based on nonlinear refraction was performed and limiting thresholds were estimated for all the three samples. The magnitude of the third-order nonlinearities measured were one of the highest reported in the continuous wave regime till date. Unsymmetrical phthalocyanine had better limiting characteristics and its nonlinear coefficients were comparatively high.

Results of the nonlinear optical studies performed with these organic dyes doped in Poly(methylmethacrylate) are also presented. They also insist that these phthalocyanines are potential candidates for optical limiting applications in low power cw regime (Mathews et al. 2007).

### **2.3 BORON COMPLEXES AS NLO MATERIALS**

The need of new materials for applications in photonics such as telecommunications, all-optical switching, data processing and optical limiting has inspired an intense research in organic compounds. These materials comprise highly polarizable  $\pi$ -electron fragments, which make possible, the observation of efficient nonlinear optical (NLO) phenomena (Zyss 1994). Furthermore, the organic materials are of major interest because of their relative low cost, easy integration, enormous design flexibility and their large and fast nonlinear optical response (Nalwa and Miyata 1997).

In the search for novel organic materials, recently, molecular and polymeric boron-containing compounds have been investigated because of their large and fast nonlinear optical response and potential applications in optical communication, data processing, optical switching, optical limiting devices, etc. They are also of interest for sensors (Liu et al. 2005) and electroluminescence applications, i.e., for the development of charge transport and luminescent materials for OLEDs (Elbing et al. 2008, Cui et al. 2007 and Zhou et al. 2008). For these applications, three-coordinated boron species have been widely studied due to the fact that their vacant p-orbital is a strong  $\pi$ -electron acceptor which can lead to significant delocalization with an adjacent organic conjugated system. In contrast to the nitro group (a well-known strong  $\pi$ -acceptor), the three-coordinated boron atom can also function as a  $\sigma$ -donor because of its low electronegativity (Entwistle and Marder 2002). Additionally, boron has been also utilized in 12-vertex clusters to form donor groups in  $\pi$ -conjugated systems (Bernard et al. 2005).

On the other hand, four-coordinated boron has also been incorporated into NLO organic systems. For instance, from experimental (Lesley et al. 1998) and theoretical (Su et al. 2001) studies it was demonstrated that the second-order NLO properties of boron complexes of stilbazoles and pyridines are enhanced with respect to their corresponding free-boron compounds; similarly, Zwitterionic borates showed much larger second-order NLO properties and higher transparency compared with their analogous uncharged push-pull species (Lambert et al 1996). Munoz et al 2008 and Reyes et al 2002 has studied second- and third-order nonlinearities in four-coordinated boron systems prepared from tridentate ligands. These studies showed that boron derivatives of salicylaldiminophenols exhibit quadratic nonlinearities with the product  $\mu \times \beta$  ( $\mu$  being the dipole moment and  $\beta$  the first molecular hyperpolarizability) ranging from 630 to  $845 \times 10^{-30} \text{ cm}^5 \text{ esu}^{-1} \text{ D}$ . These studies also showed that the appropriate combination of groups (donor-acceptor) and the formation of the N→B coordinative bond optimize quadratic nonlinear effects such as the second-harmonic generation (Reyes et al 2002). Additionally, the cubic nonlinearities in the boron complexes reported by Munoz et al 2008 have been investigated exhibiting third-order nonlinear susceptibility ( $\chi^{(3)}$ ) values in the range of  $10^{-12} \text{ esu}$ . Rodriguez M et al 2009 studied the structural-optical response in boron-containing systems, and the effect of the  $\pi$ -electronic polarization and third-order nonlinearities due to the formation of the N→B coordinative bond.

Although organo boron compounds have received considerable attention for their interesting applications in medicinal chemistry, as anticancer agents, in Boron Neutron Capture Therapy (BNCT) (Hawthorne and Lee 2003), in organic synthesis and (Suginome et al. 2004) as materials with fluorescence (Liu et al. 2004), the literature concerning organo boron complexes with NLO properties is scarce. In this respect the boron atom has been used in three different forms due to the fact that it shows excellent properties as electron acceptor (Yuang et al. 1990), as zwitter ionic complex (Lambert et al. 1996) and as acid base adduct with  $\text{BF}_3$  and  $\text{B}(\text{C}_6\text{F}_5)_3$  (Lesley et al. 1998 and Pizzotti et al. 2002).

#### 2.4 SCOPE AND OBJECTIVES OF THE WORK

With the rapid development of optical communication, the novel materials with large and ultrafast nonlinear optical responses are needed for fabricating the

ultrafast optical switching and processing devices. For these purposes, many materials, including semiconductors, polymers, nanomaterials and inorganic materials have been researched. In recent years,  $\pi$ -conjugated organic materials have received considerable interest for their high nonlinear optical (NLO) properties and fast response time of the nonlinearity. Especially, the organometallic and coordination materials have been attracting a great deal of attention in the field of nonlinear optics because they can combine the advantages of architectural flexibility, ease of fabrication, tailoring and high NLO properties of organics with good transmittancy, temporal and thermal stability of inorganics.

The study of nonlinear optical properties of the synthesized complexes will lead to the development of new NLO materials. The results of research may be useful in understanding the NLO properties of material and their applications in various optoelectronic technologies such as optical signal processing, all-optical switching, optical computing and other NLO devices. In this regard, the present work is aimed to design and characterizes suitable materials for NLO applications by selecting two types of coordination (transition metals and boron) complexes. The main objectives are

- To design and synthesize the organic  $\pi$ -conjugated donor-acceptor type ligands.
- To synthesize the transition metal complexes using the synthesized organic  $\pi$ -conjugated donor-acceptor type ligands.
- To characterize the above synthesized ligands and transition metal complexes by Elemental analysis, FT-IR, UV-visible,  $^1\text{H}$  NMR and  $^{31}\text{P}$  NMR spectroscopy.
- To design and synthesize the boron complexes using organic  $\pi$ -conjugated donor-acceptor type ligands and their characterization by Elemental analysis, FT-IR, UV-visible,  $^1\text{H}$  NMR and  $^{19}\text{F}$  NMR spectroscopy.
- To investigate the nonlinear optical properties of newly synthesized complexes by using open aperure Z-Scan and Optical Kerr gate (for selected complexes) techniques.



## CHAPTER 3

### SYNTHESIS, CHARACTERIZATION AND THIRD-ORDER NONLINEAR OPTICAL STUDIES OF Zn(II), Cd(II) AND Hg(II) COMPLEXES

#### *Abstract*

*The octupolar metal complexes [Zn(phen)(L)] (1C), [Cd(phen)(L)] (2C), [Hg(phen)(L)] (3C) [Zn(bpy)(L)] (4C), [Cd(bpy)(L)] (5C), [Hg(bpy)(L)] (6C) (phen = 1,10-phenanthroline, bpy = 2,2'-bipyridyl, L = 4-dimethylamino- $\alpha$ -cyanocinnamate) bearing diimine and one-dimensional (1D) push-pull NLO-phores with  $\pi$ -conjugation have been synthesized. The third-order nonlinear optical properties of complexes were studied using open aperture Z-scan technique at 532 nm with nanosecond laser pulses. The complexes show optical limiting behaviour. The values of the effective two-photon absorption (2PA) coefficients ( $\beta$ ) were measured.*

#### 3.1 INTRODUCTION

Metal ions being excellent templates, can gather organic 1D dipolar chromophores around to form predetermined 2D and 3D NLO-phores with various symmetries and charge-transfer dimension tunable by virtue of the coordinated metal center as well as the presence of polarizable  $d$  electrons can also contribute (Chemla et al. 1987, Zyss 1994) to greater nonlinear activity. Other advantages of using metal complexes as NLO materials include higher damage threshold, fast response time and easy synthesis. Some reports are available in the literature on Zn(II), Cd(II) and Hg(II) complexes with large second and third-order nonlinearity (Yu-Peng Tian et al. 2002 and Hongliang Yang et al. 2005).

In the case of resonant excitation, excited state absorption (ESA) is a major contributor to nonlinear absorption. In transparent materials genuine two-photon absorption (TPA) can lead to the nonlinearity, which may sometimes induce a subsequent ESA as well. Optical materials exhibiting strong two-photon absorption (2PA) have recently received considerable attention due to their numerous potential applications, such as fluorescence imaging (Sheik-Bahae 1990), up-conversion lasing (Zhan et al. 2002) and optical limiting (Sutherland et al 2005). Nonlinearity due to ESA, induced by TPA or otherwise, has been demonstrated by nonlinear transmission

and open-aperture (OA) Z-scan experiments in many materials, including charge-transfer salts, nanocomposites and organic molecules. However, only a few reports have appeared in this regard on metal complexes.

This chapter describes the synthesis, characterization and third-order NLO studies of diimine (1,10-phenanthroline, 2,2'-bipyridine) based Zn(II), Cd(II) and Hg(II) complexes (1C-6C) using open aperture Z-scan technique. The complexes show optical limiting behaviour. The operating nonlinear mechanism leading to optical power limiting was found to be reverse saturable absorption. The values of the effective two-photon absorption (2PA) coefficients ( $\beta$ ) were calculated. The values of  $\beta$  of complexes were found to be in the order of  $10^{-11}$  m/W.

## 3.2 EXPERIMENTAL

### 3.2.1 Materials

All the chemicals used were of analytical grade. Solvents were purified and dried according to the standard procedures (Vogel 1989). 4-dimethylaminobenzaldehyde, tert-butylcyanoacetate, 1,10-phenanthroline monohydrate and 2,2'-bipyridine were purchased from Sigma Aldrich and Zn(OAc)<sub>2</sub>·2H<sub>2</sub>O, Cd(OAc)<sub>2</sub>·2H<sub>2</sub>O and Hg(OAc)<sub>2</sub>·2H<sub>2</sub>O were procured from Merck chemicals.

### 3.2.2 Analysis and measurements

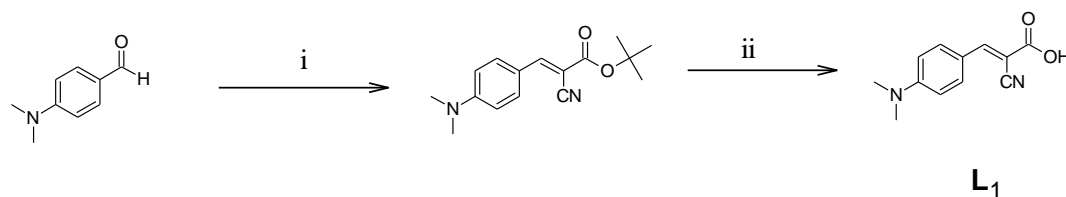
The <sup>1</sup>H NMR spectra were recorded using Bruker AV 400 spectrometer operating at the frequency of 400 MHz. The spectra were recorded in solution with DMSO as internal lock. Electronic spectra were measured on a Cintra 101 (GBC) UV-Vis double beam spectrophotometer with 0.6 nm resolution in DMSO solution of the complexes in the 200 – 800 nm range. FT - IR spectra were recorded on a Thermo Nicolet Avatar FTIR-ATR spectrometer with 4 cm<sup>-1</sup> resolution in the frequency range 400 – 4000 cm<sup>-1</sup>. The C, H and N contents were determined by Thermoflash EA1112 series elemental analyzer. The single beam Z-scan technique (Sheik-Bahae et al. 1990) was used to measure the third-order nonlinearity of the metal complexes. This technique allows measurement of nonlinear absorption (NLA). Experiment was performed using a Q-switched frequency doubled Nd: YAG laser (Spectra-Physics USA, Model-GCR170) with a temporal pulse width of 7 ns (FWHM) at 532 nm and a

repetition rate of 10 Hz. The input pulse energy used was 100  $\mu\text{J}$ , which corresponds to an on-axis-peak irradiance of 2.39  $\text{GW}/\text{cm}^2$ . The transmittance was measured using two Pyroelectric detector (RjP - 735) connected with Laser Probe Rj-7620 Energy meter. The output of the laser had a nearly Gaussian intensity profile. A lens of focal length 26 cm was used to focus the laser pulses into a 1mm quartz cuvette containing the sample solution. The laser beam waist at the focused spot was estimated to be 18.9  $\mu\text{m}$  and the corresponding Rayleigh length is 2.11 mm. The laser was run in the single shot mode using a data acquisition programme, with an approximate interval of 3 to 4 seconds between each pulse. This low repetition rate prevents sample damage and cumulative thermal effects in the medium.

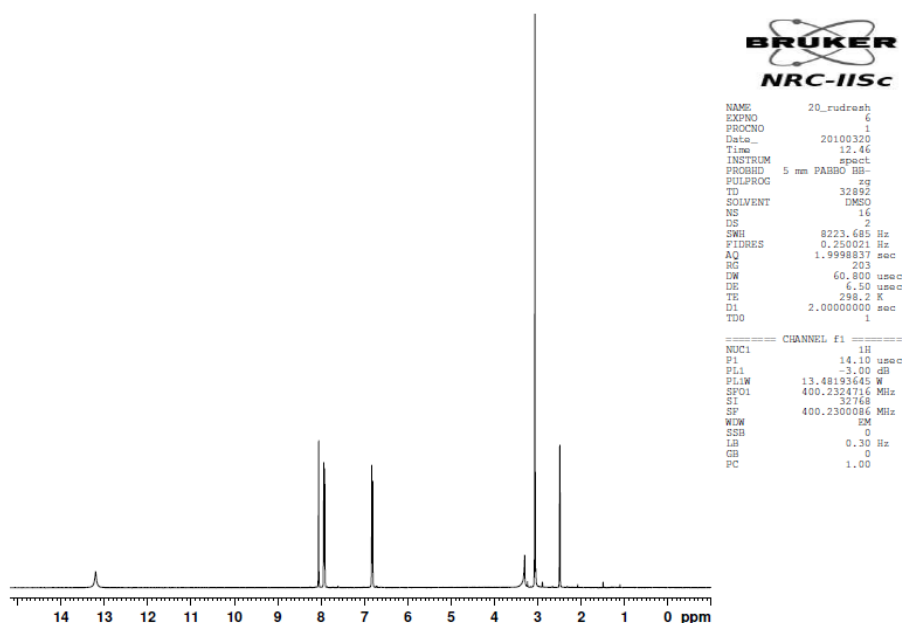
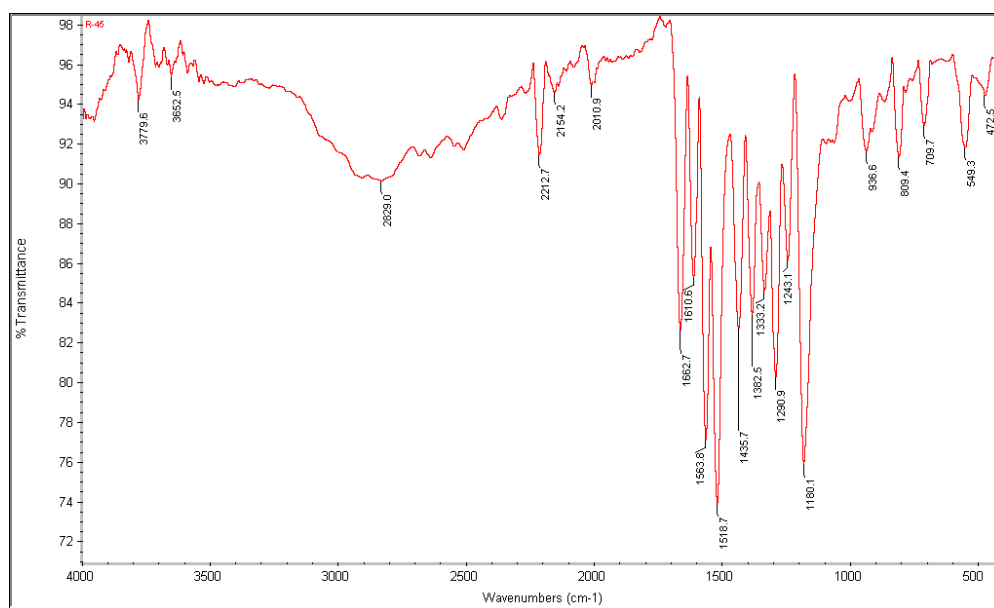
### 3.2.3 Synthesis of metal complexes

#### 3.2.3.1 Synthesis of Ligand ( $L_1$ )

The ligand  $L_1$  was prepared and characterized by following a reported procedure (Sanjib Das et al. 2006). Ethanolic (50 ml) solution of 4-dimethylaminobenzaldehyde (1.19g, 8 mmol) was added to tert-butylcyanoacetate (1.24 ml, 8.8 mmol) through a syringe all at a time followed by catalytic amount (2 drops) of piperidine. The orange yellow solid that appeared on stirring overnight at room temperature, was collected by filtration, washed thoroughly with ethanol and dried undervacuum. This solid was stirred for 2 h, with trifluoroacetic acid (6 ml) and then poured into water (50 ml) (Scheme 3.1). The orange yellow solid that separated, was collected by filtration, washed with ethanol and finally dried under vacuum. Yield: 90%.  $^1\text{H NMR}$  (400 MHz, DMSO, TMS, 25  $^\circ\text{C}$ ):  $\delta$  3.06 (s, 6H), 6.82 (d, 2H), 7.93 (d, 2H), 8.05 (s, 1H), 13.20 (bs, 1H) (Figure 3.1). IR ( $\text{cm}^{-1}$ ): 2212 ( $-\text{C}\equiv\text{N}$ ), 1662.7 ( $\text{C}=\text{O}$ ) (Figure 3.2).  $\lambda_{\text{max}}$ : 425nm. Anal. Calc. for  $\text{C}_{12}\text{H}_{12}\text{N}_2\text{O}_2$ : C, 67.03; H, 6.03; N, 13.43. Found: C, 66.59; H, 5.54; N, 12.94%.



Scheme 3.1 Synthetic scheme for ligand ( $L_1$ ). (i) tert-butyl cyanoacetate, piperidine and (ii) trifluoroacetic acid.

Figure 3.1.  $^1\text{H}$  NMR spectrum of ligand ( $L_1$ ).Figure 3.2 IR spectrum of ligand ( $L_1$ ).

### 3.2.3.2 Synthesis of $[\text{Zn}(\text{phen})(L_1)_2]$ ( $1C$ )

A methanolic solution (10 mL) containing 4-dimethylamino- $\alpha$ -cyanocinnamic acid ( $L_1$ ), (0.27 g; 1.2 mmol),  $\text{Zn}(\text{OAc})_2 \cdot 2\text{H}_2\text{O}$  (0.13 g; 0.63 mmol) and 1,10-phenanthroline monohydrate (0.12 g; 0.63 mmol) were allowed to stir for 24 h at room temperature (Scheme 3.2). The bright yellow solid that separated upon stirring

overnight was collected by filtration, washed with methanol and dried under vacuum. Yield: 87%.  $^1\text{H}$  NMR (400 MHz, DMSO, TMS, 25 °C):  $\delta$  2.90 (s, 6H),  $\delta$  6.4 to 9.2 corresponds to protons of phenyl groups and CH=C proton (Figure 3.3). IR ( $\text{cm}^{-1}$ ): 2210.3 (-CN), 553.4 (M-O), 1602.5 (C=O) (Figure 3.4). CHN found: C: 67.12, H:5.15, N: 13.03  $\text{C}_{36}\text{H}_{30}\text{N}_6\text{O}_4\text{Zn}$  requires C: 63.89, H: 4.46, N: 12.43.

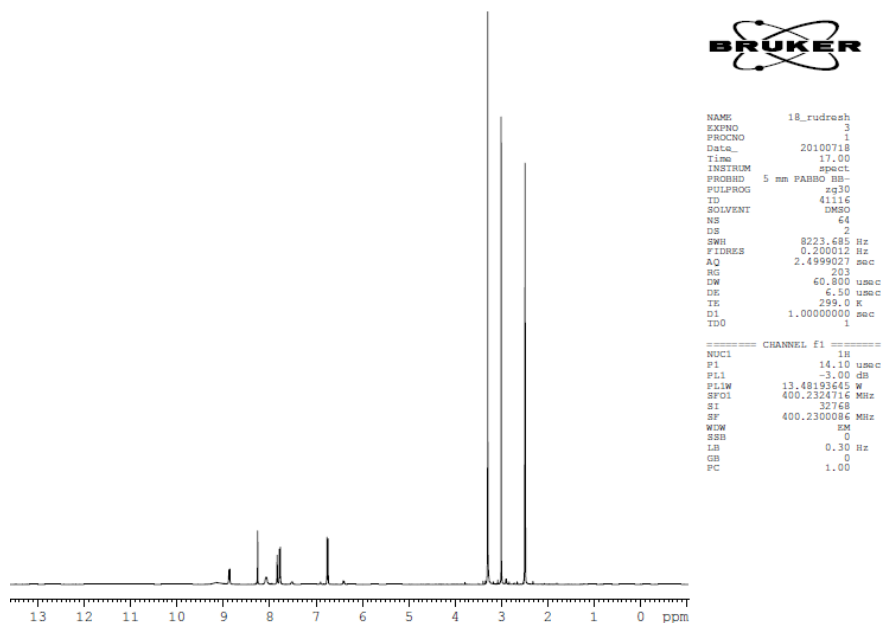


Figure 3.3  $^1\text{H}$  NMR spectrum of complex 1C.

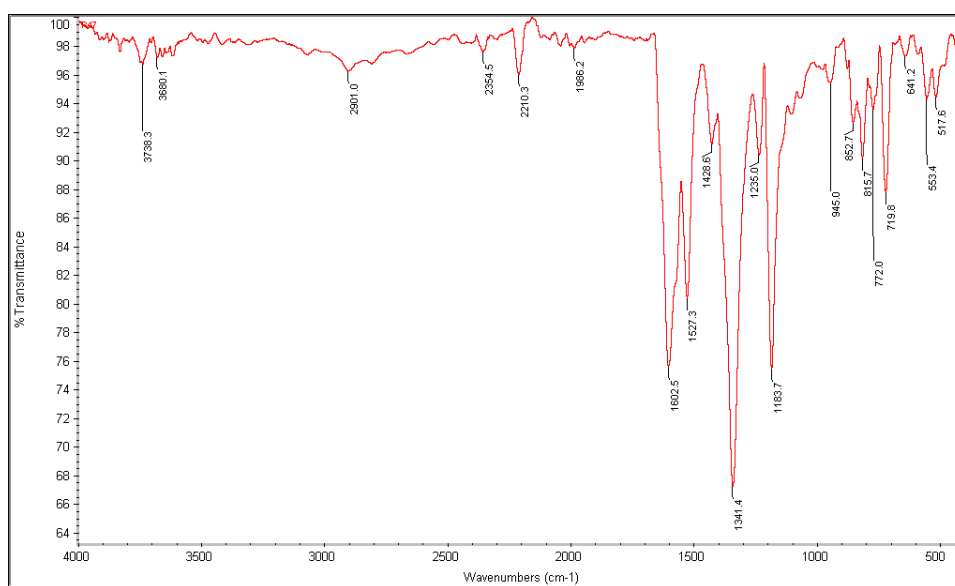
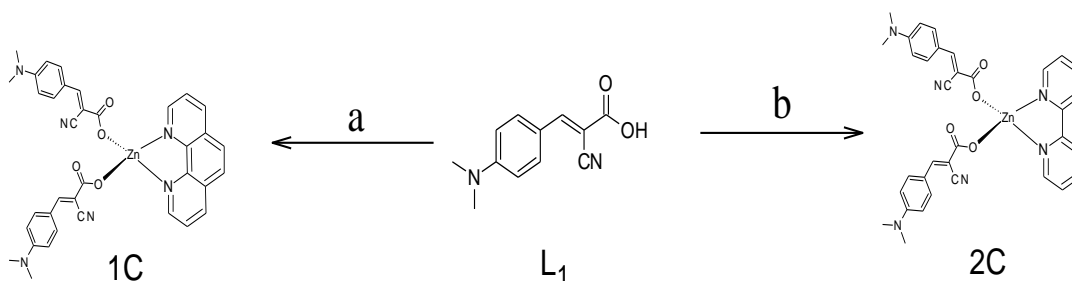


Figure 3.4 IR spectrum of complex 1C.

### 3.2.3.3 Synthesis of $[Zn(bpy)(L_1)_2]$ (2C)

This compound was isolated in a similar manner as complex 1C taking bipyridine (0.098 g; 0.63mmol) in place of 1,10-phenanthroline keeping other reactants unchanged (Scheme 3.2). The yellow solid was collected by filtration, washed thoroughly with methanol and dried under vacuum. Yield: 85%.  $^1H$  NMR (400 MHz, DMSO, TMS, 25 °C):  $\delta$  2.90 (s, 6H),  $\delta$  6.4 to 9.2 corresponds to protons of phenyl groups and CH=C proton (Figure 3.5). IR ( $cm^{-1}$ ): 2200.1 (CN), 554.6 (M-O), 1600.1 (C=O) (Figure 3.6). CHN found: C: 63.54, H:5.78, N: 13.55.  $C_{34}H_{30}N_6O_4Zn$  requires C: 62.62, H: 4.63, N: 12.88.



Scheme 3.2 Synthetic scheme for complexes 1 and 2. (a) 1,10-phenanthroline monohydrate and (b) 2, 2'-bipyridine.

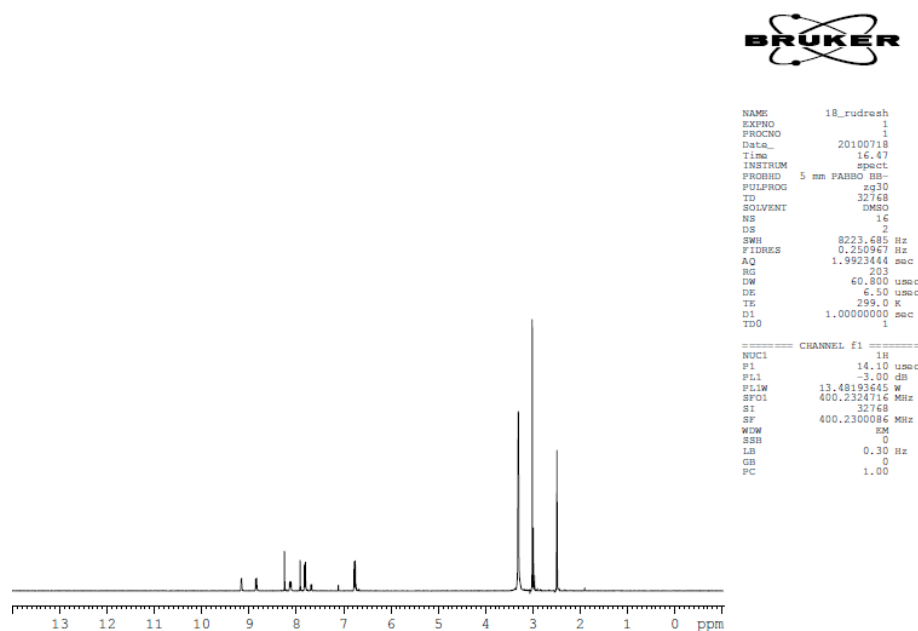


Figure 3.5  $^1H$  NMR spectrum of complex 2C.

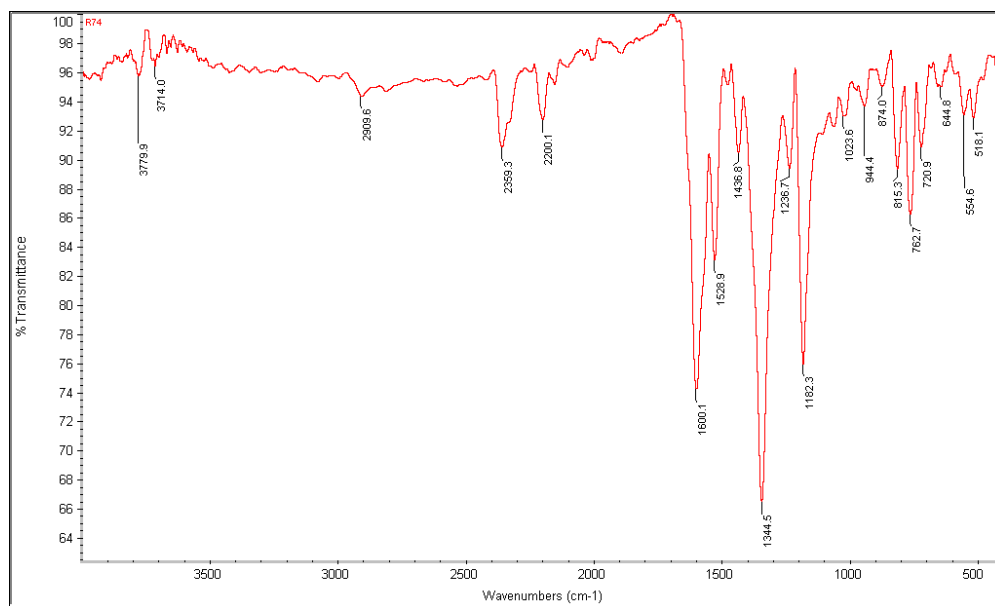
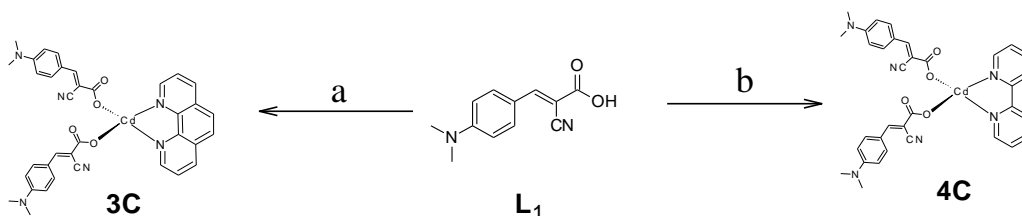


Figure 3.6 IR spectrum of complex 2C.

### 3.2.3.4 Synthesis of $[Cd(phen)(L_1)_2]$ (3C)

Synthesis of this complex is also accomplished following a similar procedure of complex 1C taking  $Cd(OAC)_2 \cdot 2H_2O$  (0.168 g; 0.63mmol) in place of  $Zn(OAC)_2 \cdot 2H_2O$ . The bright yellow solid that separated upon stirring overnight was collected by filtration, washed with methanol and dried under vacuum (Scheme 3.3). Yield: 80%.  $^1H$  NMR (400 MHz, DMSO, TMS, 25 °C):  $\delta$  2.90 (s, 6H),  $\delta$  6.7 to 9.2 corresponds to protons of phenyl groups and  $CH=C$  proton (Figure 3.7). IR ( $cm^{-1}$ ): 2207.2 (CN), 516.6 (M-O), 1583.5 (C=O) (Figure 3.8). CHN found: C: 60.13, H:4.55, N: 11.95.  $C_{36}H_{30}N_6O_4Cd$  requires C: 59.79, H: 4.18, N: 11.62.



Scheme 3.3 Synthetic scheme for complexes 3 and 4 . (a) 1,10-phenanthroline monohydrate and (b) 2, 2'-bipyridine.

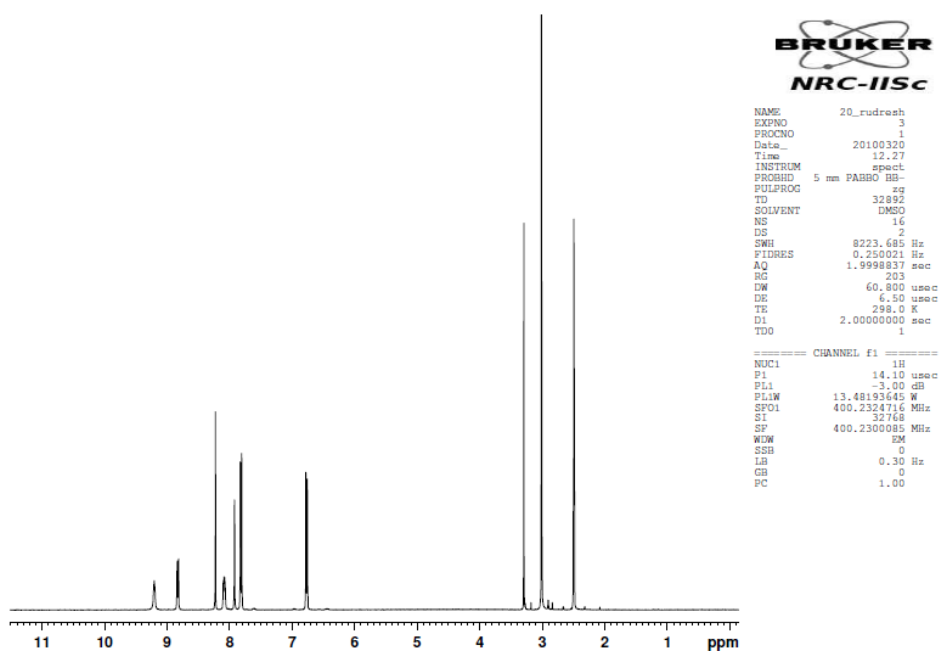
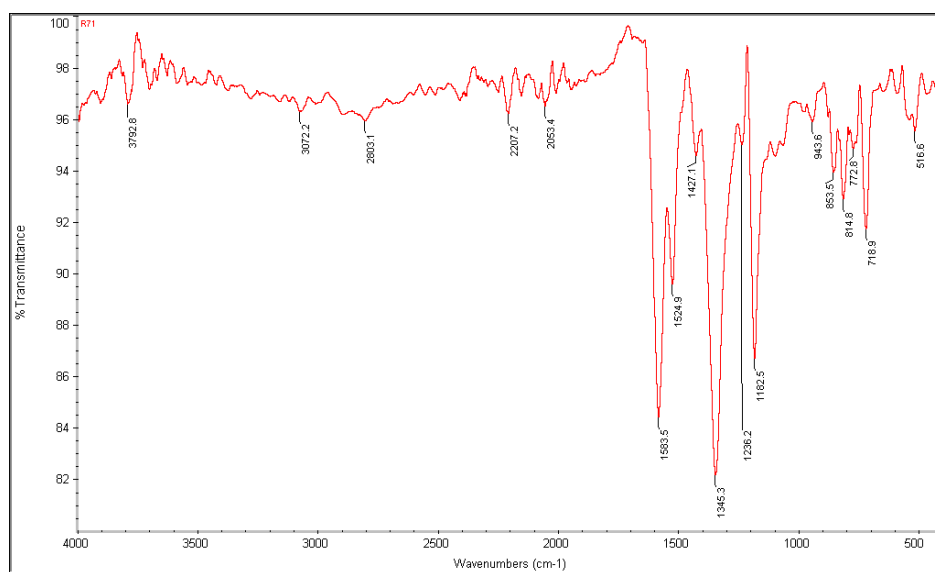
Figure 3.7  $^1\text{H}$  NMR spectrum of complex 3C.

Figure 3.8 IR spectrum of complex 3C.

### 3.2.3.5 Synthesis of $[\text{Cd}(\text{bpy})(\text{L}_1)_2]$ (4C)

Synthesis of this complex is also accomplished following a similar procedure of complex 3C taking bipyridine (0.098 g; 0.63 mmol) in place of 1,10-phenanthroline keeping other reactants unchanged (Scheme 3.3). The bright yellow solid that separated upon stirring overnight was collected by filtration, washed with methanol and dried under vacuum. Yield: 87%.  $^1\text{H}$  NMR (400 MHz, DMSO, TMS,

25 °C):  $\delta$  2.90 (s, 6H),  $\delta$  6.7 to 8.7 corresponds to protons of phenyl groups and CH=C proton (Figure 3.9). IR ( $\text{cm}^{-1}$ ): 2207.3 (CN), 516.8 (M-O), 1583.5 (C=O) (Figure 3.10). CHN found: C: 59.17, H:4.51, N: 12.73.  $\text{C}_{34}\text{H}_{30}\text{N}_6\text{O}_4\text{Cd}$  requires C: 58.41, H: 4.32, N: 12.02.

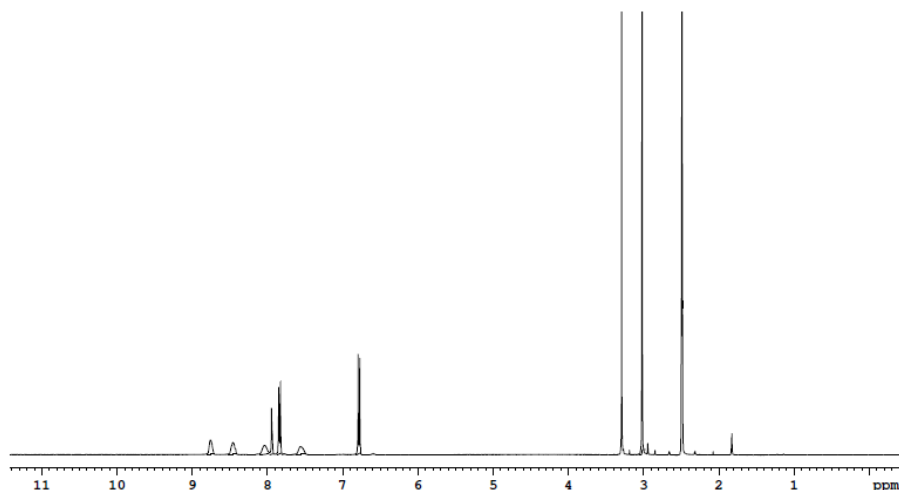


Figure 3.9  $^1\text{H}$  NMR spectrum of complex 4C.

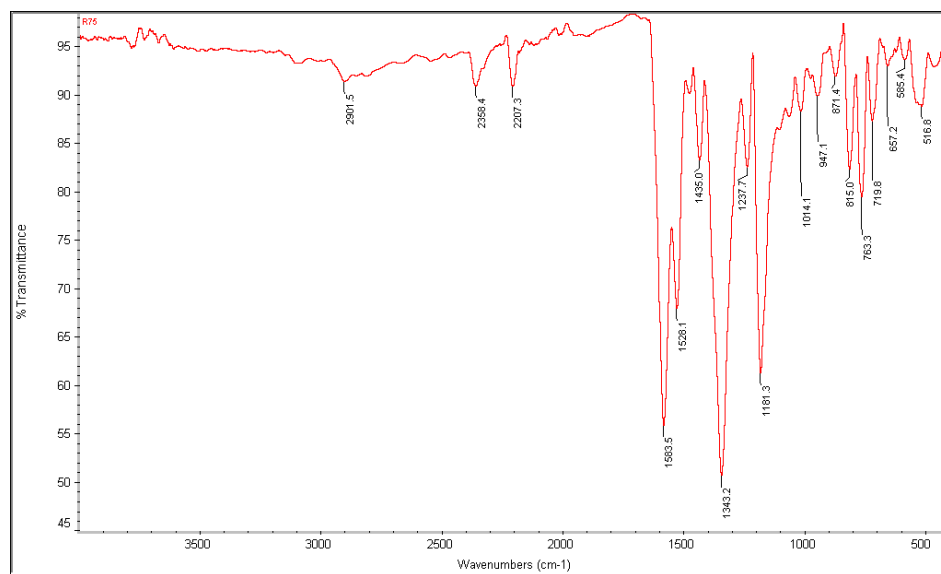
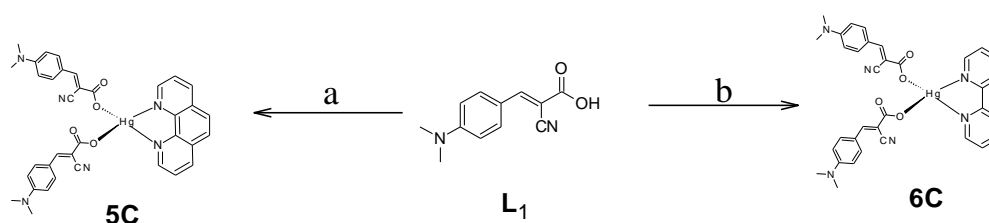


Figure 3.10 IR spectrum of complex 4C.

### 3.2.3.6 Synthesis of $[Hg(phen)(L_1)_2]$ (**5C**)

Synthesis of this complex is also accomplished following a similar procedure of complex **1C** taking  $Hg(OAc)_2 \cdot 2H_2O$  (0.20 g; 0.63 mmol) in place of  $Zn(OAc)_2 \cdot 2H_2O$  (Scheme 3.4). The brightly yellow solid that separated upon stirring overnight was collected by filtration, washed with methanol and dried under vacuum. Yield: 82%.  $^1H$  NMR (400 MHz, DMSO, TMS, 25 °C):  $\delta$  2.90 (s, 6H),  $\delta$  6.4 to 9.2 corresponds to protons of phenyl groups and CH=C proton (Figure 3.11). IR ( $cm^{-1}$ ): 2206.7 (CN), 515.3 (M-O), 1576.9 (C=O) (Figure 3.12). CHN found: C: 53.86, H:3.88, N: 11.03.  $C_{36}H_{30}N_6O_4Hg$  requires C: 53.29, H: 3.72, N: 10.35.



Scheme 3.4 Synthetic scheme for complexes **3** and **4**. (a) 1,10-phenanthroline monohydrate and (b) 2, 2'-bipyridine.

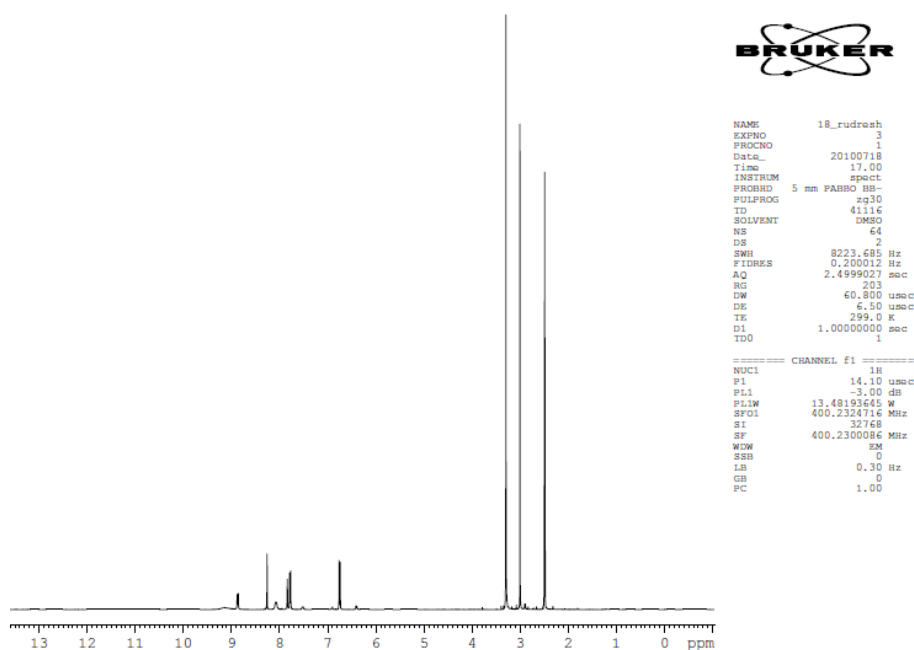


Figure 3.11  $^1H$  NMR spectrum of complex **5C**.

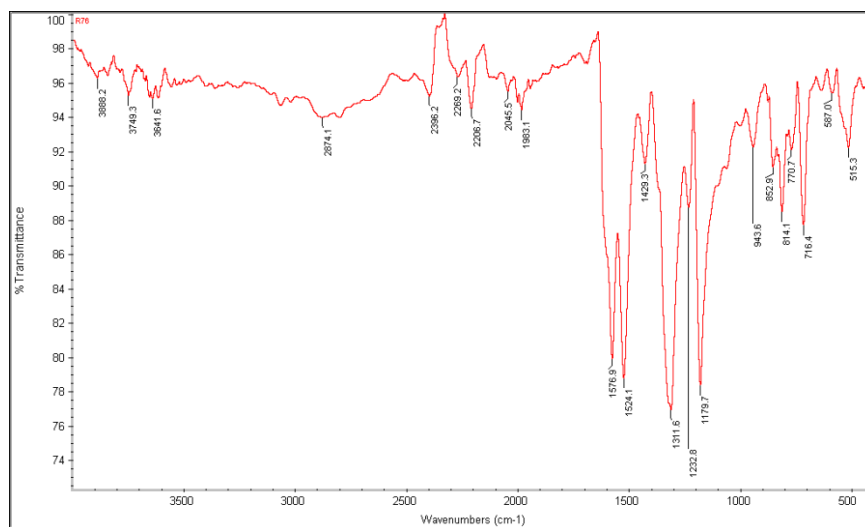
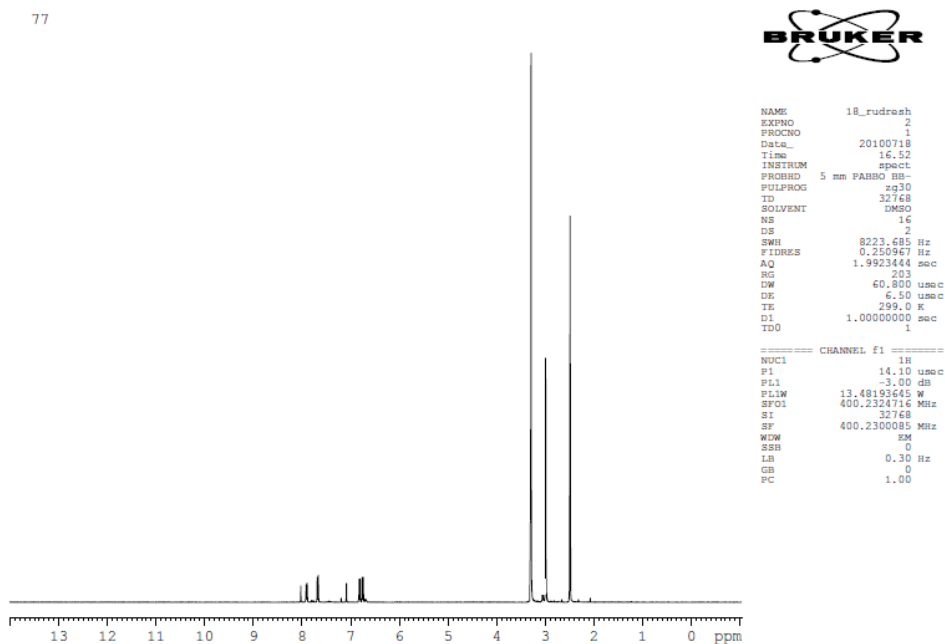


Figure 3.12 IR spectrum of complex 5C.

### 3.2.3.7 Synthesis of $[Hg(bpy)(L_1)_2]$ (6C)

Synthesis of this complex is also accomplished following a similar procedure of complex 5C taking bipyridine (0.098 g; 0.63 mmol) in place of 1,10-phenanthroline keeping other reactants unchanged (Scheme 3.4). The bright yellow solid that separated upon stirring overnight was collected by filtration, washed with methanol and dried under vacuum. Yield: 84%.

Figure 3.13 <sup>1</sup>H NMR spectrum of complex 6C.

$^1\text{H}$  NMR (400 MHz, DMSO, TMS, 25 °C):  $\delta$  2.90 (s, 6H),  $\delta$  6.7 to 8.2 corresponds to protons of phenyl groups and CH=C proton (Figure 3.13). IR ( $\text{cm}^{-1}$ ): 2206.3 (CN), 515.1 (M-O), 1571.2 (C=O) (Figure 3.14). CHN found: C: 52.06, H:4.02, N: 10.87.  $\text{C}_{34}\text{H}_{30}\text{N}_6\text{O}_4\text{Zn}$  requires C: 51.87, H: 3.84, N: 10.67.

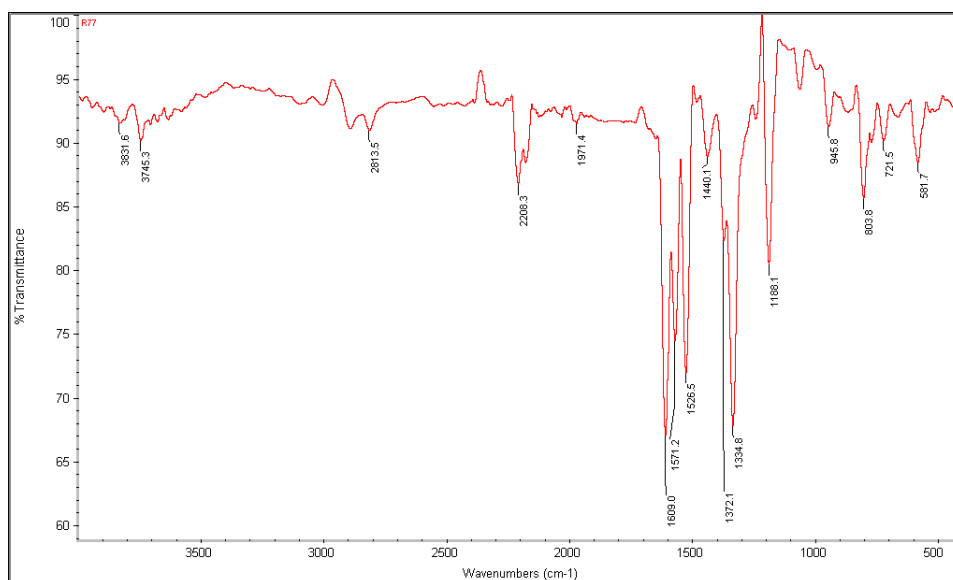


Figure 3.14 IR spectrum of complex 6C.

### 3.2.4 UV-visible spectra of complexes

The UV-Vis spectral data of the ligand and complexes recorded in dry DMSO are displayed in Figures 3.15-3.21. The spectra shows that complexes exhibit two intra ligand charge transfer absorptions ( $\lambda_{\text{max}}$  ~ at 250 and 420 nm) compared to ligand which shows only one intramolecular charge transfer absorptions at  $\lambda_{\text{max}}$  425 nm.

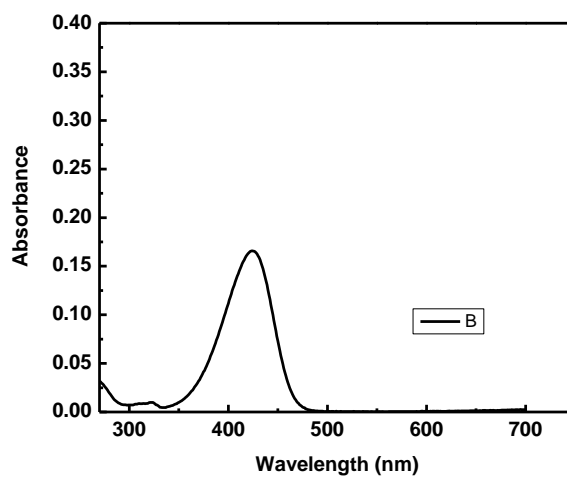
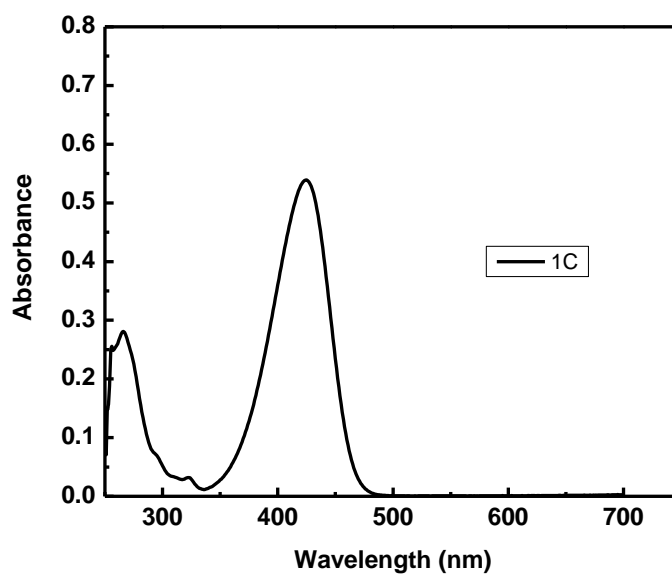
Figure 3.15 UV-visible spectrum of ligand L<sub>1</sub>.

Figure 3.16 UV-visible spectrum of complex 1C.

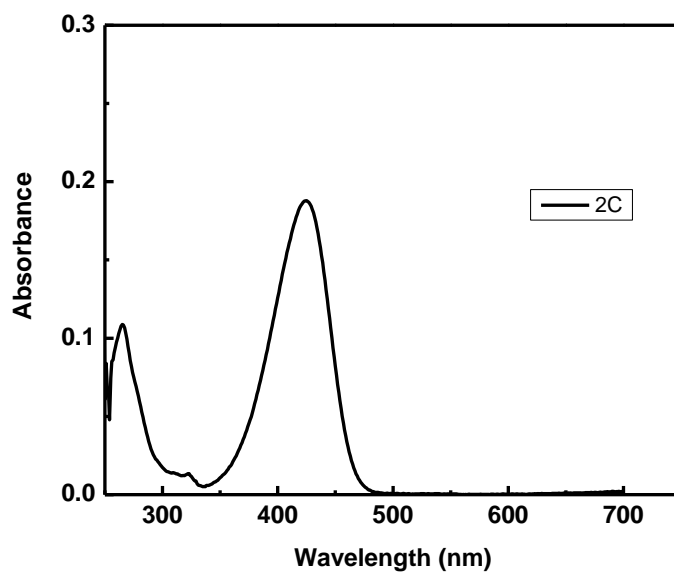


Figure 3.17 UV-visible spectrum of complex 2C.

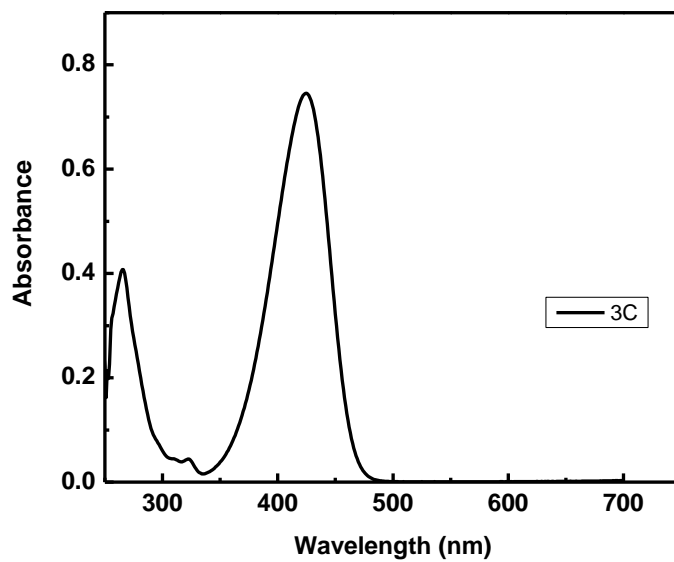


Figure 3.18 UV-visible spectrum of complex 3C.

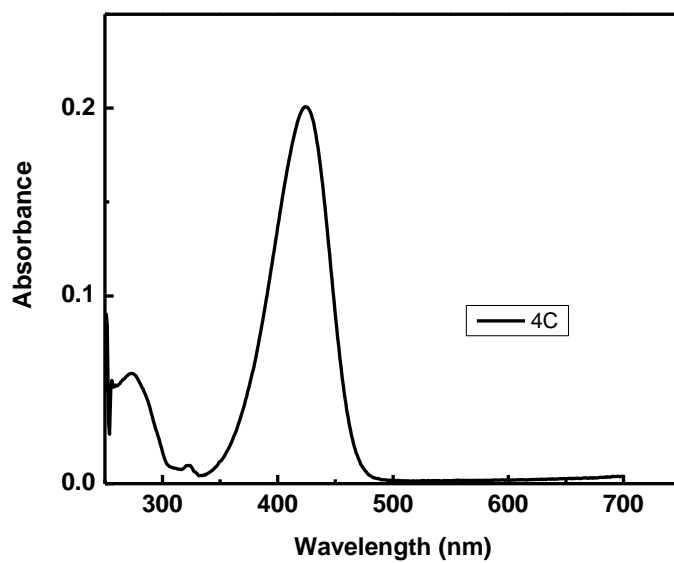


Figure 3.19 UV-visible spectrum of complex 4C.

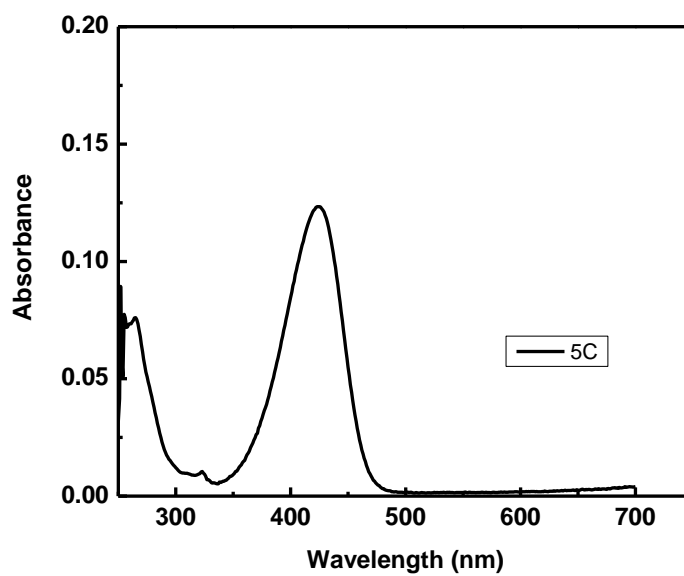


Figure 3.20 UV-visible spectrum of complex 5C.

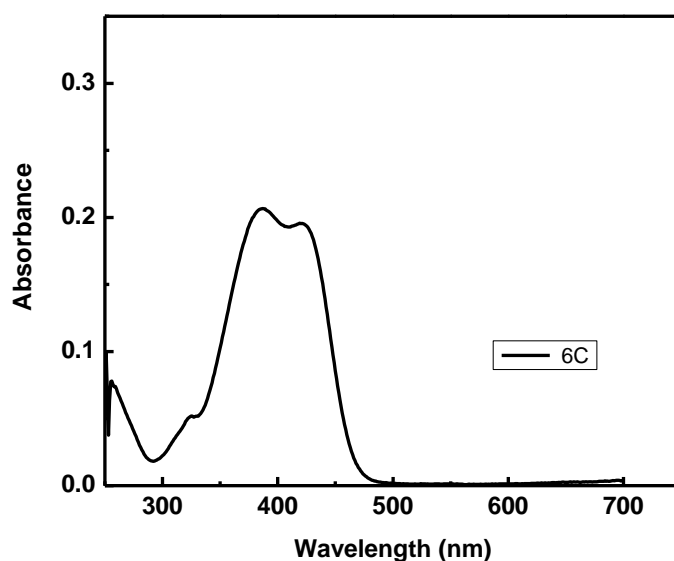


Figure 3.21 UV-visible spectrum of complex 6C.

### 3.3 RESULTS AND DISCUSSION

#### 3.3.1 Spectral analysis

The analytical data shows that the observed values are in good agreement with the theoretical values. The IR spectra of complexes 1C-6C shows that the coordination geometry around the Zn(II), Cd (II) and Hg (II) ions are almost same for all the complexes. The characteristic stretching frequencies of ligand and complexes are shown in Figures (3.2, 3.4, 3.6, 3.8, 3.10, 3.12 and 3.14). The cyano group in complexes remains non-interacting with the metals and shows a strong peak at  $\sim 2210\text{ cm}^{-1}$ . Metal-coordinated cyano groups show the stretching frequency above  $2250\text{ cm}^{-1}$ . The stretching frequencies carbonyl (C=O) group of complexes shows a strong peak at lower frequency ( $\sim 1600\text{ cm}^{-1}$ ) compared free ligand ( $\sim 1660\text{ cm}^{-1}$ ). The stretching frequency of metal-oxygen (M-O) bond in complexes show peak at  $\sim 530\text{ cm}^{-1}$ . The  $^1\text{H}$  NMR spectra of ligand and complexes show peaks at  $\delta$ :  $\sim 3.00$  due to dimethyl amino groups,  $\sim 8.2$  due to (H-C=C-CN-) proton and remaining characteristics peaks of aromatic proton are shown in Figures (3.1, 3.3, 3.5, 3.7, 3.9, 3.11 and 3.13).

### 3.3.2 Linear optical study

The linear absorption spectrum of ligand and complexes in DMSO solution was obtained at room temperature by using the UV-Vis double beam spectrophotometer. Spectra indicate (Figure 3.15-3.21) that negligible linear absorption at 532nm wavelength. Hence, our NLO measurement corresponds to non-resonant nonlinearity.

### 3.3.3 Nonlinear Optical Study

The solutions required for the analysis were prepared by dissolving complexes in dry dimethylsulphoxide with concentration  $1 \times 10^{-3}$  mol/L and filtered off, prepared solutions to remove the undissolved residue.

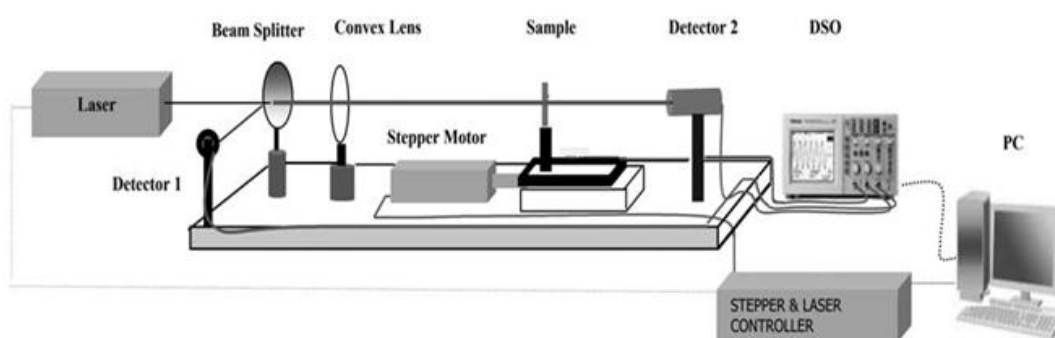


Figure 3.22 The open aperture Z-scan setup.

The open aperture Z-scan experiments (Figure 3.22) were performed to determine nonlinear absorption with input pulse energy of 100  $\mu$ J, which corresponds to on-axis peak irradiance of 2.39  $\text{GW}/\text{cm}^2$ . Open aperture Z-scan curves show minimum transmittance at the focus indicating nonlinear absorption in the complexes. The nonlinear absorption coefficient  $\beta$  of the complexes were calculated using the open aperture curve. The third-order nonlinear absorption coefficient,  $\beta$  (molecular TPA coefficient) of complexes are presented in Table 3.1.

Table 3.1 The values of the two-photon absorption (2PA) coefficients  $\beta$  of the complexes 1C-6C

Complex	$\beta$ ( $\times 10^{-11}$ m/W)
1C	6.6332
2C	6.2557
3C	4.7432
4C	5.0722
5C	4.9894
6C	5.0722

The Open aperture Z-scan (i.e. without aperture in front of the detector) was performed to measure the nonlinear absorption in the sample, which is related to imaginary part of third-order optical susceptibility  $\chi^{(3)}$ . Figures 3.24-3.29 show the open aperture Z-scan curve of the complexes which are symmetric with respect to the focus indicating intensity dependent absorption. The absorption may be due to two photon absorption (TPA), excited state absorption (ESA), reverse saturable absorption (RSA), etc. Nonlinear absorption of nano second pulses can be understood using the five level model (Feng et al. 2005 and Unikrishnan et al. 2002) shown in Figure. 3.23. The relevant energy levels are the singlet levels  $S_0$ ,  $S_1$ , and  $S_2$  and the triplet levels are  $T_1$  and  $T_2$ . Each of these states contains number of vibrational levels. When the molecule is excited by the laser pulse, electrons are initially excited from lowest vibrational level of  $S_0$  to upper vibrational levels of  $S_1$ , where they relax in picoseconds by nonradiative decay. In nano second time scale, singlet transition does not deplete the population of  $S_1$  level appreciably, since atoms excited to  $S_2$  decay to  $S_1$  itself within picoseconds. From  $S_1$ , electrons are transferred to  $T_1$  via intersystem crossing (ISC), from where transitions to  $T_2$  occur. The process ( $S_0 \rightarrow S_1$ ) is known as ground state absorption. The two process ( $S_1 \rightarrow S_2$ ) and ( $T_1 \rightarrow T_2$ ) are known as ESA (Excited state absorption) and if the excited state absorption cross-sections ( $\sigma_s$ ) are larger than that of the ground state ( $\sigma_G$ ) the process is called RSA (reverse saturable absorption). With excitation of laser pulses on the nanosecond scale, which

is true in our case, triplet-triplet transitions are expected to make significant contribution to nonlinear absorption.

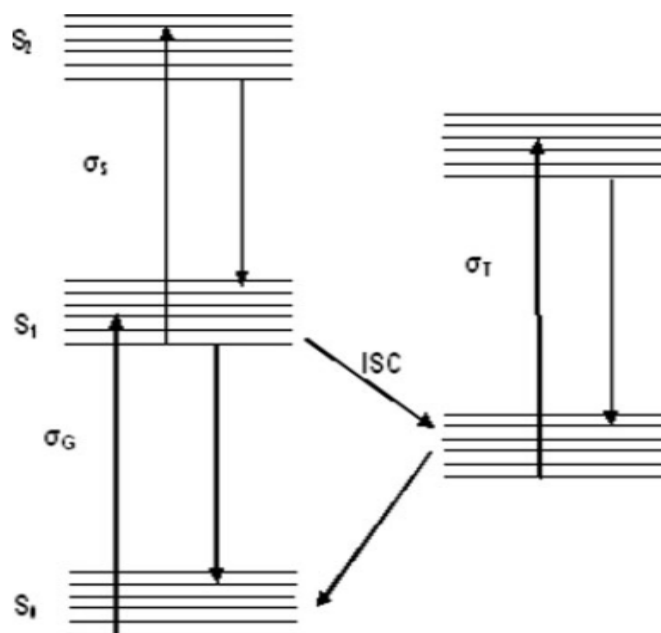


Figure 3.23 Energy level diagram (Five level model) adopted from W. Feng et al. 2005.

Since the residual absorption of the samples at the excitation wavelength is in the vicinity of 50%, the nonlinearity can be expected to arise from a two-step or three-step excitation process involving real excited states, which essentially amounts to reverse saturable absorption (RSA). Genuine two-photon (2PA) and three-photon (3PA) absorption involving virtual states also can take place in the system, but these will be relatively weak compared to the RSA process. However, an excitation where two photons are involved will numerically fit to a two-photon absorption equation irrespective of whether real or virtual states are involved. Similarly, if three photons are involved, it will fit to a three-photon absorption equation. Therefore we tried to fit our data to two-photon and three-photon equations, and the best fit was obtained to the two-photon process described by the nonlinear transmission equation (Sutherland 1996)

$$T = \left( \frac{(1-R)^2 \exp(-\alpha L)}{\sqrt{\pi q_0}} \right) \int_{-\infty}^{\infty} \ln \left[ \sqrt{1 + q_0 \exp(-t^2)} \right] dt \quad \text{----- (3.1)}$$

where  $T$  is the actual  $z$ -dependent sample transmission (product of linear transmission and normalized transmittance), and  $L$  and  $R$  are the length and surface reflectivity of the sample respectively.  $\alpha$  is the linear absorption coefficient.  $q_0$  is given by  $\beta(1 - R)I_0L_{eff}$ , where  $\beta$  is the two-photon absorption coefficient, and  $I_0$  is the on-axis peak intensity.  $L_{eff}$  is given by  $1 - \exp^{-\alpha l}/\alpha$ . The quantity  $\beta$  here is the *effective* 2PA coefficient, as it is a lumped coefficient for the effects of RSA as well as genuine 2PA. The  $\beta$  values of complexes are found to be in the order of  $10^{-11}$  m/W. For comparison, under similar excitation conditions, the measured values of nonlinear absorption coefficient,  $\beta$ , of the complexes are comparable to those obtained for the organic NLO materials viz, polyoxadiazoles (Udayakumar et al. 2006), polythiophenes (Poornesh et al. 2010), copolymer containing oxadiazole and thiophene units (John Kiran et al. 2007), chalcones (Poornesh et al. 2009, John Kiran et al. 2007 and Seetharam Shettigar et al. 2008) and hydrazones (Naseema et al. 2010). In all these materials strong excited state absorption was found to happen concurrently with genuine 2PA, since the samples used had some residual absorption at the excitation wavelength of 532 nm.

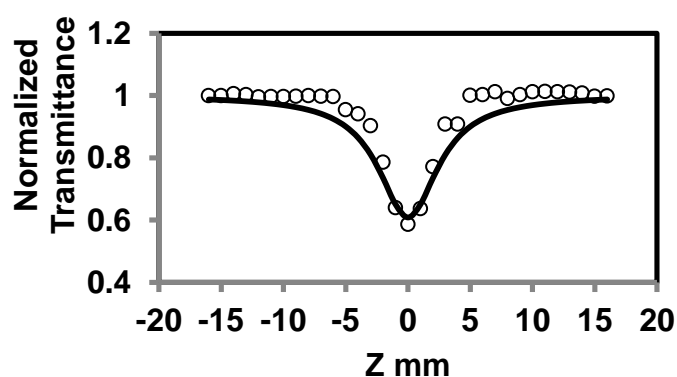


Figure 3.24 Open aperture z-scan curve for complex 1C. The filled circles are measured data points and solid curve is the numerically calculated fit for a two-photon absorption process using Equation 3.1.

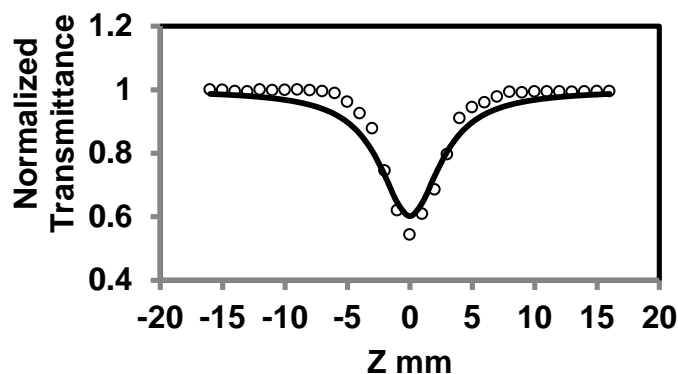


Figure 3.25 Open aperture z-scan curve for complex 2C. The filled circles are measured data points and solid curve is the numerically calculated fit for a two-photon absorption process using Equation 3.1.

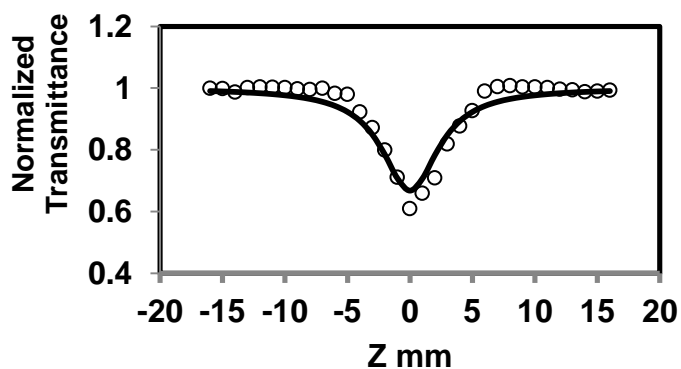


Figure 3.26 Open aperture z-scan curve for complex 3C. The filled circles are measured data points and solid curve is the numerically calculated fit for a two-photon absorption process using Equation 3.1.

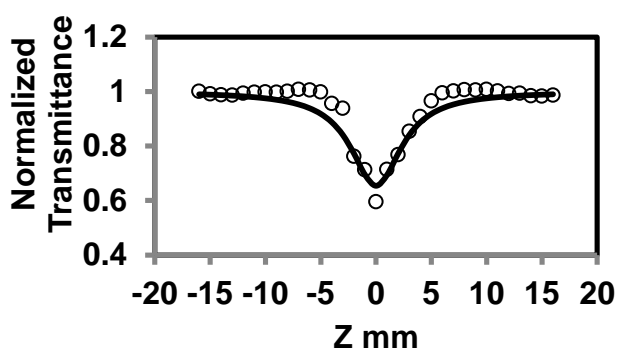


Figure 3.27 Open aperture z-scan curve for complex 4C. The filled circles are measured data points and solid curve is the numerically calculated fit for a two-photon absorption process using Equation 3.1.

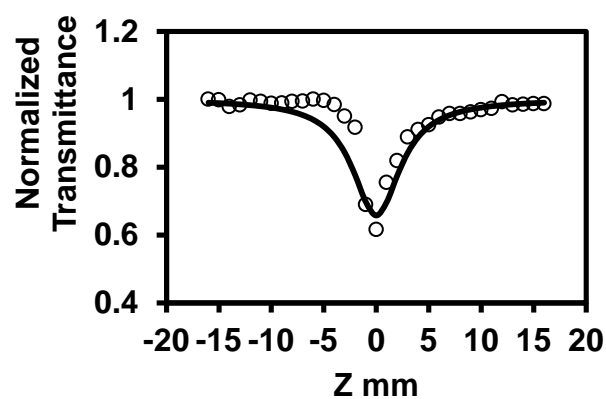


Figure 3.28 Open aperture z-scan curve for complex 5C. The filled circles are measured data points and solid curve is the numerically calculated fit for a two-photon absorption process using Equation 3.1.

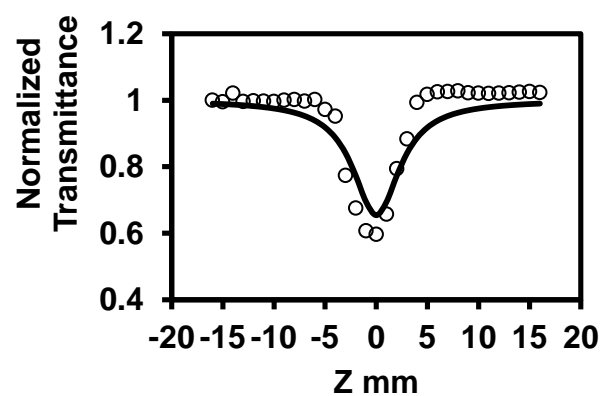


Figure 3.29 Open aperture z-scan curve for complex 6C. The filled circles are measured data points and solid curve is the numerically calculated fit for a two-photon absorption process using Equation 3.1.

---

## CHAPTER 4

### SYNTHESIS AND THIRD-ORDER NONLINEAR OPTICAL STUDIES OF Co(II) AND Pd(I) COMPLEXES

#### *Abstract*

*The third-order optical nonlinearity of the composite film of coordination complexes, [CoL<sub>2</sub>PPh<sub>3</sub>Cl] (7C) and [PdL<sub>2</sub>PPh<sub>3</sub>] (8C) (L<sub>2</sub>=N-(2-pyridyl)-N'-(salicylidene)hydrazine, PPh<sub>3</sub> = triphenylphosphine) and PMMA have been investigated by using Differential Optical Kerr Gate (DOKG) and open aperture Z-scan measurements. Large values of the third-order nonlinear optical susceptibility ( $\chi^{(3)}$ ) of the order of  $10^{-10}$  esu were measured. The nonlinear response time were found to be  $\leq 90$  fs. The single beam Z-scan technique was used to investigate the nonlinear absorption property of the composite near 800 nm. The complexes exhibit saturable absorption. The nonlinear absorption coefficient ( $\beta$ ) of complexes was found to be in the order  $-10^{-11}$  m/W.*

#### 4.1 INTRODUCTION

With the rapid development of optical communication, the novel materials with large and ultrafast nonlinear optical responses are needed for fabricating the ultrafast optical switching and processing devices (Halvorson et al. 1994, Marder et al. 1997, Slepko et al. 2002, Qiyang Chen et al. 2003, Bing Gu et al. 2004). For these purposes, many materials, including semiconductors, polymers, nanomaterials and inorganic materials have been investigated. Among metal-organic compounds, first report being on the NLO properties of a ferrocene derivative (Green et al. 1997). The results show that these compounds possess good NLO properties, it is thought that ferrocenyl conjugated system offers the possibility of electronic communication between terminal subunits, this being of particular interest in nonlinear optics (Mata et al. 2001). The incorporation of transition metal ions introduces more sublevels into the energy hierarchy, thus permitting more allowed electronic transitions and giving larger NLO effects (Chao et al. 1999). Metal ions being excellent templates, can gather organic one dimensional dipolar chromophores around to form predetermined two or three dimensional NLO-phores with various symmetries and charge-transfer

dimensions. By virtue of which the coordinated metal center as well as the presence of polarisable *d* orbital electrons would contribute to the larger nonlinear activity (Long 1995 and Evans and Lin 2002).

From last few decades, scientists have searched for materials with high nonlinear susceptibilities and ultrafast response times. For practical applications, nonlinear materials will also require adequate transparency, stability, speed, and processability (Prasad and Williams 1991). Furthermore, transition-metal based nonlinear optical organometallic fullerene derivatives  $C_{60}M_2$  ( $M = Pd, Pt$ ) shown to exhibit large value  $\chi^{(3)}$  compared to that of  $C_{60}$ . Considering the existence of partial charge transfer from metal atom to  $C_{60}$  molecule, would result in a larger nonlinear optical response (Yanghui Lin et al. 1999). It is shown that the metal–ligand bonding in coordination complexes displays very large molecular hyperpolarizability because of transfer of electron density between the metal atom and the conjugated ligands. These materials possess additional advantages in that they can be grown as crystals as well as being incorporated into polymers such as poly(methyl methacrylate) (PMMA) to fabricate films. Despite a number of previous reports on the NLO properties of various metal complexes in solutions, the interest in ultrafast NLO properties of high quality thin film and crystalline forms of novel metal complexes has been sustained over recent years since they are crucial for any photonic devices.

Based on the above consideration, in this chapter we have described ultrafast and nonresonant nonlinear optical characteristics of metal complexes,  $[CoL_2PPh_3Cl]$  and  $[PdL_2PPh_3]$ , incorporated into PMMA film was studied using time-resolved differential optical Kerr gate (DOKG) and Open aperture Z-scan experiments. From DOKG experiment third-order NLO susceptibility  $\chi^{(3)}$  of composite film of complexes were derived to be in the order of  $10^{-10}$ esu and open aperture Z-scan measurement shows the complexes exhibit saturable absorption property.

## 4.2 EXPERIMENTAL

### 4.2.1 Materials

All the chemicals used were of analytical grade. Solvents were purified and dried according to standard procedure (Vogel 1989). Salicylaldehyde, 2-hydrazinopyridine, anhydrous  $PdCl_2$  and  $CoCl_2 \cdot 6H_2O$  were purchased from Merck

and were used without further purification. Detailed synthesis, characterization of ligand and complexes were reported in the literature (Dileep and Bhat 2010 and Dileep and Bhat 2010).

#### 4.2.2 Synthesis of ligand N-(2-pyridyl)-N'-(salicylidene) hydrazine (L<sub>2</sub>)

A solution of salicylaldehyde (0.03 mmol) in methanol (10 cm<sup>3</sup>) was added to a solution of 2-hydrazinopyridine (0.006g, 0.03 mmol) in methanol (10 cm<sup>3</sup>). The mixture was stirred for 15 minutes at room temperature. The yellow colored solid formed was filtered, washed with water and recrystallized using alcohol.

#### 4.2.3 Synthesis of [CoL<sub>2</sub>PPh<sub>3</sub>Cl] (7C) and [PdL<sub>2</sub>PPh<sub>3</sub>] (8C) complexes.

The complexes 7C and 8C (Figure 4.1 and 4.2) were prepared and characterised according to the following procedure reported elsewhere (Dileep et al. 2010). The complexes were prepared by refluxing a dichloromethane solutions of [CoCl<sub>2</sub>(PPh<sub>3</sub>)<sub>2</sub>] and [PdCl<sub>2</sub>(PPh<sub>3</sub>)<sub>2</sub>] and N-(2-pyridyl)-N'-(salicylidene) hydrazine (L<sub>2</sub>) in a 1:1 molar ratio for 3 h yielding a corresponding complexes 7C and 8C. The complexes were soluble in common organic solvents such as CH<sub>3</sub>OH, CH<sub>3</sub>CN, C<sub>6</sub>H<sub>6</sub>, DMSO and DMF and were found to be thermally stable up to 300 °C.

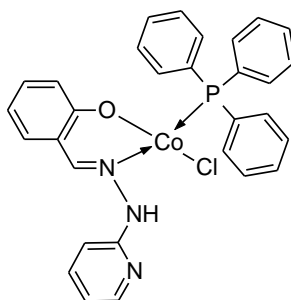


Figure 4.1 Molecular structures of 7C.

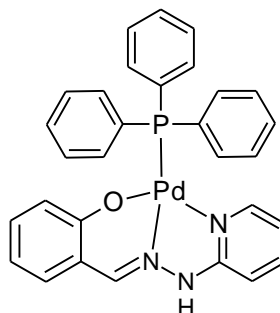


Figure 4.2 Molecular structures of 8C.

## 4.2.4 Nonlinear optical measurements

### 4.2.4.1 Film preparation

In order to prepare composite film of complexes and PMMA, 250 mg of PMMA (M.W. 140,000) and 2 mg of corresponding complexes were dissolved in 2.5 mL of dichlorobenzene (DCB). The concentration of complex in the solution was 1 mmol/L. The solution was mixed thoroughly by stirring and via ultra sonication to ensure homogenous mixing. The solution was subsequently spin coated at 1200 rpm on a glass substrate and the coated film was dried in a vacuum oven at 100°C for about 20 h. The film thickness (L) of composite film was measured to be 1.48  $\mu\text{m}$ , by an Alpha-step surface profiler (Tencor P-10).

### 4.2.4.2 Differential Optical Kerr Gate (DOKG) and Z-scan measurements

The time-resolved DOKG (Sutherland et al. 2003) experiment with a Ti:sapphire laser delivering 90 fs pulses at a repetition rate of 92 MHz at 800 nm was used to investigate the nonlinear response time and third-order nonlinear optical susceptibility of the composite film (Figure 4.5). The laser beam was divided into pump and probe beams with 20:1 intensity ratio by a beam splitter. The polarization of the probe beam was set to 45° with respect to that of the pump beam by a half wave plate. Two beams were focused on the sample by a convex lens of focal length of 7 cm. The time delay of the probe with respect to the pump was controlled by a PC-driven linear translator (PI, M-014.D01). At the zero time delay, the two beams overlap spatially and temporally, and the probe beam polarization rotates due to the birefringence induced in the sample by the pump beam. The pump beam, after passing through the sample, was blocked and the probe beam was passed through a quarter wave plate. The circularly polarized probe beam was then split into two beams by a polarizing cube beam splitter and the two beams were detected by a photo detector pair connected to a lock-in amplifier. CS<sub>2</sub> was used to check the reliability of the setup as well as to estimate the  $\chi^{(3)}$  of the sample. Additionally, single beam Z-scan technique (Sheik-Bahae et al. 1990) was used to investigate the nonlinear absorption property of the composite near 800 nm. An optical parametric oscillator synchronously pumped with a Ti:sapphire laser operating at 92 MHz (800 nm, 110 fs), was employed in the study. The laser beam was focused by a convex lens on the

sample. The beam waist at 800 nm was estimated to be 16  $\mu\text{m}$ , by the knife edge method.

### 4.3 RESULTS AND DISCUSSION

#### 4.3.1 Linear optical studies

The linear absorption spectra of the complexes are displayed in Figure 4.3 and Figure 4.4. The metal complexes shows absorption peaks in the region 250–490 nm. The bands appearing in the region 250–350 nm were assigned to intra ligand charge transfer transitions (ILCT) and less intense bands in the range 390–490 nm corresponds to the d-d forbidden transitions.

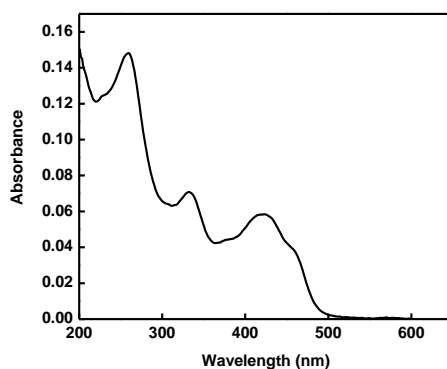


Figure 4.3 Absorption spectrum of the complex 7C.

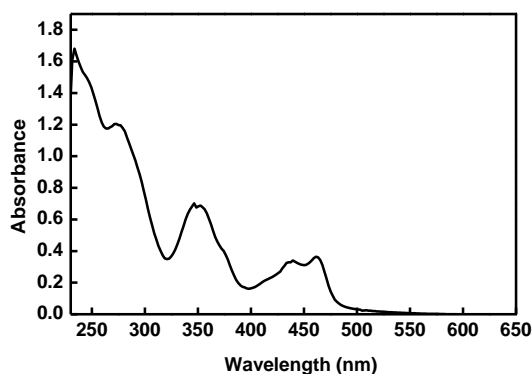


Figure 4.4 Absorption spectrum of the complex 8C.

### 4.3 NONLINEAR OPTICAL STUDIES

#### 4.3.1 Differential Optical Kerr Gate study

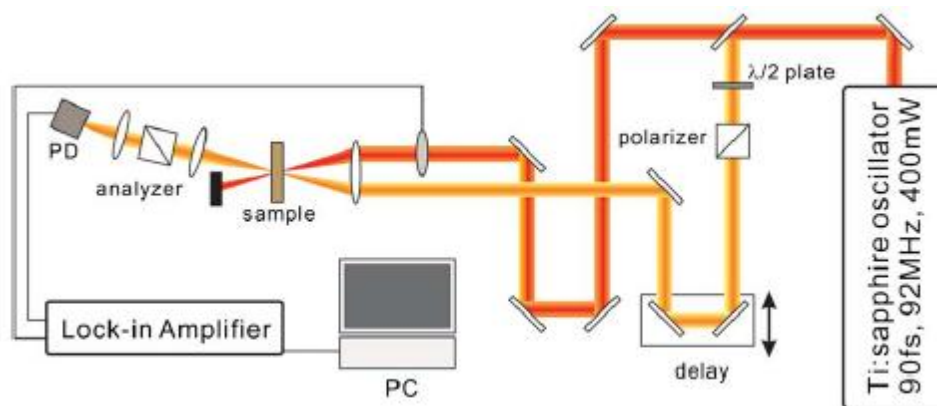


Figure 4.5 Schematic diagram of optical Kerr gate experiment.

The result of the DOKG experiment performed at 800nm is depicted in Figure 4.6 and 4.7. In the present optical Kerr gate experiment, the peak-on-axis intensity was  $\sim 2 \text{ GW/cm}^2$  at the focus. The solid line shows a fit to the experimental data. The optical Kerr effect (OKE) signal is symmetric about the zero time delay, shows that the nonlinear response time of the composite film is faster than or comparable to the laser pulse width used (90 fs). To verify the reliability of our experimental setup, we used  $\text{CS}_2$  as a reference and its optical Kerr effect (OKE) signal was recorded at the same experimental conditions.  $\text{CS}_2$  exhibited a biexponential nonlinear response curve with response times of 0.2 and 1.8 ps, respectively. These values agree well with the previously reported values (Minoshima et al 1991). Maximum signal is observed at zero probe delay times, suggesting that the ultrafast electronic response is the dominant contributor to the observed nonlinearities. The magnitude of  $\chi^{(3)}$  of the complexes can be estimated by comparing its OKE signal amplitude with that of  $\text{CS}_2$  using the following equation (4.1) (Sutherland et al. 2003).

$$\chi_s^{(3)} = \chi_r^{(3)} \left( \frac{I_s}{I_r} \right)^{1/2} \left( \frac{n_s}{n_r} \right)^2 \left( \frac{L_r}{L_s} \right) \frac{\alpha L_s}{\exp\left(-\frac{\alpha L_s}{2}\right) \cdot [1 - \exp(-\alpha L_s)]} \quad (4.1)$$

where the subscripts  $s$  and  $r$  represent the sample and the reference,  $I$  the absolute magnitude of OKE signal,  $n$  the refractive index,  $L$  the thickness and  $\alpha$  the linear absorption coefficient respectively. The  $\chi_r^{(3)}$  of CS<sub>2</sub> was taken as  $1 \times 10^{-13}$  esu (Lee et al. 2009) and that of the composite film of complexes **7C** and **8C** were derived to be  $3.9 \times 10^{-10}$  and  $3.9 \times 10^{-10}$  esu respectively. The  $\chi^{(3)}$  value of the composite film of complexes are one order of magnitude larger than that of an organometallic polymer film measured near 1054 nm using picosecond pulses (Afanasev et al. 2002). Also response time of our investigated complexes are comparable with porous anodized aluminum oxide (AAO) nanostructures (Lee et al. 2009), and chloro(1,10-phenanthroline- $N,N'$ ) (triphenylphosphine)copper(I) complex (Kiran et al 2010) measured under same experimental conditions. Such an ultrafast response and third-order nonlinearity originates in these complexes due to the  $\pi$ -conjugated triphenylphosphine ligand with its electron accepting character ( $d$  to  $\sigma^*$ ) (Horst Kunkely and Arnd Vogler 2002), which facilitating effective electronic communication and CT transitions between metal (Co and Pd) and ligands. This results in the large dipole moment changes between the excited states. The simplest way to achieve this is to have a donor (D) – acceptor (A) system with a bridge (D– $\pi$ –A) which can help the electronic communication between donor and the acceptor. Most metal complexes can be prepared within an above mentioned D– $\pi$ –A system, in which donor and/or acceptor, or the bridge moieties are selectively replaced by an organometallic group. This is because metal complexes possess intense, low energy MLCT, LMCT or intraligand charge transfer (ILCT) excitations. Therefore they can effectively behave as donor and/or acceptor groups of the D– $\pi$ –A system, or as constituents of the polarisable bridge (Poornima et al. 2003). Furthermore, the strength of the NLO properties can be altered by the  $\pi$ -back-donation capacity of the metal ions to the ligands and the increased  $\pi$ -back donation capacity of the metal ions to the ligands may enhance the extension of the electronic  $\pi$  system and improve the NLO properties.

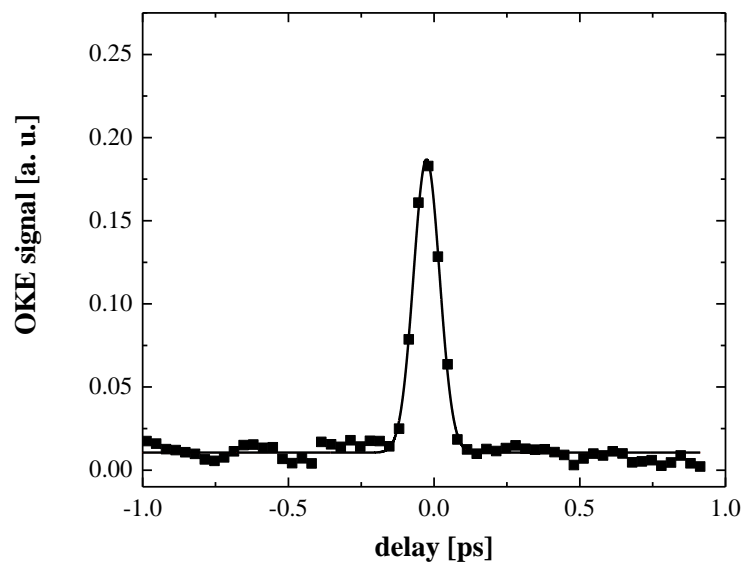


Figure 4.6 Optical Kerr effect signal from 7C/PMMA composite film at 800 nm.

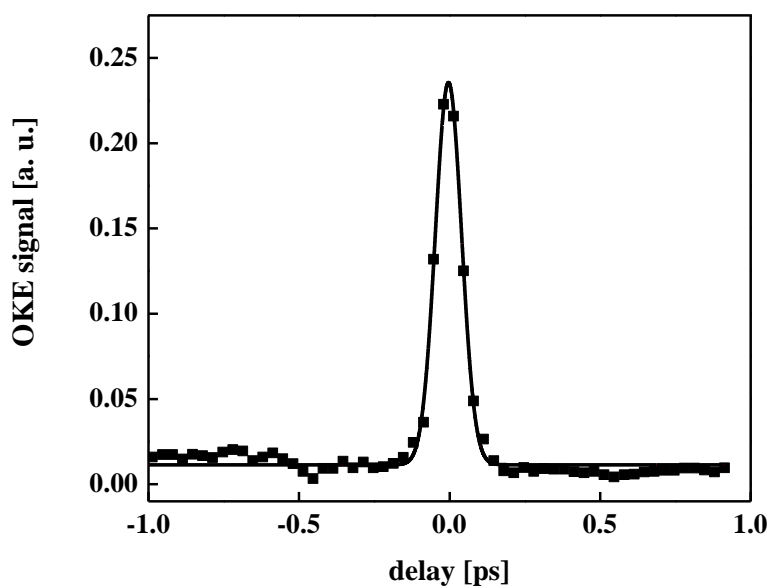


Figure 4.7 Optical Kerr effect signal from 8C/PMMA composite film at 800 nm.

### 4.3.2 Open aperture Z-scan study

Figure 4.8 and 4.9 show the open-aperture Z-scan data obtained for composite film of complexes at 800 nm. The negative nonlinear absorption coefficient of the complexes **7C** and **8C** are found to be  $-3.2 \times 10^{-11}$  m/W and  $-2.3 \times 10^{-11}$  m/W respectively. The open aperture traces could be reproduced in the input intensity range involved in the experiments and also shows that presence of strong saturable absorption. The combined saturable absorption and the two-photon absorption (TPA) coefficient, yielding the total absorption coefficient, can be obtained from a best fitting performed on the experimental data of the OA measurement by the equation with a negative  $\beta \propto -\alpha_0/I_s$ ,

$$\alpha(I) = \alpha_0 \frac{1}{1 + I/I_s} + \beta I \quad \text{-----} \quad (4.2)$$

where the first term describes negative nonlinear absorption such as saturable absorption, and the second term describes positive nonlinear absorption such as reverse saturable absorption and/or two-photon absorption.  $\alpha_0$  is the linear absorption coefficient.  $I$  and  $I_s$  are laser radiation intensity and saturation intensity, respectively.  $\beta$  is the two-photon absorption coefficient. As for open aperture Z-scan, the normalized transmittance may be expressed as (Sheik-Bahae et al 1990),

$$T(z) = \sum_{m=0}^{\infty} \frac{\left[ \frac{-\alpha I_0 L_{eff}}{1 + z^2/z_0^2} \right]^m}{(m+1)} \quad \text{-----} \quad (4.3)$$

where  $L_{eff} = (1 - e^{-\alpha_0 L})/\alpha_0$ ,  $z$  is the longitudinal displacement of the sample from the focus ( $z = 0$ ),  $\alpha$  is the nonlinear absorption coefficient,  $I_0$  is the on-axis peak intensity at the focus,  $L_{eff}$  is the effective interaction length,  $L$  is the sample length,  $z_0$  is the Rayleigh diffraction length. Theoretical fit of the experimental data could be conducted by the substitution of Eq. (4.2) into Eq. (4.3). A direct comparison of this study with those of other organometallic or coordination compounds is rather hard because of different experimental conditions and reports on solutions. As for the

observed negative nonlinear absorption (saturable absorption) in the present case, more work is required to identify the exact phenomena causing such behavior in these materials. Recent literature shows that, some metal complexes have been reported in solution state for saturable absorption phenomenon (Maria Konstantaki et al 2001, Wang et al 2008 and Yan-Ling Wang et al. 2008). These compounds are thermally stable up to 300 °C and exhibit no remarkable laser damage in the intensity range ( $\sim 9 \text{ GWcm}^{-2}$ ) involved in the experiment.

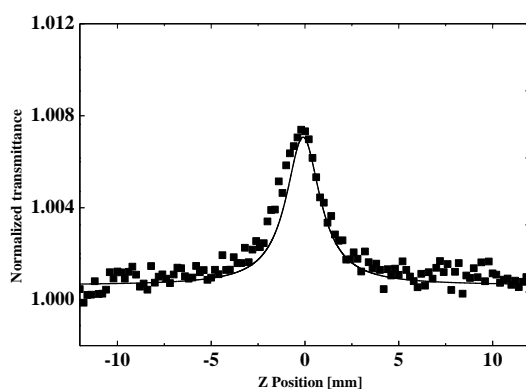


Figure 4.8 Open aperture Z-scan traces for the **7C** in PMMA at 800 nm. The data corresponds to the input intensity  $8\text{GW}/\text{cm}^2$ . The solid line is a theoretical fit of the experimental data.

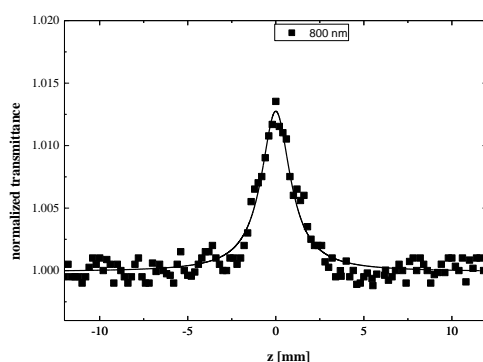


Figure 4.9 Open aperture Z-scan traces for the **8C** in PMMA at 800 nm. The data corresponds to the input intensity  $8\text{GW}/\text{cm}^2$ . The solid line is a theoretical fit of the experimental data.

## CHAPTER 5

### SYNTHESIS, CHARACTERISATION AND THIRD-ORDER NLO STUDIES OF Cu(I) COMPLEXES

#### *Abstract*

*This chapter describes the synthesis, characterization and third-order nonlinear optical studies of copper (I) complexes [Cu(Cl)(N,N'-C<sub>12</sub>H<sub>6</sub>N<sub>2</sub>O<sub>2</sub>)(PPh<sub>3</sub>)], [Cu(Br)(N,N'-C<sub>12</sub>H<sub>6</sub>N<sub>2</sub>O<sub>2</sub>)(PPh<sub>3</sub>)] and [Cu(I)(N,N'-C<sub>12</sub>H<sub>6</sub>N<sub>2</sub>O<sub>2</sub>)(PPh<sub>3</sub>)] abbreviated as [CuClL<sub>3</sub>PPh<sub>3</sub>] (9C), [CuBrL<sub>3</sub>PPh<sub>3</sub>] (10C) and [CuIL<sub>3</sub>PPh<sub>3</sub>] (11C) (L<sub>3</sub> = 1,10-phenanthroline-5,6-dione). Nonlinear optical properties of the complexes are investigated at 532 nm using single beam Z-scan technique employing nanosecond laser pulses. The complexes show optical limiting behaviour due to “effective” two-photon absorption. The values of the effective two-photon absorption (2PA) coefficients ( $\beta$ ) are calculated.*

#### 5.1 INTRODUCTION

Copper (I) ion is an important metal ion, which has a strong tendency to form covalent bonds with ligands containing S or P donor atoms (Hadjikakou et al. 1993 and Hadjidakou et al. 2005, Aslanidis et al 1994 and Aslanidis et al 2002, Karagiannidis et al. 1990 and Akrivos et al. 1993). Intramolecular electron transfer between the two redox sites of metals and ligands often generates characteristic CT bands that are regulated by external stimuli such as photo-irradiation, heat reactions, and redox reactions. Therefore, metal complexes having redox active ligands are feasible candidates for molecular switching (Rei Okamura et al. 2006). Compounds which contain an electron donor and acceptor moiety are frequently characterized by charge transfer (CT) bands in their electronic spectra. Light absorption leads to charge separation which attracts much interest owing to important applications such as artificial photosynthesis (Dixon et al. 2001) and nonlinear optical properties (Pati et al. 2001). It should be quite interesting to modify an organic donor–acceptor molecule by placing a metal ion between the donor and acceptor which then become separate ligands. As a consequence an optical ligand to metal or metal to ligand or ligand to

ligand charge transfers (Vogler and Kunkely 1990 and Vogler and Kunkely 1997) could exist.

Based on this approach, this chapter describes the synthesis, characterisation and the third-order NLO properties of new Cu(I) complexes with two electron withdrawing ligands (1,10-Phenanthroline-5,6-dione and triphenylphosphine (PPh<sub>3</sub>)) using the Z-scan technique. The values obtained for the effective two-photon absorption (2PA) coefficients ( $\beta$ ) are compared to those measured recently for other systems.

## **5.2 EXPERIMENTAL**

### **5.2.1 Materials**

All chemicals used were of analytical grade. Cuprous chloride, Cuprous bromide, Cuprous iodide, 1,10-phenanthroline and triphenylphosphine were procured from Sigma Aldrich. Literature method was used for the preparation of 1,10-phenanthroline-5,6-dione (Catharina et al. 1993).

### **5.2.2 Analysis and measurements**

The <sup>1</sup>H and <sup>31</sup>P spectra were recorded using Bruker AV 400 spectrometer operating at the frequency of 400 MHz. The spectra were recorded in solution with DMSO as internal lock. DMSO and 85% H<sub>3</sub>PO<sub>3</sub> were used as reference and external standards for <sup>1</sup>H and <sup>31</sup>P respectively. Electronic spectra were measured on a Cintra 101 (GBC) UV-Vis double beam spectrophotometer with 0.6 nm resolution in DMSO solution of the complexes in the 200 – 800 nm range. FT - IR spectra were recorded on a Thermo Nicolet Avatar FTIR-ATR spectrometer with 4 cm<sup>-1</sup> resolution in the frequency range 400 – 4000 cm<sup>-1</sup>. The C, H and N contents were determined by Thermoflash EA1112 series elemental analyzer.

### **5.2.3 Z-scan measurement**

Open-aperture Z-scan measurements were performed to determine the nonlinear transmission of laser light through the samples. The Z-scan is a widely used technique developed by Sheik Bahae et al. 1990 to measure optical nonlinearity of materials and the open aperture Z-scan gives information about the nonlinear absorption coefficient. Here a laser beam is focused using a lens and passed through the sample. The beam's propagation direction is taken as the Z-axis, and the focal

point is taken as  $Z = 0$ . The beam will have maximum energy density at the focus, which will symmetrically reduce towards either side for the positive and negative values of  $Z$ . The experiment is done by placing the sample in the beam at different positions with respect to the focus (different values of  $z$ ), and measuring the corresponding light transmission. The graph plotted between the sample position  $z$  and the normalized transmittance of the sample  $T$  (norm.) (transmission normalized to the linear transmission of the sample) is known as the  $z$ -scan curve. The nonlinear absorption coefficient of the sample can be numerically calculated from the  $Z$ -scan curve. In our experiment, DMF solutions of the samples taken in 1 mm cuvettes were irradiated by plane polarized 5 ns laser pulses at 532 nm obtained from the second harmonic output of a Q-switched Nd:YAG laser (MiniLite, Continuum). The laser pulse energy was 100 micro Joules and the beam focal spot radius ( $\omega_0$ ) was 18 microns. These values yield a Rayleigh range ( $z_0$ ) of 1.9 mm, and on-axis peak intensity ( $I_0$ ) of  $6.29 \times 10^9$  W/cm<sup>2</sup>, for a spatially Gaussian beam. The laser was run in the single shot mode using a data acquisition programme, with an approximate interval of 3 to 4 seconds between each pulse. This low repetition rate prevents sample damage and cumulative thermal effects in the medium.

#### 5.2.4 Synthesis of the complexes

##### 5.2.4.1 Synthesis of ligand ( $L_3$ )

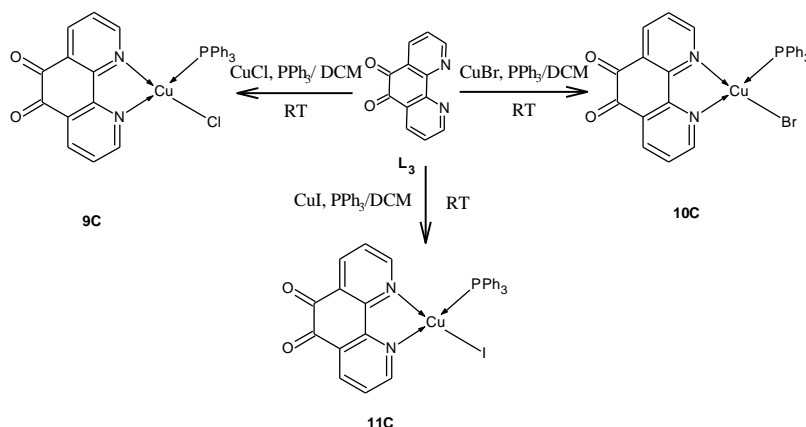
1,10-Phenanthroline (5.00 g) was dissolved in portions during stirring in 30 ml of concentrated sulfuric acid in a 100 ml round bottom flask equipped with a reflux condenser. Sodium bromide (2.50 g) was then added, followed by 15 ml of 70% nitric acid. The mixture was heated to boiling and then kept refluxing for 40 min. heating was then reduced and the reflux condenser removed to allow the bromine vapors to escape during 15 min of gentle boiling. After being cooled the mixture was poured onto 400 g of ice, carefully neutralized to pH 7 with about 150 mL of 10 M sodium hydroxide and allowed to stand for 30 min. The turbid solution was filtered and the solids were extracted with 100 ml of boiling water. The insoluble material was removed from the cooled extract by filtration and the combined aqueous solutions extracted with 5×100 ml dichloromethane. The organic phase was washed with 50 ml of water, dried over anhydrous sodium sulfate, and evaporated under reduced pressure. The crystalline residue was recrystallized from 400 ml of toluene to give the

dione: yield: 45%, yellow-orange needles, MP 257 °C. Anal.Calc for  $C_{12}H_6O_2N_2$ : C, 68.75; H, 2.84; N, 13.25. Found: C, 68.26; H, 2.17; N, 13.19%.

#### 5.2.4.2 Synthesis of $[CuClL_3PPh_3]$ (9C)

CuCl (235 mg, 2.378mmol) was added to the DCM ( $20\text{ cm}^3$ ) solution of  $PPh_3$  (623mg, 2.378mmol) and 1,10-phenanthroline-5,6-dione (500mg, 2.378mmol). After the reaction mixture was stirred 3hrs at room temperature under nitrogen, the blackish brown solid formed was filtered off, washed with ethanol, diethyl ether and dried under reduced pressure (scheme 5.1). Yield: 70%, M.P:  $> 300^\circ\text{C}$ .

Anal.Calc for  $C_{30}H_{21}O_2CuClN_2P$ : C, 63.08; H, 3.67; N, 4.90. Found: C, 57.43; H, 3.40; N, 4.48%. NMR:  $\delta\text{H}$  (400 MHz; DMSO- $d_6$ ; referenced with respect to DMSO- $d_6$ ). There are two sets of aromatic protons found:  $^1\text{H}$ , 7.20-7.80 $\delta$ , from 1,10-phenanthroline-5,6-dione and  $PPh_3$  (Figure 5.2) and  $^{31}\text{P}$  NMR: 28.54  $\delta$ ; referenced with respect to  $\text{H}_3\text{PO}_4$  (Figure 5.3). UV-vis:  $\lambda_{\text{max}}$ /nm (DMF)  $\sim 350$  and 278.7 (Figure 5.10). IR:  $\nu_{\text{max}}$ / $\text{cm}^{-1}$  1684.1 (C=O), 1569.2 (C=N) (Figure 5.1).



Scheme 5.1 Synthetic Scheme for complexes 9C-11C.

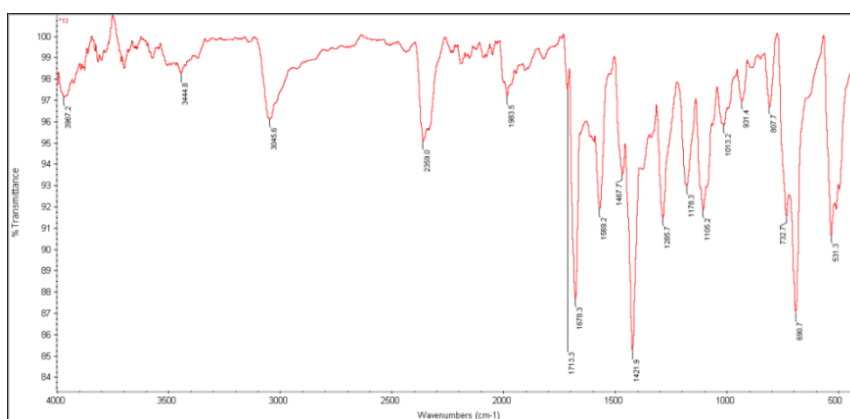
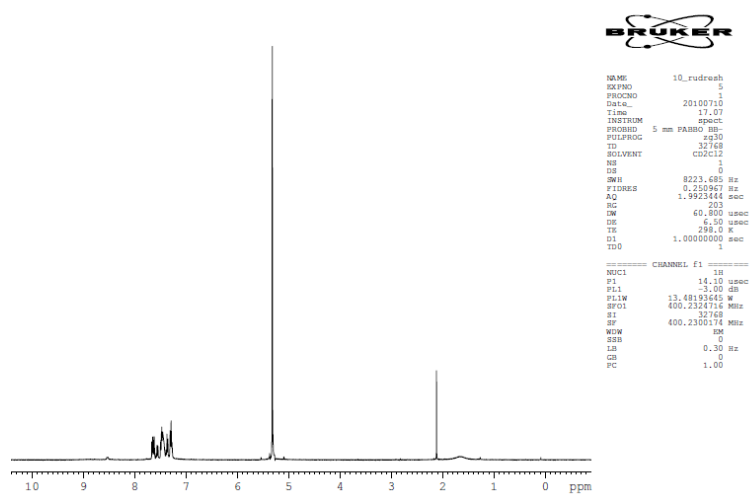
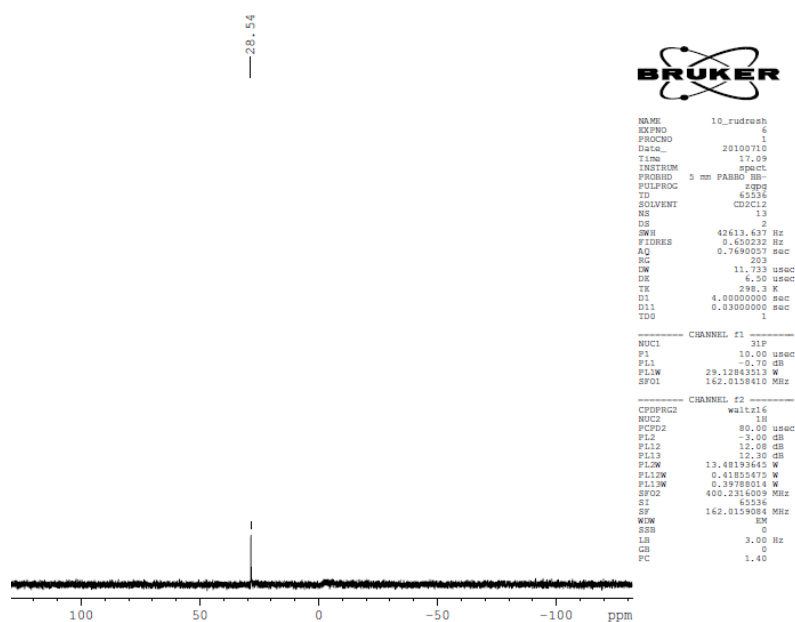


Figure 5.1 IR spectrum of complex 9C.

Figure 5.2  $^1\text{H}$  NMR spectrum of complex 9C.Figure 5.3  $^{31}\text{P}$  NMR spectrum of complex 9C.

### 5.2.4.3 Synthesis of $[\text{CuBrL}_3\text{PPh}_3]$ (10C)

Synthesis of this complex is accomplished following a similar procedure taking CuBr (341mg, 2.378mmol) in place of CuCl. The blackish brown solid formed was filtered off, washed with ethanol, diethyl ether and dried under reduced pressure (scheme 5.1). Yield:70%. M.P:  $> 300^\circ\text{C}$ .

Anal.Calc for  $C_{30}H_{21}O_2CuBrN_2P$ : C, 58.52; H, 3.41; N, 4.54. Found: C, 57.43; H, 3.40; N, 4.48%. NMR:  $\delta$ H (400 MHz; DMSO- $d_6$ ; referenced with respect to DMSO- $d_6$ ). There are two sets of aromatic protons found:  $^1$ H, 7.20-7.80 $\delta$ , from 1,10-phenanthroline-5,6-dione and  $PPh_3$  (Figure 5.5) and  $^{31}$ P NMR: 26.49  $\delta$ ; referenced with respect to  $H_3PO_4$  (Figure 5.6). UV-vis:  $\lambda_{max}/nm$  (DMF)  $\sim$ 350 and 278.7 (Figure 5.11). IR:  $\nu_{max}/cm^{-1}$  1684.1 (C=O), 1566.8 (C=N) (Figure 5.4).

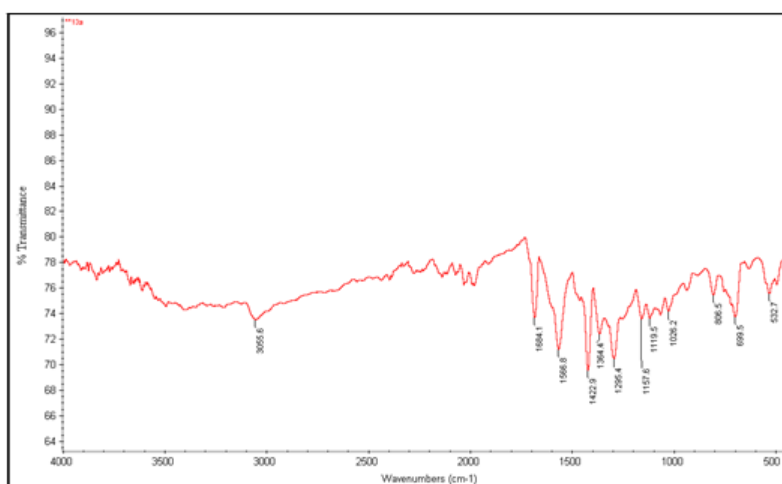


Figure 5.4 IR spectrum of complex 10C.

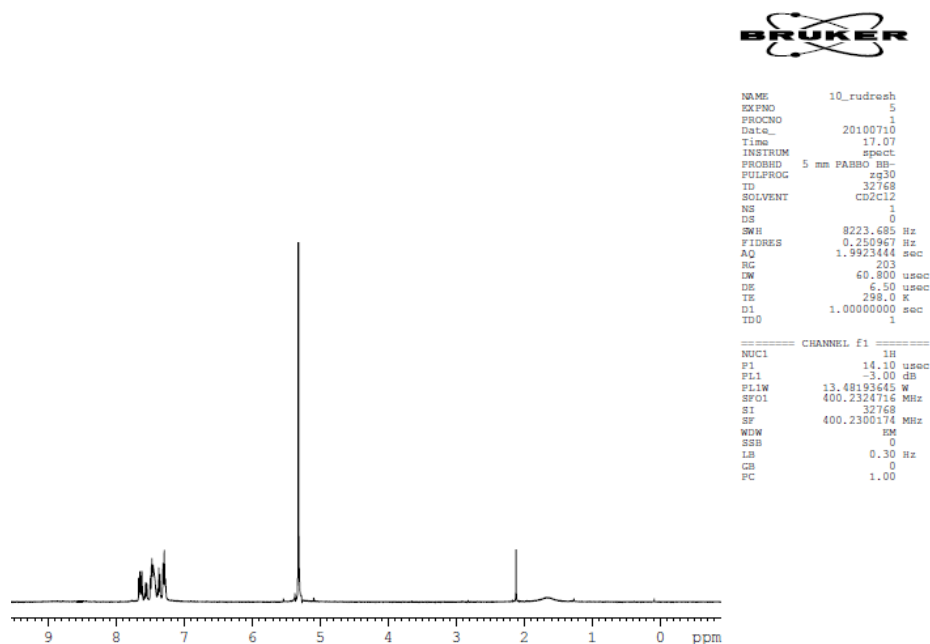


Figure 5.5  $^1$ H NMR spectrum of complex 10C.

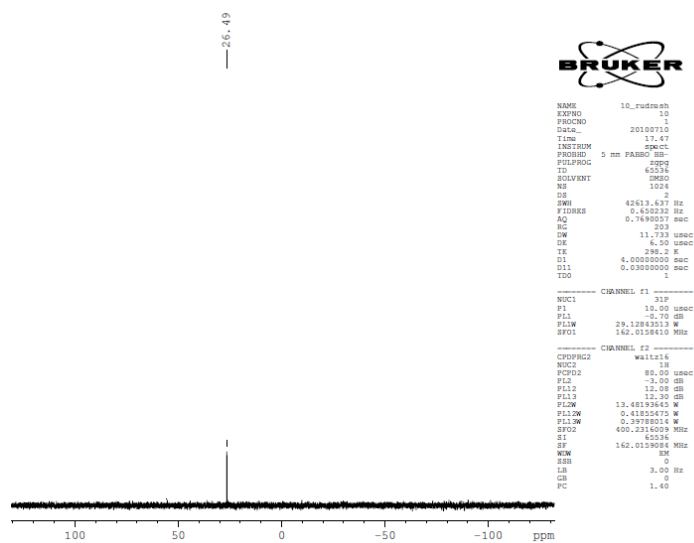


Figure 5.6  $^{31}\text{P}$  NMR spectrum of complex 10C.

#### 5.2.4.4 Synthesis of $[\text{CuIL}_3\text{PPh}_3]$ (11C)

Synthesis of this complex is accomplished following a similar procedure taking CuI (452mg, 2.378mmol) in place of CuCl. The blackish brown solid formed was filtered off, washed with ethanol, diethyl ether and dried under reduced pressure (scheme 5.1). Yield: 70%. M.P.:  $> 300^\circ\text{C}$ .

Anal. Calc for  $\text{C}_{30}\text{H}_{21}\text{O}_2\text{CuIN}_2\text{P}$ : C, 54.37; H, 3.16; N, 4.22. Found: C, 53.26; H, 3.17; N, 4.19%. NMR:  $\delta\text{H}$  (400 MHz; DMSO- $d_6$ ; referenced with respect to DMSO- $d_6$ ). There are two sets of aromatic protons found:  $^1\text{H}$ , 7.20-7.80 $\delta$ , from 1,10-phenanthroline-5,6-dione and  $\text{PPh}_3$  (Figure 5.8) and  $^{31}\text{P}$  NMR: 26.54  $\delta$ ; referenced with respect to  $\text{H}_3\text{PO}_4$  (Figure 5.9). UV-vis:  $\lambda_{\text{max}}/\text{nm}$  (DMF)  $\sim 350$  and 278.3 (Figure 5.12). IR:  $\nu_{\text{max}}/\text{cm}^{-1}$  1678.3 (C=O), 1569.2 (C=N) (Figure 5.7).

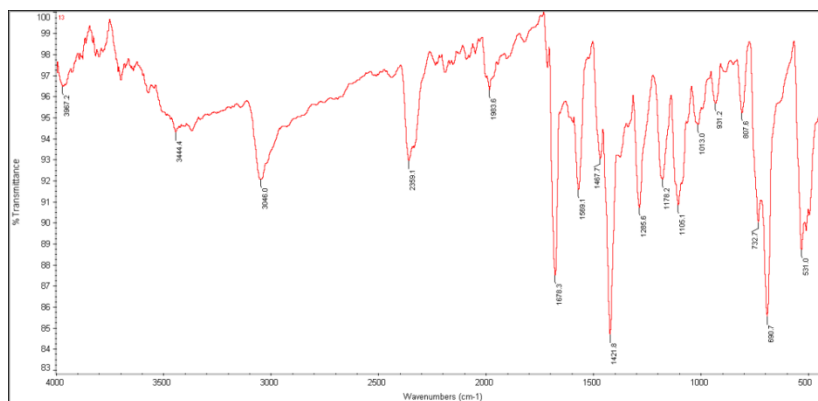
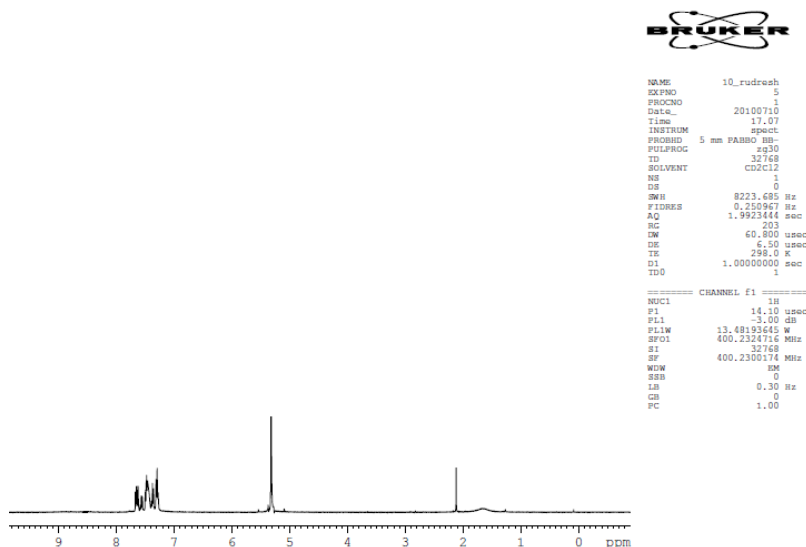
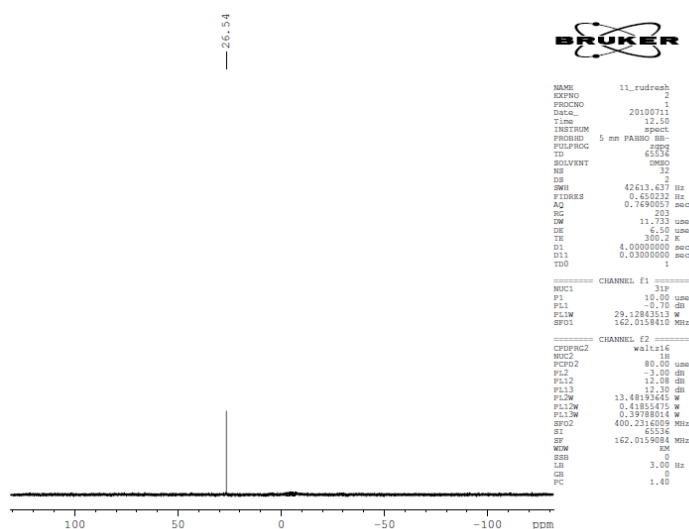


Figure 5.7 IR spectrum of complex 11C.

Figure 5.8  $^1\text{H}$  NMR spectrum of complex 11C.Figure 5.9  $^{31}\text{P}$  NMR spectrum of complex 11C.

## 5.3 RESULTS AND DISCUSSION

### 5.3.1 Spectral analysis of complexes

The electronic spectra of the complexes are shown in Figure 5.10-5.12. Spectrum of complexes are dominated by one main absorption band in the region 275-290 nm and a shoulder near 350nm which are ascribed to the intra-ligand ( $\pi$  to  $\pi^*$ ) transitions of triphenylphosphine. Also absence of bands ( $d-d$ ) above 400 nm shows  $d^{10}$  electronic configuration of copper (Cu(I)) in the complexes. Since Cu(I) is

reducing as well as oxidizing, MLCT and LMCT transitions will be occur at relatively low energies (Horst et al. 2002). Free triphenylphosphine shows a broad band with  $\lambda_{\max}$  at 262 nm (Kubicki et al. 2001). The IR spectra of complexes show absorption bands at near  $1680\text{ cm}^{-1}$ , assigned to the CO stretching of 1,10-phenanthroline-5,6-dione coordinated to the metal through the nitrogen atoms. These bands are slightly higher shifted wavenumber compared with free uncomplexed 1,10-phenanthroline-5,6-dione ( $1672\text{ cm}^{-1}$ ). The complexes show absorption bands at near  $1430\text{ cm}^{-1}$ ,  $1090\text{ cm}^{-1}$ ,  $720\text{ cm}^{-1}$ ,  $690\text{ cm}^{-1}$  and  $520\text{ cm}^{-1}$  due to triphenylphosphine ligand. The appearance of the  $\nu(\text{CO})$  bands (at  $1684.1\text{ cm}^{-1}$  and  $1679\text{ cm}^{-1}$ ) in the IR spectrum and the absence of bands in the region of 400 to 500 nm in the electronic absorption spectrum of complexes further confirms that 1,10-phenanthroline-5,6-dione is bound to Cu(I) with the N,N'-chelate (Rei Okamura et al. 2006). The magnetic susceptibility measurement show that the complexes are diamagnetic and copper is in +1 oxidation state. From the above spectral information, it was confirmed that structure of the complexes are distorted tetrahedral ( $d^{10}$ ) and copper atom bonding with nitrogen atoms of 1,10-phenanthroline-5,6-dione.

### 5.3.2 Linear optical study

The electronic spectra of the complexes are shown in Figure 5.10-5.12. Spectrum of complexes are dominated by one main absorption band in the region 275-290 nm and a shoulder near 350nm which are ascribed to the intra-ligand ( $\pi$  to  $\pi^*$ ) transitions of triphenylphosphine. Also absence of bands ( $d-d$ ) above 400 nm shows  $d^{10}$  electronic configuration of copper (Cu(I)) in the complexes. Since Cu(I) is reducing as well as oxidizing, MLCT and LMCT transitions will be occur at relatively low energies (Horst et al. 2002). Free triphenylphosphine shows a broad band with  $\lambda_{\max}$  at 262 nm (Kubicki et al. 2001).

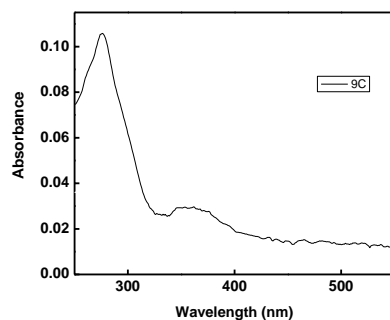


Figure 5.10 UV-visible spectrum of complex 9C.

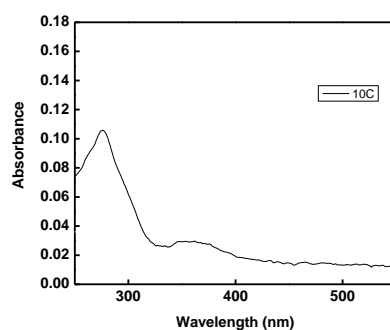


Figure 5.11 UV-visible spectrum of complex 10C.

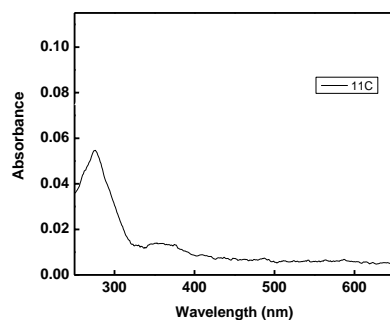


Figure 5.12 UV-visible spectrum of complex 11C.

### 5.3.3 Nonlinear optical studies

The solutions required for the analysis were prepared by dissolving complexes in dichloromethane with concentration  $1 \times 10^{-3}$  mol/L and filtered off, prepared solutions to remove the undissolved residue.

The open aperture z-scan curves of complexes are given in Figure 5.13-5.15. Curves shows an increase in absorption when the sample is nearing the beam focus,

indicating a reverse saturable absorption behaviour. Numerically, a TPA type process described by the nonlinear transmission equation (5.1) (Sutherland et al.1996).

$$T = \left( \frac{(1-R)^2 \exp(-\alpha L)}{\sqrt{\pi q_0}} \right) \int_{-\infty}^{\infty} \ln \left[ \sqrt{1 + q_0 \exp(-t^2)} \right] dt \text{----- (5.1)}$$

The above equation was found to give the best fit to the data. Here T is the actual z-dependent sample transmission (product of linear transmission and normalized transmittance) and L and R are the length and surface reflectivity of the sample respectively.  $\alpha$  is the linear absorption coefficient.  $q_0$  is given by  $\beta(1-R)I_0L_{eff}$ , where  $\beta$  is the TPA coefficient, and  $I_0$  is the on-axis peak intensity.  $L_{eff}$  is given by  $1 - \exp^{-\alpha l/\alpha}$ . The values of the two-photon absorption (2PA) coefficients  $\beta$  of the complexes are presented in the Table 5.1. For comparison, under similar excitation conditions, the NLO materials such as Cu nanocomposite glasses (Karthikeyan et al. 2008) and Schiff base complexes of N, N'-bis(2-hydroxynaphthalidene)phenylene-1,2-diamine ligand with metal M (M= Ni(II), Zn(II) and Fe (III)) (Sampath Kumar et al. 2010) had given TPA coefficient values of  $10^{-10}$  to  $10^{-12}$  m/W. Similarly, Bismuth nanorods (Sivaramakrishnan et al. 2007) and CdS quantum dots (Kurian et al. 2007) gave values of  $5.3 \times 10^{-11}$  m/W and  $1.9 \times 10^{-9}$  m/W respectively. In all these materials strong excited state absorption will happen concurrently with genuine TPA at the excitation wavelength of 532 nm, and hence the effect is usually referred to as an effective TPA process. The coefficients calculated are therefore effective TPA coefficients.

The Open aperture Z-scan (i.e. without aperture in front of the detector) was performed to measure the nonlinear absorption in the sample, which is related to imaginary part of third-order optical susceptibility  $\chi^{(3)}$ . Figures 5.13-5.15 show the open aperture Z-scan curve of the complexes which are symmetric with respect to the focus indicating intensity dependent absorption. The absorption may be due to two photon absorption (TPA), excited state absorption (ESA), reverse saturable absorption (RSA), etc. Nonlinear absorption of nano second pulses can be understood using the five level model (Feng et al. 2005 and Unikrishnan et al. 2002) shown in Figure. 3.25. The relevant energy levels are the singlet levels  $S_0$ ,  $S_1$ , and  $S_2$  and the triplet levels are  $T_1$  and  $T_2$ . Each of these states contains number of vibrational levels. When the

molecule is excited by the laser pulse, electrons are initially excited from lowest vibrational level of  $S_0$  to upper vibrational levels of  $S_1$ , where they relax in picoseconds by nonradiative decay. In nanosecond time scale, singlet transition does not deplete the population of  $S_1$  level appreciably, since atoms excited to  $S_2$  decay to  $S_1$  itself within picoseconds. From  $S_1$ , electrons are transferred to  $T_1$  via intersystem crossing (ISC), from where transitions to  $T_2$  occur. The two processes ( $S_1 \rightarrow S_2$ ) and ( $T_1 \rightarrow T_2$ ) are known as ESA (Excited state absorption) and if the excited state absorption cross-sections ( $\sigma_s$ ) are larger than that of the ground state ( $\sigma_G$ ) the process is called RSA (reverse saturable absorption). With excitation of laser pulses on the nanosecond scale, which is true in our case, triplet-triplet transitions are expected to make significant contribution to nonlinear absorption.

Table 5.1 The values of the two-photon absorption (2PA) coefficients  $\beta$  of the complexes 9C-11C.

Complex	$\beta$ ( $\times 10^{-11}$ m/W)
9C	2.4
10C	2.4
11C	7.7

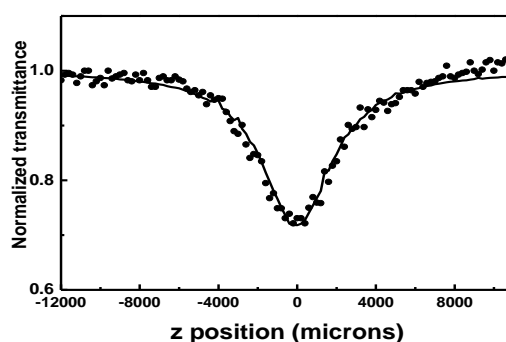


Figure 5.13 Open aperture z-scan curve for complex 9C. The filled circles are measured data points and solid curve is the numerically calculated fit for a two-photon absorption process using Equation 5.1.

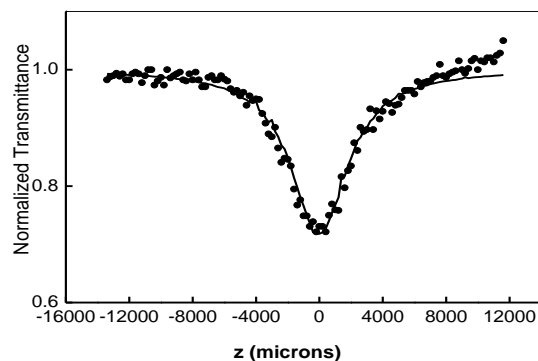


Figure 5.14 Open aperture z-scan curve for complex 10C. The filled circles are measured data points and solid curve is the numerically calculated fit for a two-photon absorption process using Equation 5.1.

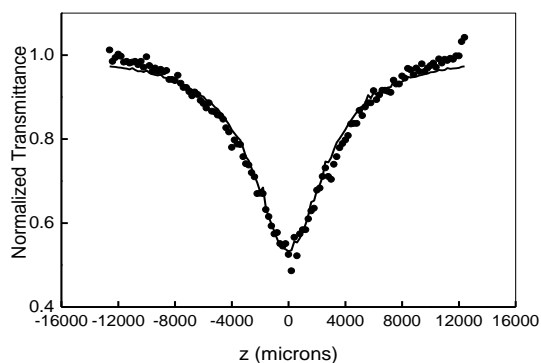


Figure 5.15 Open aperture z-scan curve for complex 11C. The filled circles are measured data points and solid curve is the numerically calculated fit for a two-photon absorption process using Equation 5.1.



---

## CHAPTER 6

### SYNTHESIS, CHARACTERIZATION AND THIRD-ORDER NONLINEAR OPTICAL STUDIES OF BORON CHALCONE COMPLEXES

#### *Abstract*

*This chapter describes the synthesis, characterization and third-order nonlinear optical studies of boron 2-hydroxychalcone complexes. From the analytical and spectral studies, the formation of the complexes was confirmed. Nonlinear optical properties of the complexes are investigated at 532 nm using single beam Z-scan technique employing nanosecond laser pulses. The complexes show optical limiting behaviour due to ‘‘effective’’ two-photon absorption. The values of the effective two-photon absorption (2PA) coefficients ( $\beta$ ) are calculated. Strong donor-acceptor mechanism (‘‘push-pull’’ system), is the responsible factors for this observed third-order nonlinear optical response.*

#### 6.1 INTRODUCTION

At present there is great interest in materials with high nonlinear optical (NLO) responses both from the scientific and technological points of view. Although inorganic solids such as  $\text{LiNbO}_3$  and  $\text{KH}_2\text{PO}_4$  have traditionally attracted the widest attention (Kurtz 1972), it has been recognized that molecular materials possess superior NLO characteristics such as faster response times, lower dielectric constants and enhanced NLO responses (Dalton et al. 1995, Benning 1995 and Verbiest et al 1997). Along this line, chalcones which are naturally occurring substances with fungicidal (Lorimer and Perry 1994), antibacterial (Li et al. 1995) and carcinogenic (Makita et al. 1996) activities, as well as potent anti-platelet agents (Lin et al. 1996) have been recently used as NLO materials (Wang et al. 1994 and Twieg and Jain 1983) due to the fact that they exhibit fluorescent properties as sensors (Jiang et al. 1994).

The 2'-hydroxychalcones, in particular, have been widely used in coordination chemistry with different metals such as Co(II), Ni(II), Cu(II) (Palaniandavar and Natarajan 1980), Sn(IV) (Biradar et al. 1976) and Te(IV) (Rudzinski et al. 1983). Moreover, the efficiency of the 2'-hydroxychalcones to form complexes has been used

to identify different metal cations like Ge(IV) (Birdar et al. 1975), Al(III) (Debattista and Pappano 1997), Eu(III) (Montana et al. 1998) and Be(II) (Raghava Naidu 1975).

In this chapter we have described, the formation of “push-pull” boron complexes derived from chalcones. These derivatives present a  $\pi$  system, in which boron atom can act as electron acceptor and a substituent at the *para* position acting as the electron donor/acceptor atom with potential NLO properties.

## 6.2 EXPERIMENTAL

### 6.2.1 Materials

All the chemicals used were of analytical grade. Solvents were purified and dried according to standard procedure (Vogel 1989). 2-hydroxyacetophenone, benzaldehyde derivatives and boron trifluoride etherate were purchased from Sigma Aldrich.

### 6.2.2 Analysis and measurements

The  $^1\text{H}$  and  $^{19}\text{F}$  spectra were recorded using Bruker AV 400 spectrometer operating at the frequency of 400 MHz. The spectra were recorded in chloroform solvent. Electronic spectra were measured on a Cintra 101 (GBC) UV-Vis double beam spectrophotometer with 0.6 nm resolution in DMSO solution of the complexes in the 200 – 800 nm range. FT - IR spectra were recorded on a Thermo Nicolet Avatar FTIR-ATR spectrometer with  $4\text{ cm}^{-1}$  resolution in the frequency range 400 – 4000  $\text{cm}^{-1}$ . The C, H and N contents were determined by Thermoflash EA1112 series elemental analyser.

### 6.2.3 Z-scan measurement

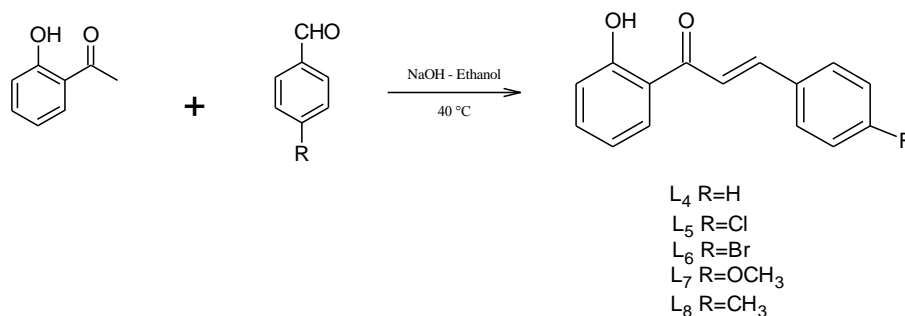
Open-aperture Z-scan measurements were performed to determine the nonlinear transmission of laser light through the samples. The Z-scan is a widely used technique developed by Sheik Bahae et al. (1990) to measure optical nonlinearity of materials, and the open aperture Z-scan gives information about the nonlinear absorption coefficient. Here a laser beam is focused using a lens and passed through the sample. The beam's propagation direction is taken as the z-axis, and the focal point is taken as  $z = 0$ . The beam will have maximum energy density at the focus, which will symmetrically reduce towards either side for the positive and negative values of z. The experiment is done by placing the sample in the beam at different

positions with respect to the focus (different values of  $z$ ), and measuring the corresponding light transmission. The graph plotted between the sample position  $z$  and the normalized transmittance of the sample  $T$  (norm.) (transmission normalized to the linear transmission of the sample) is known as the  $z$ -scan curve. The nonlinear absorption coefficient of the sample can be numerically calculated from the  $z$ -scan curve. In our experiment, DMF solutions of the samples taken in 1 mm cuvettes were irradiated by plane polarized 5 ns laser pulses at 532 nm obtained from the second harmonic output of a Q-switched Nd:YAG laser (MiniLite, Continuum). The laser pulse energy was 100 micro Joules and the beam focal spot radius ( $\omega_0$ ) was 18 microns. These values yield a Rayleigh range ( $z_0$ ) of 1.9 mm, and on-axis peak intensity ( $I_0$ ) of  $6.29 \times 10^9 \text{ W/cm}^2$ , for a spatially Gaussian beam. The laser was run in the single shot mode using a data acquisition programme, with an approximate interval of 3 to 4 seconds between each pulse. This low repetition rate prevents sample damage and cumulative thermal effects in the medium.

### 6.3 SYNTHESIS OF BORON CHALCONE COMPLEXES

#### 6.3.1 General procedure for synthesis of ligands ( $L_4$ - $L_8$ )

Ligands ( $L_4$ - $L_8$ ) were prepared by adding sodium hydroxide to the 2-hydroxyacetophenone and benzaldehyde derivatives in ethanol at  $40^\circ\text{C}$ . The mixture was stirred for 20 min and cooled to room temperature. The precipitate that formed was dissolved in water. The solution was made slightly acidic using dilute hydrochloric acid. The precipitate formed was filtered, washed with ice cold ethanol, and dried over calcium chloride to obtain crude chalcones. These were purified by column chromatography, eluting with a mixture of ethyl acetate and hexane (Scheme 6.1).



Scheme 6.1 Synthetic scheme for synthesis of ligands ( $L_4$ - $L_8$ )

### 6.3.1.1 Synthesis of (2-Hydroxyphenyl)-3-phenyl-2-propen-1-one ( $L_4$ )

Sodium hydroxide, 3.85 g (96.36 mmol), in 10 ml water, was added to the ethanolic solution (30 ml) of 2-hydroxyacetophenone 3.20g (23.5 mmol), the mixture was stirred for 20 minutes. To this solution 2.50g (23.5 mmol) of benzaldehyde in 20 ml of ethanol was added at 40°C. The mixture was stirred for 2hrs and cooled to room temperature. The precipitate that formed was dissolved in 100 ml of water. The solution was made slightly acidic using dilute hydrochloric acid (50% 20 ml). The precipitate formed was filtered, purified by column chromatography, eluting with a mixture of ethyl acetate and hexane (1:9). Yield 80%.  $^1\text{H}$  NMR (400MHz,  $\text{CDCl}_3$ ), [ $\delta$ , ppm]: 12.79 (1H, s), 7.94-7.90 (3H, m), 7.68-7.64 (4H, m), 7.52-7.48 (1H, m), 7.45-7.42 (2H, m), 7.04-7.02 (1H, dd) and 6.96-6.92 (1H, m) (Figure 6.1). IR ( $\text{cm}^{-1}$ ): 1635.5, 1565.8, 1199.4, 734.2 (Figure 6.2). Anal calcd for  $\text{C}_{15}\text{H}_{12}\text{O}_2$ , C 80.33%, H 5.35%. Found C 80.20 %, H 5.23%. UV-vis:  $\lambda_{\text{max}}$ /nm (DCM) 317.48 (Figure 6.26).

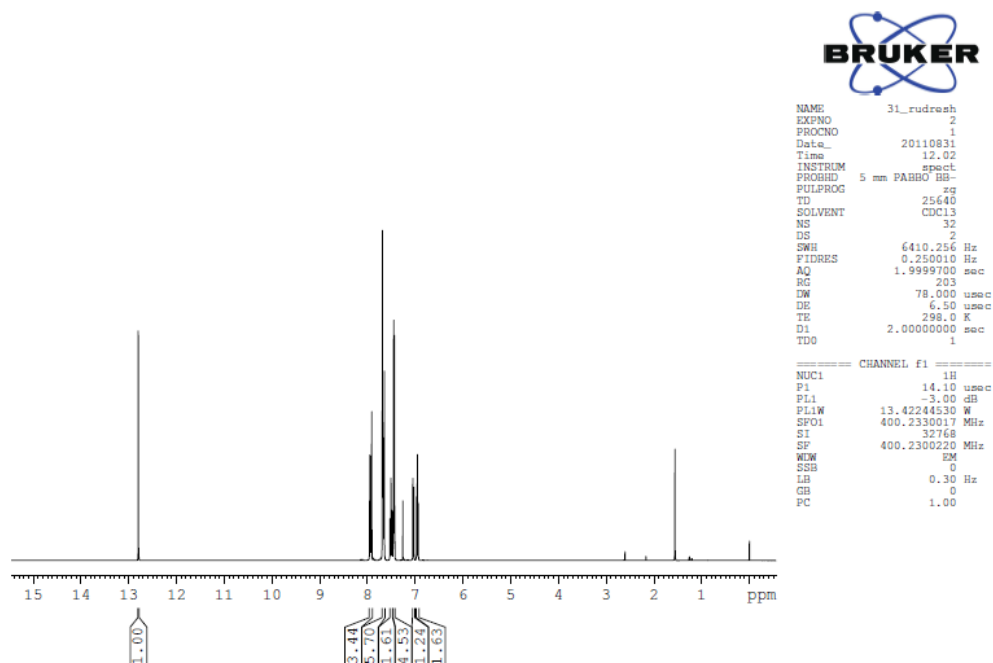


Figure 6.1  $^1\text{H}$  NMR spectrum of ligand  $L_4$

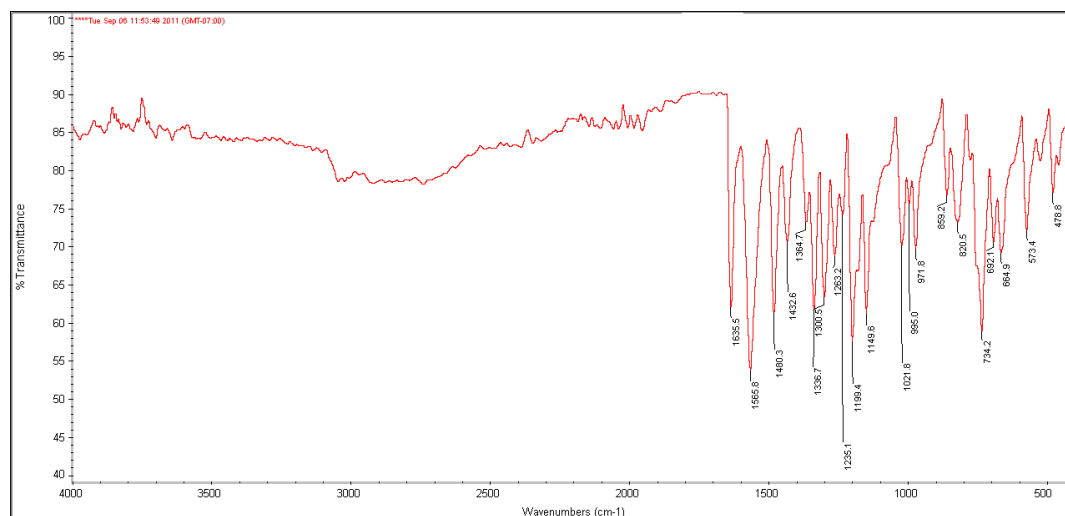
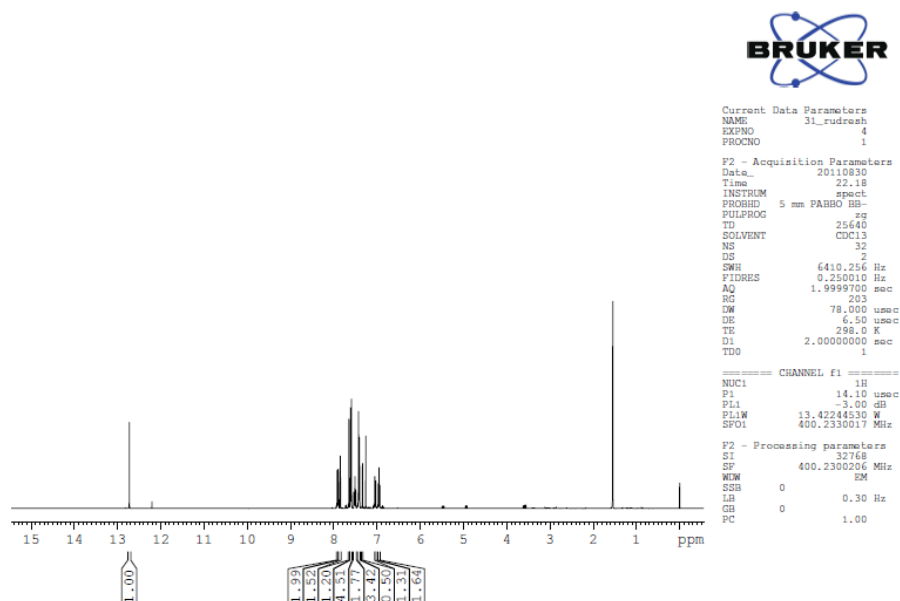
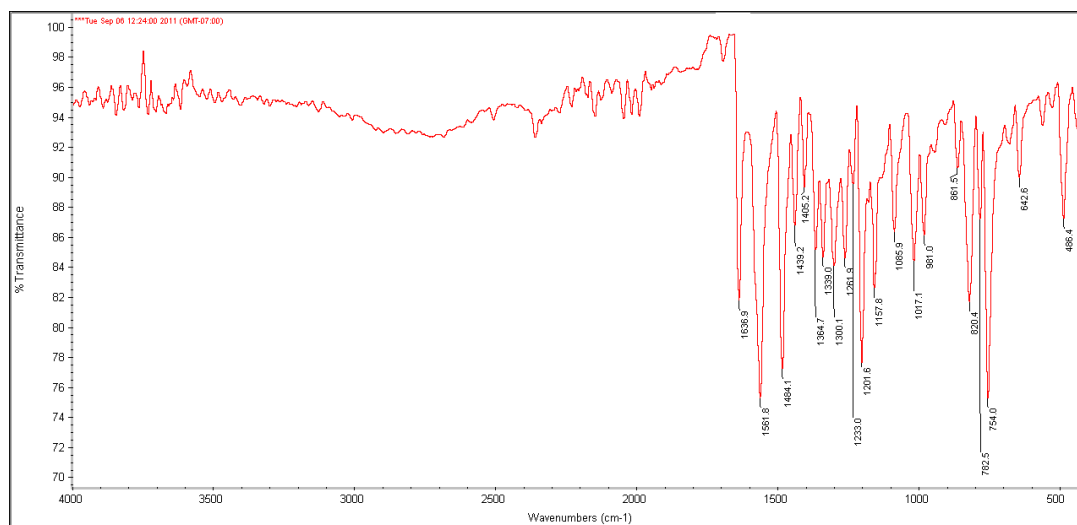


Figure 6.2 IR spectrum of ligand **L<sub>4</sub>**.

### 6.3.1.2 Synthesis of (2-Hydroxyphenyl)-3-(4-chlorophenyl)-2-propen-1-one (**L<sub>5</sub>**)

The compound **L<sub>5</sub>** was prepared following the same procedure used for **L<sub>4</sub>**. Sodium hydroxide, 3.61 g (90.34 mmol), in 10 ml water, was added to the ethanolic solution (30 ml) of 2-hydroxyacetophenone 3.00g (22.03 mmol), the mixture was stirred for 20 minutes. To this solution 4.02g (28.64 mmol) of 4-chlorobenzaldehyde in 20 ml of ethanol was added at 40°C. The mixture was stirred for 2hrs and cooled to room temperature. The precipitate that formed was dissolved in 100 ml of water. The solution was made slightly acidic using dilute hydrochloric acid (50% 20 ml). The precipitate formed was filtered, washed with ice cold ethanol, and dried over calcium chloride to obtain crude chalcone. It was purified by column chromatography, eluting with a mixture of ethyl acetate and hexane (1:9). Yield 75%. <sup>1</sup>H NMR (400MHz, CDCl<sub>3</sub>), [δ, ppm]: 12.72 (1H, s), 7.92-7.88 (1H, m), 7.84 (1H, s), 7.64 (1H, s), 7.61-7.58 (2H, m), 7.53-7.49 (1H, m), 7.43-7.40 (2H, m), 7.05-7.02 (1H, m) and 6.97-6.93 (1H, m) (Figure 6.3). IR (cm<sup>-1</sup>): 1636.9, 1561.8, 1201.6, 754.0 (figure 6.4). Anal calcd for C<sub>15</sub>H<sub>11</sub>ClO<sub>2</sub>, C 69.63%, H 4.25%. Found C 69.43 %, H 4.18%. UV-vis: λ<sub>max</sub>/nm (DCM) 322.3 (Figure 6.27).

Figure 6.3  $^1\text{H}$  NMR spectrum of ligand  $\text{L}_5$ Figure 6.4 IR spectrum of ligand  $\text{L}_5$ .

### 6.3.1.3 Synthesis of (2-Hydroxyphenyl)-3-(4-bromophenyl)-2-propen-1-one ( $\text{L}_6$ )

The compound  $\text{L}_6$  was prepared following the same procedure used for  $\text{L}_4$ . Sodium hydroxide, 1.77 g (44.3 mmol), in 8 ml water, was added to the ethanolic solution (20 ml) of 2-hydroxyacetophenone 1.47g (10.8 mmol), the mixture was stirred for 20 minutes. To this solution 2.0g (10.8 mmol) of 4-bromobenzaldehyde in 20 ml of ethanol was added at  $40^\circ\text{C}$ . The mixture was stirred for 2hrs and cooled to room temperature. The precipitate that formed was dissolved in 100 ml of water. The solution was made slightly acidic using dilute hydrochloric acid (50% 20 ml). The

precipitate formed was filtered, washed with ice cold ethanol, and dried over calcium chloride to obtain crude chalcone. It was purified by column chromatography, eluting with a mixture of ethyl acetate and hexane (1:9). Yield 75%.  $^1\text{H}$  NMR (400MHz,  $\text{CDCl}_3$ ), [ $\delta$ , ppm]: 12.72 (1H, s), 7.91-7.89 (1H, dd), 7.87-7.83 (1H, d), 7.66-6.62 (1H, d), 7.59-7.49 (5H, m), 7.04-7.02 (1H, dd) and 6.97-6.93 (1H, m) (Figure 6.5). IR (KBr,  $\text{cm}^{-1}$ ): 1639.3, 1561.6, 1201.8, 750.1 (Figure 6.6). Anal calcd for  $\text{C}_{15}\text{H}_{11}\text{BrO}_2$ , C 59.42%, H 3.62%. Found C 59.23 %, H 3.40%. UV-vis:  $\lambda_{\text{max}}$ /nm (DCM) 361.95 (Figure 6.28).

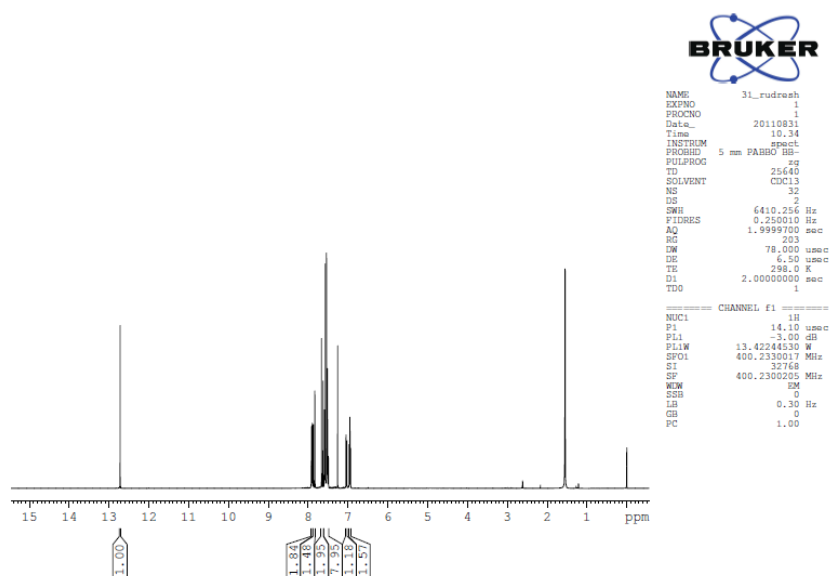


Figure 6.5  $^1\text{H}$  NMR spectrum of ligand  $\text{L}_6$

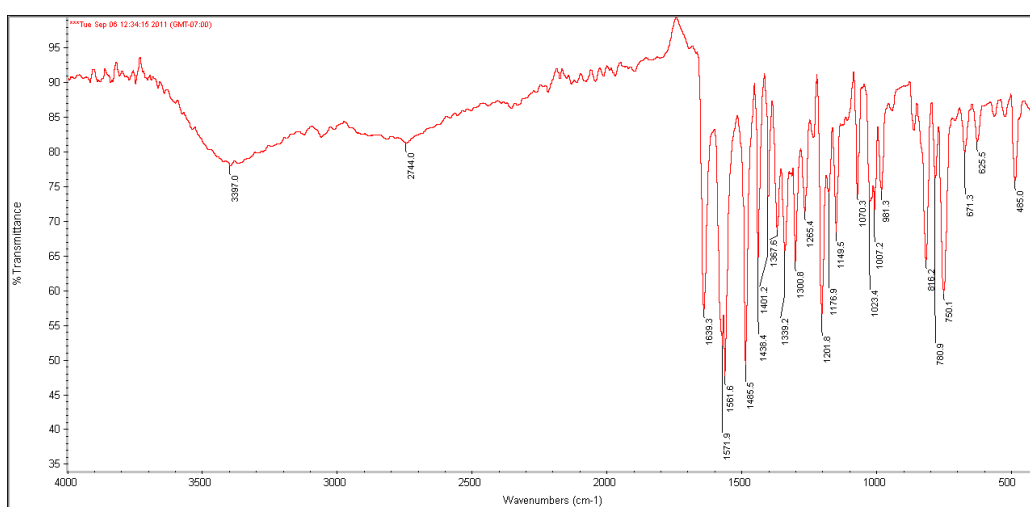


Figure 6.6 IR spectrum of ligand  $\text{L}_6$

#### 6.3.1.4 Synthesis of (2-Hydroxyphenyl)-3-(4-methoxyphenyl)-2-propen-1-one ( $L_7$ )

The compound  $L_7$  was prepared following the same procedure used for  $L_4$ . Sodium hydroxide, 2.40g (60.2 mmol), in 8 ml water, was added to the ethanolic solution (20 ml) of 2-hydroxyacetophenone 2.0g (14.68 mmol), the mixture was stirred for 20 minutes. To this solution 2.0g (14.68 mmol) of 4-methoxybenzaldehyde in 20 ml of ethanol was added at 40°C. The mixture was stirred for 2hrs and cooled to room temperature. The precipitate that formed was dissolved in 100 ml of water. The solution was made slightly acidic using dilute hydrochloric acid (50% 20 ml). The precipitate formed was filtered, washed with ice cold ethanol, and dried over calcium chloride to obtain crude chalcone. It was purified by column chromatography, eluting with a mixture of ethyl acetate and hexane (1:9). Yield 75%.  $^1\text{H}$  NMR (400MHz,  $\text{CDCl}_3$ ), [ $\delta$ , ppm]: 12.91 (1H, s), 7.93-7.88 (2H, m), 7.65-7.61 (2H, m), 7.56-7.52 (1H, d), 7.50-7.46 (1H, m), 7.03-7.01 (1H, m), 6.97-6.91 (3H, m) and 3.86 (3H, s) (Figure 6.7). IR ( $\text{cm}^{-1}$ ): 1634.3, 1558.2, 1203.4, 757.3 (Figure 6.8). Anal calcd for  $\text{C}_{15}\text{H}_{14}\text{O}_3$ , C 75.57%, H 5.50%. Found C 75.32 %, H 5.22%. UV-vis:  $\lambda_{\text{max}}$ /nm (DCM) 365.91 (Figure 6.29).

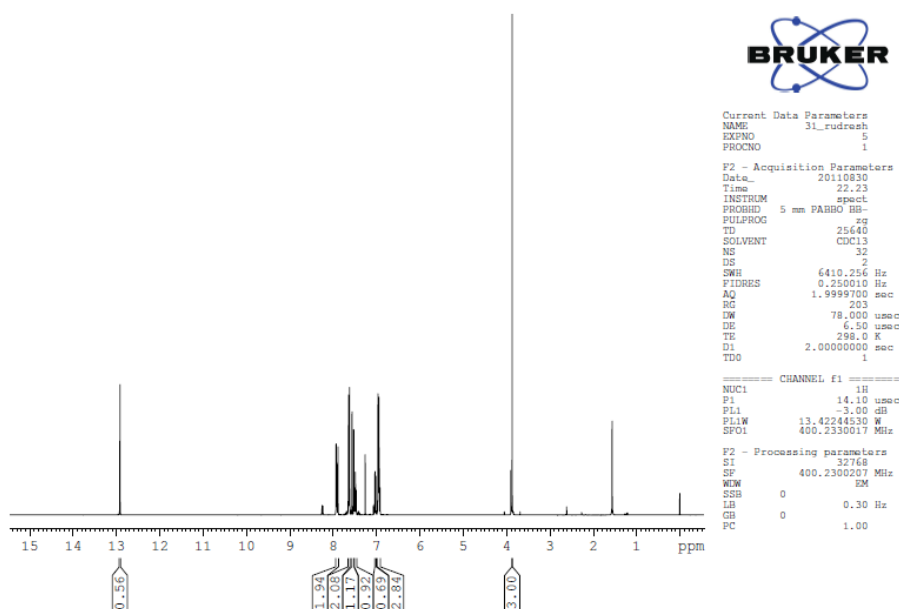


Figure 6.7  $^1\text{H}$  NMR spectrum of ligand  $L_7$

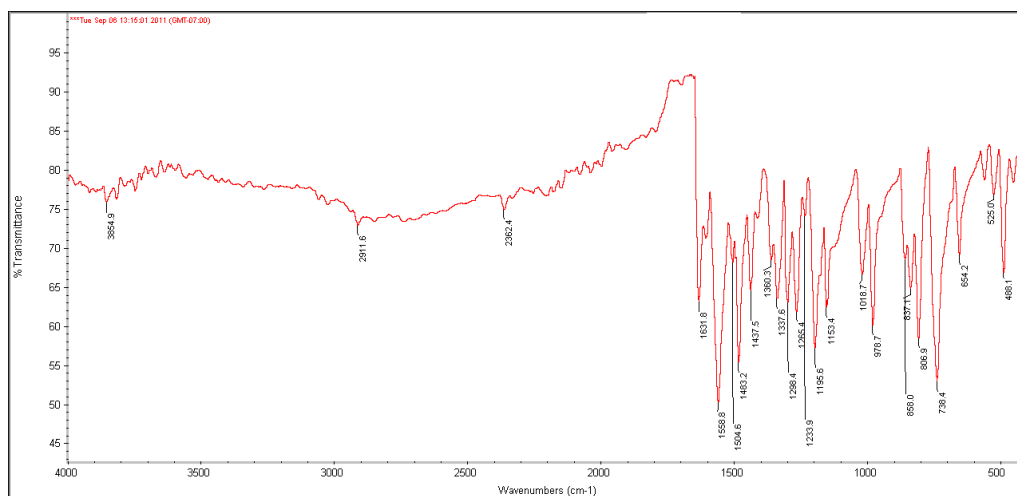
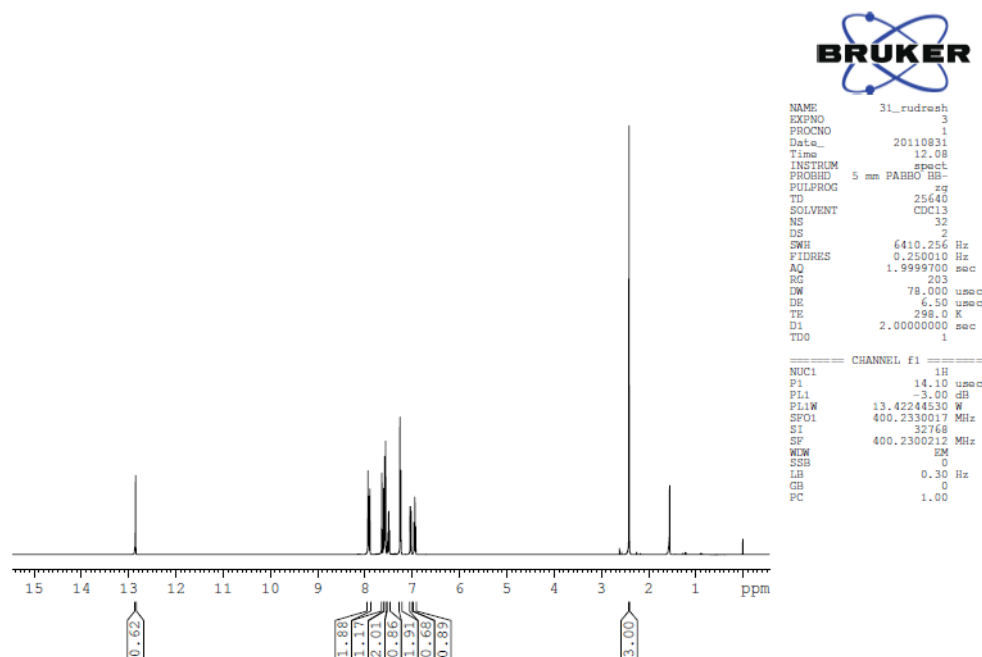
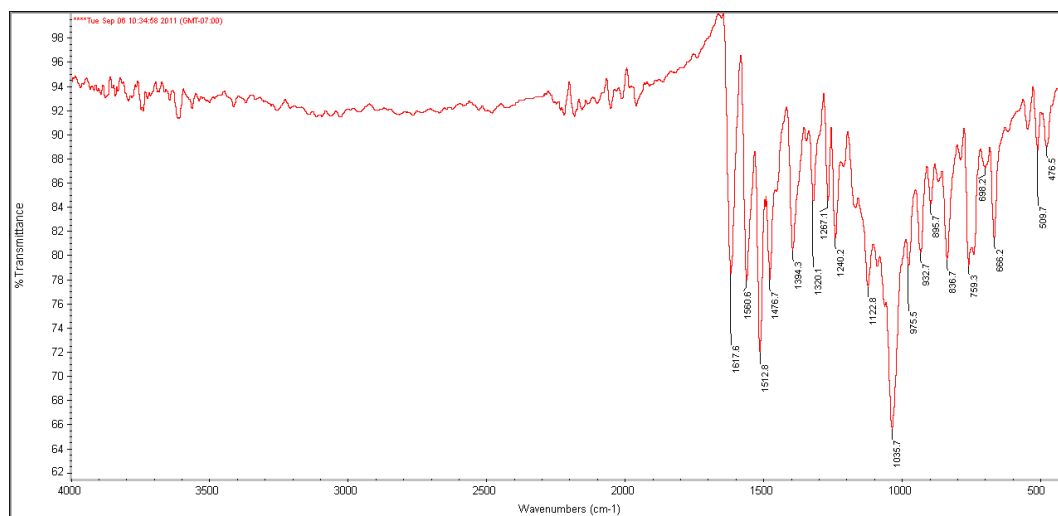


Figure 6.8 IR spectrum of ligand **L<sub>7</sub>**

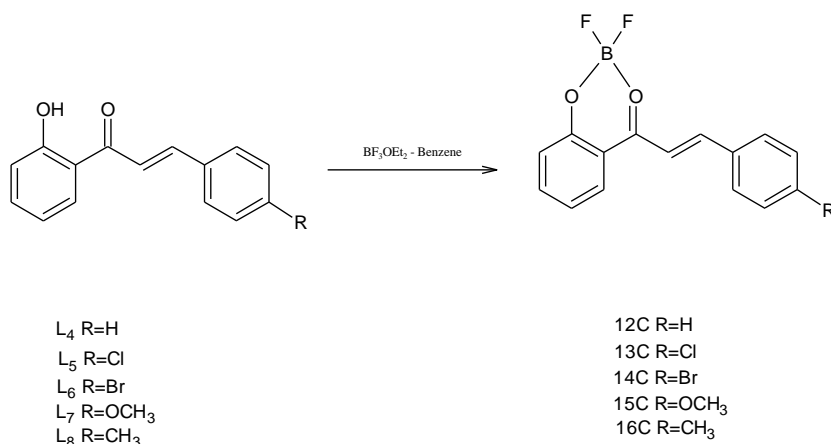
#### 6.3.1.5 Synthesis of (2-Hydroxyphenyl)-3-(4-methylphenyl)-2-propen-1-one (**L<sub>8</sub>**)

The compound **L<sub>8</sub>** was prepared following the same procedure used for **L<sub>4</sub>**. Sodium hydroxide, 2.73g (68.32 mmol), in 8 ml water, was added to the ethanolic solution (20 ml) of 2-hydroxyacetophenone 2.26g (16.66 mmol), the mixture was stirred for 20 minutes. To this solution 2.0g (16.66 mmol) of 4-methylbenzaldehyde in 20 ml of ethanol was added at 40°C. The mixture was stirred for 2 hrs and cooled to room temperature. The precipitate that formed was dissolved in 100 ml of water. The solution was made slightly acidic using dilute hydrochloric acid (50% 20 ml). The precipitate formed was filtered, washed with ice cold ethanol, and dried over calcium chloride to obtain crude chalcone. It was purified by column chromatography, eluting with a mixture of ethyl acetate and hexane (1:9). Yield 75%. <sup>1</sup>H NMR (400MHz, CDCl<sub>3</sub>), [δ, ppm]: 12.85 (1H, s), 7.93-7.89 (2H, m), 7.64-7.60 (1H, d), 7.57-7.56 (2H, m), 7.51-7.47 (1H, m), 7.25-7.23 (2H, d), 7.03-7.01 (1H, s), 6.96-6.92 (1H, s) and 2.40 (3H, s) (Figure 6.9). IR (cm<sup>-1</sup>): 1631.8, 1558.8, 1195.6, 738.4 (Figure 6.10). Anal calcd for C<sub>15</sub>H<sub>14</sub>O<sub>2</sub>, C 80.64%, H 5.87%. Found C 80.62%, H 5.02%. UV-vis: λ<sub>max</sub>/nm (DCM) 331.0 (Figure 6.30).

Figure 6.9  $^1\text{H}$  NMR spectrum of ligand  $\text{L}_8$ Figure 6.10 IR spectrum of ligand  $\text{L}_8$ 

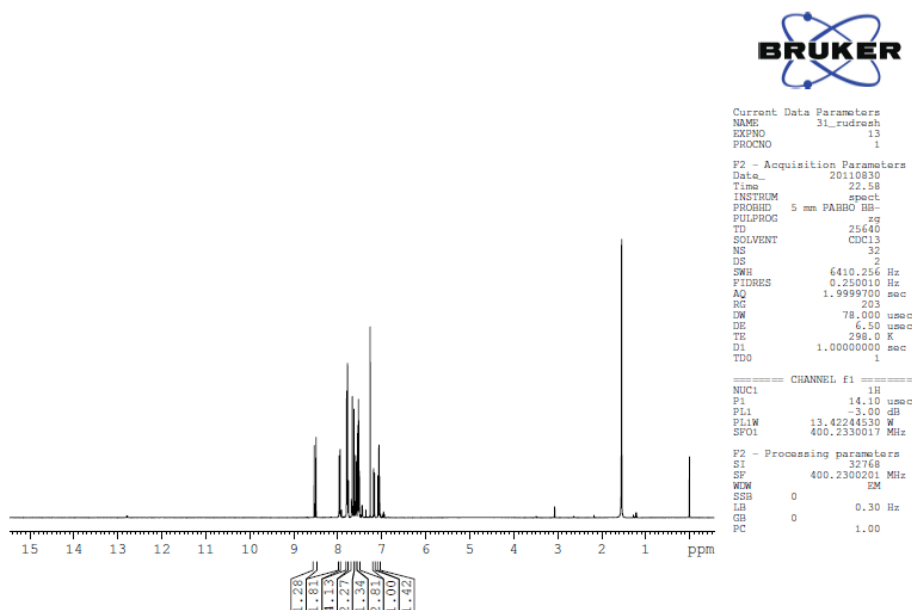
### 6.3.2 General method for the synthesis of boron chalcone complexes (12C-16C)

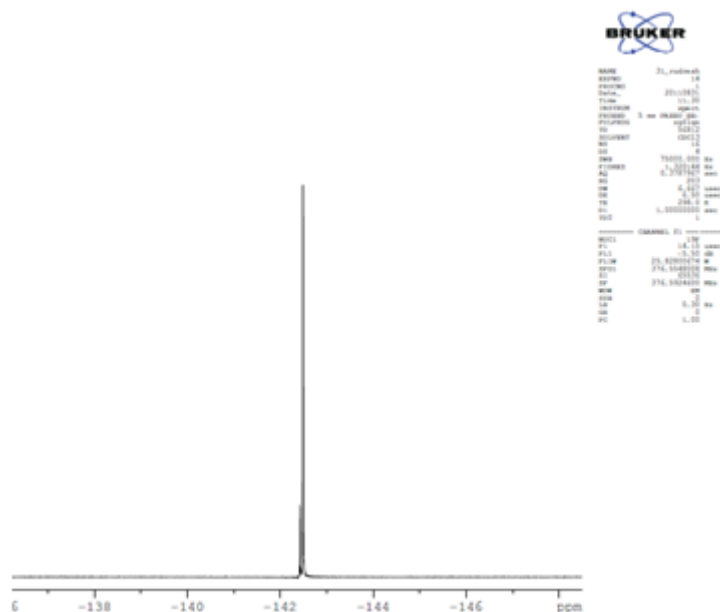
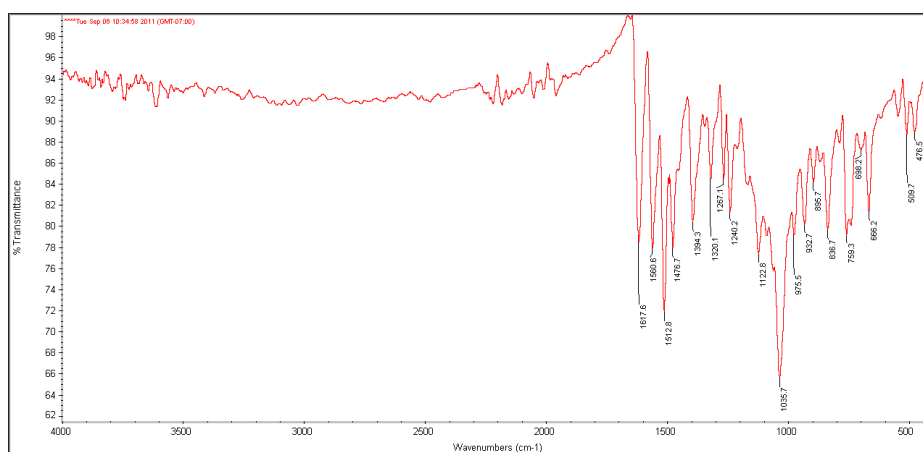
Equimolecular quantities of the 2'-hydroxychalcone ( $\text{L}_4$ - $\text{L}_8$ ) and boron trifluoride etherate were stirred at room temperature on magnetic stirrer for 4 hrs in dry benzene to give a solid which was filtered and washed with dry benzene (Scheme 6.2).

Scheme 6.2 Synthesis of complexes **12C-16C**

### 6.3.2.1 Synthesis of 12C

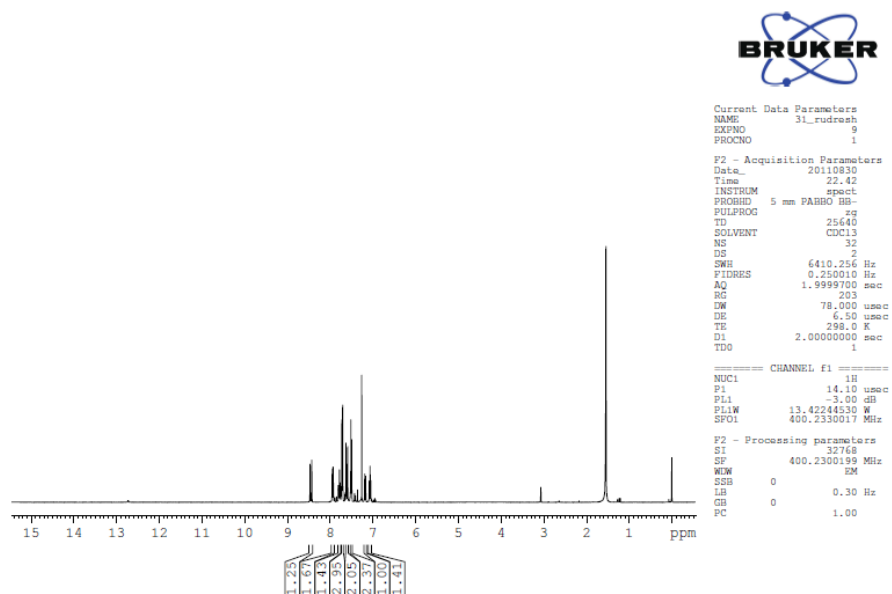
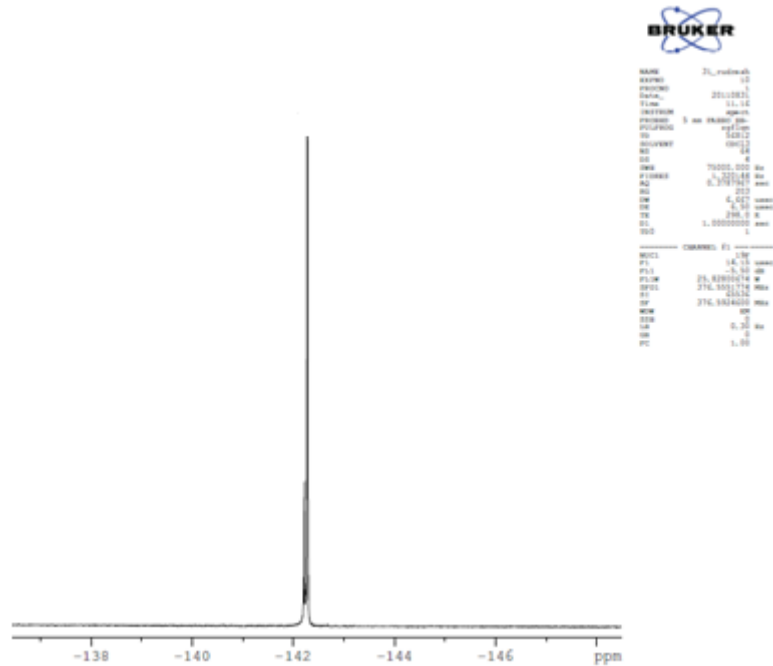
Compound **12C** was prepared from 0.3g (1.00 mmol) of 2'-hydroxychalcone (L<sub>4</sub>) and 0.20 mL (1.20 mmol) of boron trifluoride in dry benzene to give yellow powder with 85 % yield, mp 247-251 °C. <sup>1</sup>H NMR (400MHz, CDCl<sub>3</sub>), [δ, ppm]: 8.53-8.49 (1H, d), 7.96-7.94 (1H, dd), 7.8-7.77 (2H, m), 7.76-7.66 (2H, d), 7.63-7.56 (1H, m), 7.52-7.5 (2H, m), 7.18-7.16 (1H, dd) and 7.06-7.04 (1H, m) (Figure 6.11). <sup>19</sup>F NMR (400MHz, CDCl<sub>3</sub>), [δ, ppm]:142.49 (Figure 6.12). IR (cm<sup>-1</sup>): 1617.6, 1560.6, 1035.7, 666.2 (Figure 6.13). Anal calcd for C<sub>15</sub>H<sub>11</sub>BF<sub>2</sub>O<sub>2</sub>, C 66.21%, H 4.04%. Found C 66.15 %, H 4.02 %. UV-vis: λ<sub>max</sub>/nm (DCM) 375.5 (Figure 6.31).

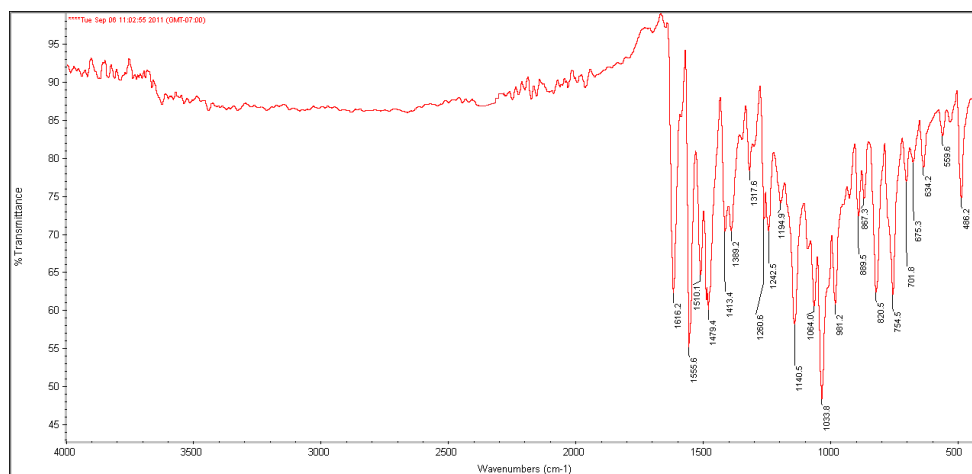
Figure 6.11 <sup>1</sup>H NMR spectrum of complex **12C**

Figure 6.12  $^{19}\text{F}$  NMR spectrum of complex **12C**.Figure 6.13 IR spectrum of complex **12C**

### 6.3.2.2 Synthesis of **13C**

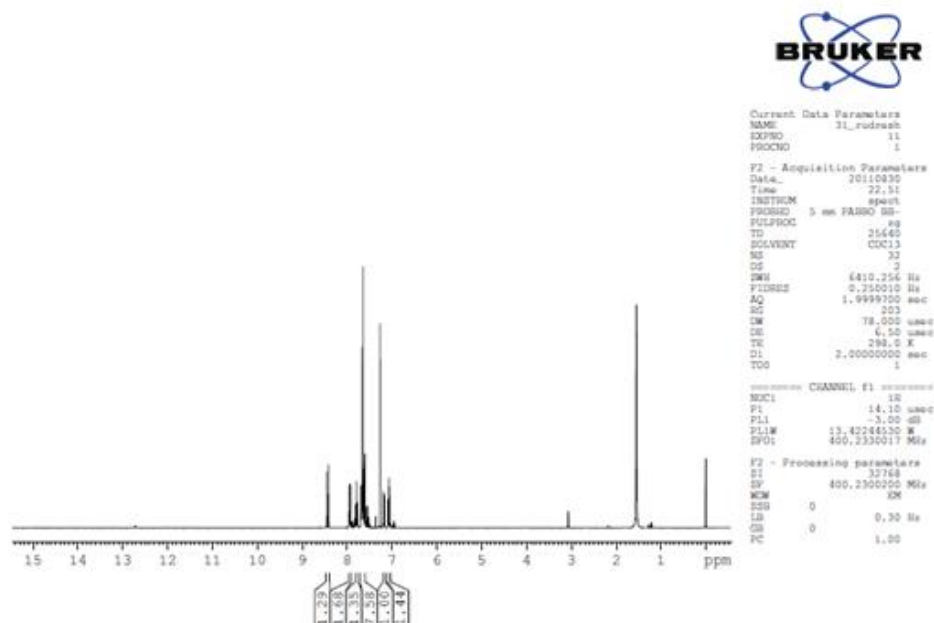
Compound **13C** was prepared from 0.2g (0.77 mmol) of 2'-hydroxychalcone (**L5**) and 0.11 mL (0.92 mmol) of boron trifluoride in dry benzene to give orange precipitate with 85 % yield, mp 247-251 °C.  $^1\text{H}$  NMR (400MHz,  $\text{CDCl}_3$ ), [ $\delta$ , ppm]: 8.46-8.43 (1H, d), 7.95-7.92 (1H, dd), 7.80-7.76 (1H, m), 7.72-7.70 (2H, m), 7.62-7.58 (1H, d), 7.51-7.49 (2H, m), 7.18-7.16 (1H, d) and 7.08-7.04 (1H, m) (Figure 6.14).  $^{19}\text{F}$  NMR (400MHz,  $\text{CDCl}_3$ ), [ $\delta$ , ppm]: 142.28 (Figure 6.15). IR ( $\text{cm}^{-1}$ ): 1618.5, 1556.2, 1037.4, 646.7 (Figure 6.16). Anal. calcd for  $\text{C}_{15}\text{H}_{10}\text{BF}_2\text{ClO}_2$ , C 59.21%, H 3.26%. Found C 59.15 %, H 3.18 %. UV-vis:  $\lambda_{\text{max}}$ /nm (DCM) 366.34 (Figure 6.32).

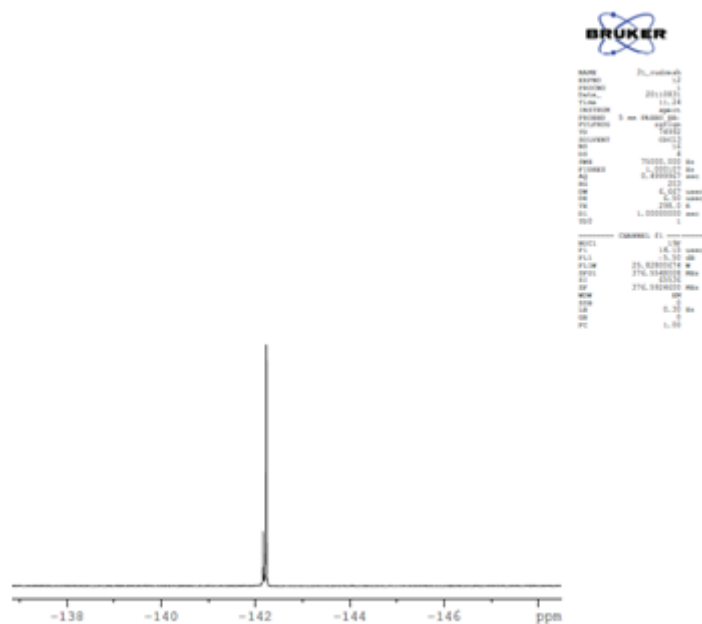
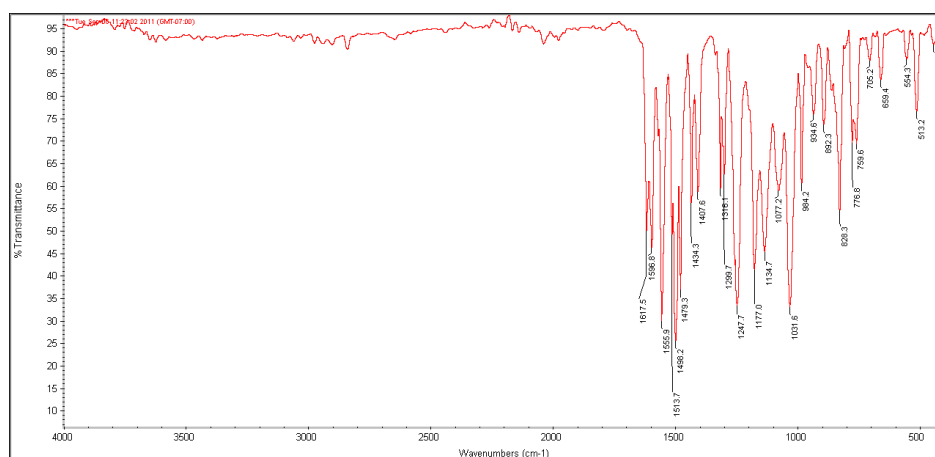
Figure 6.14  $^1\text{H}$  NMR spectrum of complex **13C**Figure 6.15  $^{19}\text{F}$  NMR spectrum of complex **13C**

Figure 6.16 IR spectrum of complex **13C**

### 6.3.2.3 Synthesis of **14C**

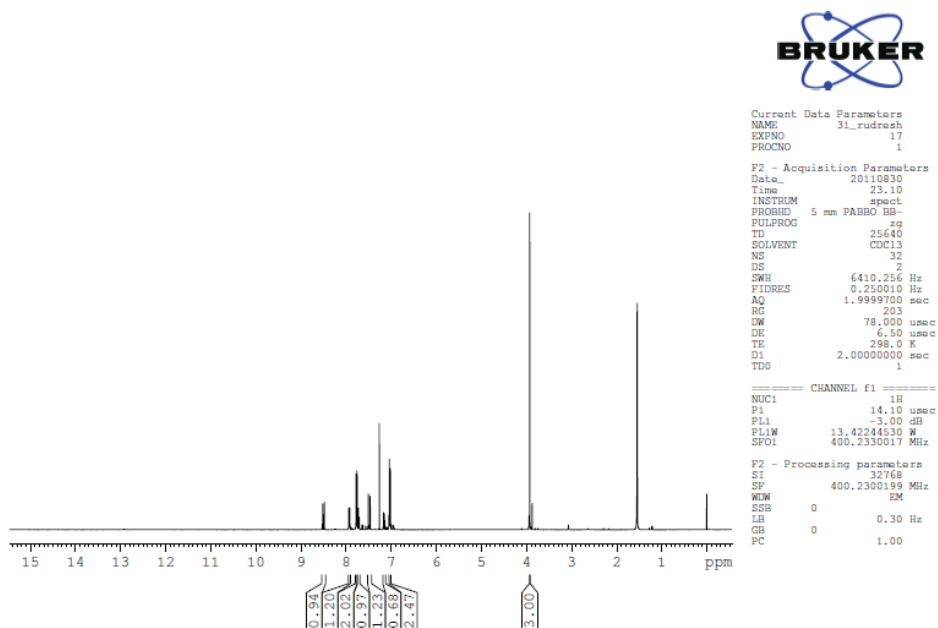
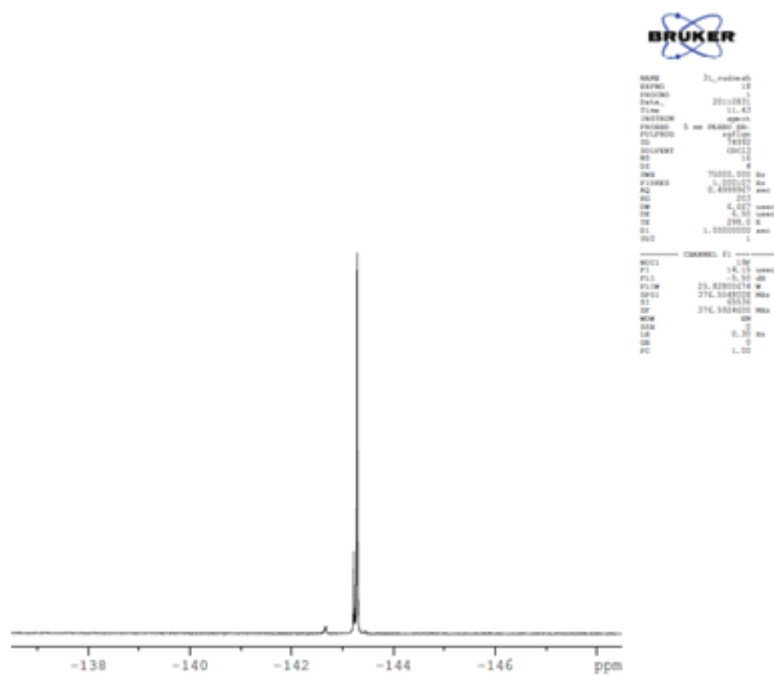
Compound **14C** was prepared from 0.4g (1.31 mmol) of 2'-hydroxychalcone (**L6**) and 0.199 mL (1.58 mmol) of boron trifluoride in dry benzene to give orange precipitate with 85 % yield, mp 247-251 °C.  $^1\text{H}$  NMR (400MHz,  $\text{CDCl}_3$ ), [ $\delta$ , ppm]: 8.44-8.41 (1H, d), 7.94-7.92 (1H, dd), 7.80-7.76 (1H, m), 7.68-7.54 (5H, m), 7.18-7.16 (1H, dd) and 7.08-7.04 (1H, m) (Figure 6.17).  $^{19}\text{F}$  NMR (400MHz,  $\text{CDCl}_3$ ), [ $\delta$ , ppm]: 142.23 (figure 6.18). IR ( $\text{cm}^{-1}$ ): 1616.2, 1555.6, 1033.8, 634.2 (Figure 6.19). Anal calcd for  $\text{C}_{15}\text{H}_{10}\text{BF}_2\text{BrO}_2$ , C 55.33 %, H 2.84 %. Found C 55.20 %, H 2.60 %. UV-vis:  $\lambda_{\text{max}}$ /nm (DCM) 377.54 (Figure 6.33).

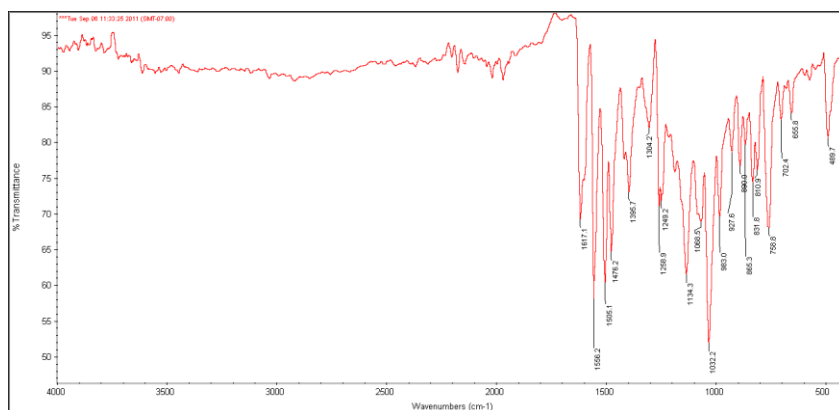
Figure 6.17  $^1\text{H}$  NMR spectrum of complex **14C**

Figure 6.18  $^{19}\text{F}$  NMR spectrum of complex **14C**Figure 6.19 IR spectrum of complex **14C**

#### 6.3.2.4 Synthesis of **15C**

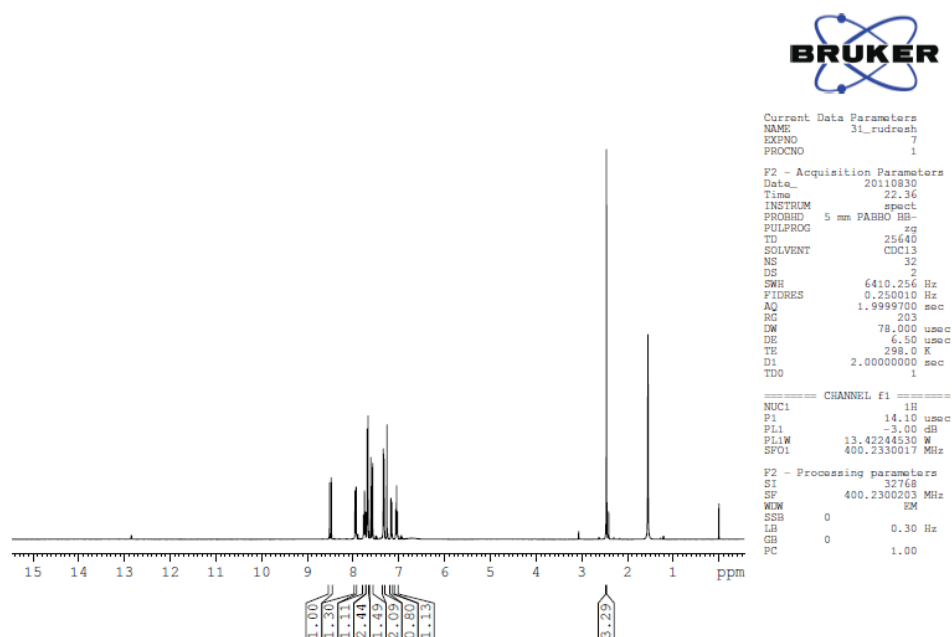
Compound **15C** was prepared from 0.4g (1.57 mmol) of 2'-hydroxychalcone (**L**<sub>7</sub>) and 0.23 mL (1.88 mmol) of boron trifluoride in dry benzene to give orange precipitate with 85 % yield, mp 247-251 °C.  $^1\text{H}$  NMR (400MHz,  $\text{CDCl}_3$ ), [ $\delta$ , ppm]: 8.51-8.48 (1H, d), 7.94-7.91 (1H, dd), 7.78-7.74 (2H, m), 7.73-7.70 (1H, m), 7.50-7.46 (1H, d), 7.16-7.14 (1H, dd), 7.05-7.01 (3H, m) and 3.92 (3H, s) (Figure 6.20).  $^{19}\text{F}$  NMR (400MHz,  $\text{CDCl}_3$ ), [ $\delta$ , ppm]: 143.29 (Figure 6.21). IR ( $\text{cm}^{-1}$ ): 1617.5, 1559.9, 1031.6, 659.4 (Figure 6.22). Anal calcd for  $\text{C}_{15}\text{H}_{13}\text{BF}_2\text{O}_3$ , C 63.61 %, H 4.30 %. Found C 63.15 %, H 4.20 %. UV-vis:  $\lambda_{\text{max}}$ /nm (DCM) 454.00 (Figure 6.34).

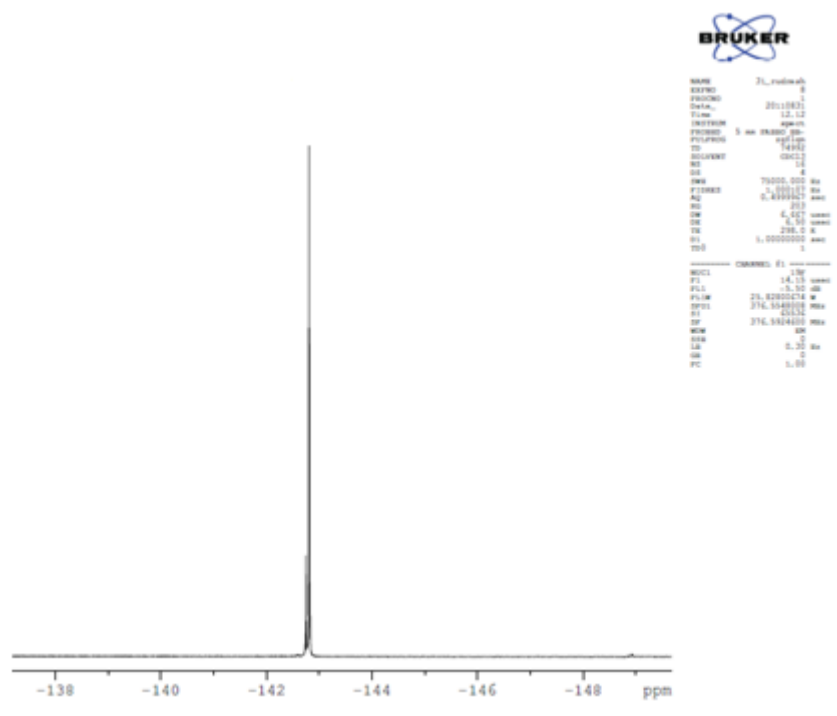
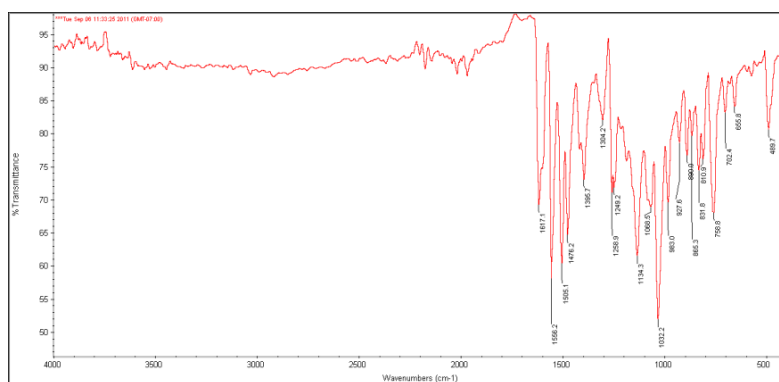
Figure 6.20  $^1\text{H}$  NMR spectrum of complex **15C**Figure 6.21  $^{19}\text{F}$  NMR spectrum of complex **15C**

Figure 6.22 IR spectrum of complex **15C**.

### 6.3.2.5 Synthesis of **16C**

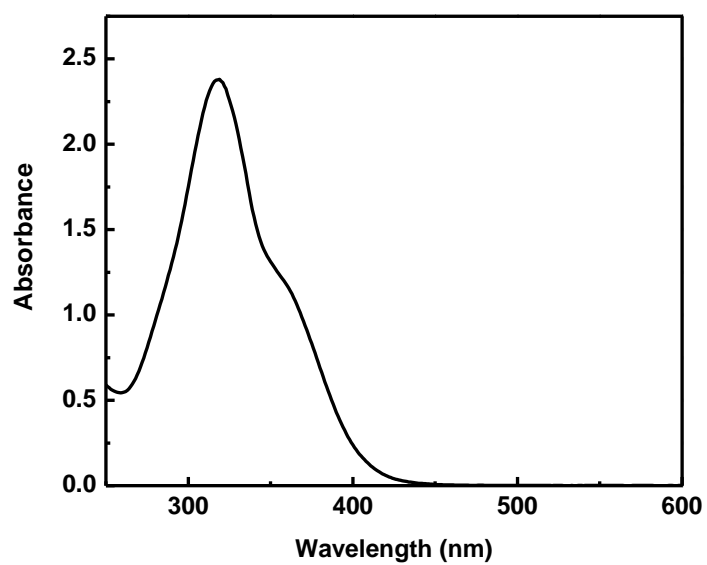
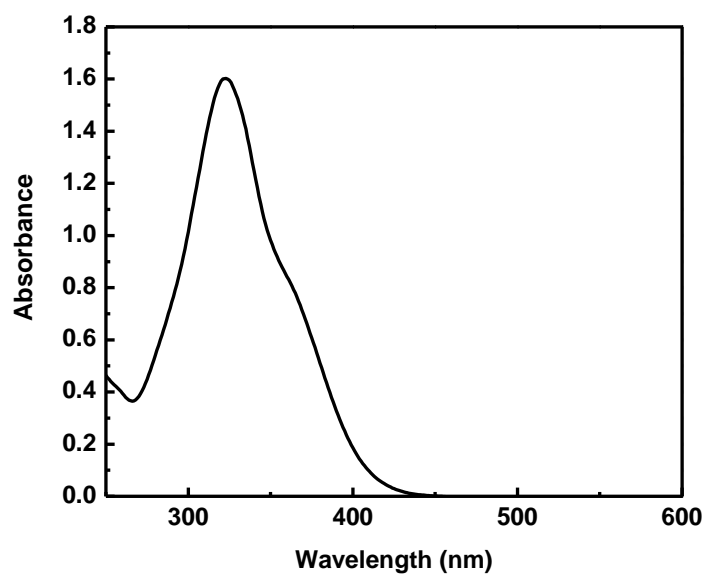
Compound **16C** was prepared from 0.4g (1.67 mmol) of 2'-hydroxychalcone (**L<sub>8</sub>**) and 0.25 mL (2.01 mmol) of boron trifluoride in dry benzene to give orange precipitate with 85 % yield, mp 247-251 °C. <sup>1</sup>H NMR (400MHz, CDCl<sub>3</sub>), [δ, ppm]: 8.51-8.47 (1H, d), 7.95-7.93 (1H, dd), 7.77-7.73 (1H, m), 7.69-7.67 (2H, m), 7.61-7.57 (1H, d), 7.33-7.31 (2H, d), 7.17-7.14 (1H, dd), 7.06-7.02 (1H, m) and 2.49 (3H, s) (Figure 6.23). <sup>19</sup>F NMR (400MHz, CDCl<sub>3</sub>), [δ, ppm]: 142.81 (Figure 6.24). IR (cm<sup>-1</sup>): 1617.1, 1556.2, 1032.2, 655.8 (Figure 6.25). Anal calcd for C<sub>15</sub>H<sub>13</sub>BF<sub>2</sub>O<sub>2</sub>, C 67.17 %, H 4.54%. Found C 67.02 %, H 4.34 %. UV-vis: λ<sub>max</sub>/nm (DCM) 382.0 (Figure 6.35).

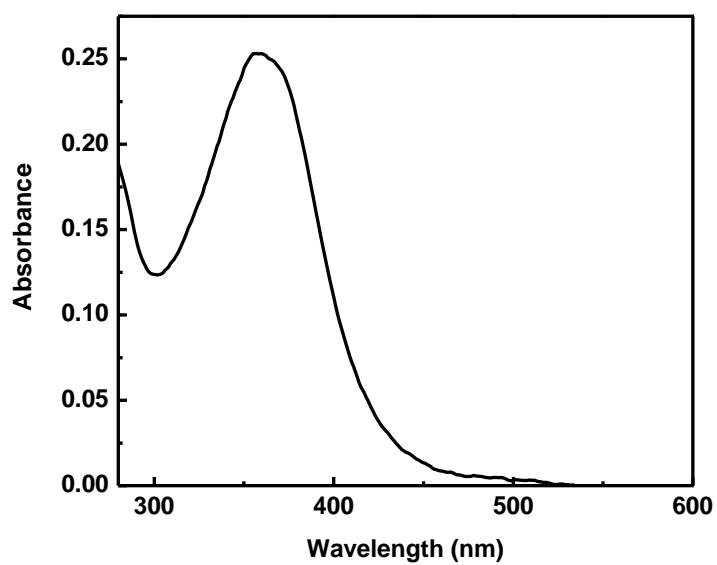
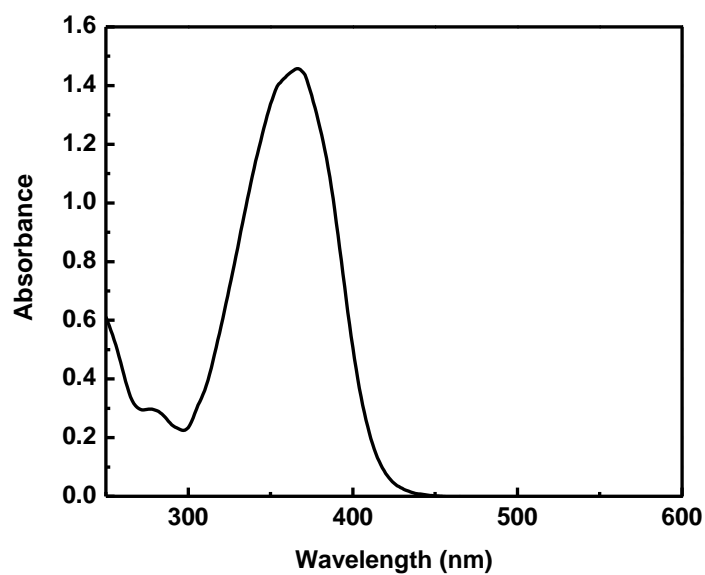
Figure 6.23 <sup>1</sup>H NMR spectrum of complex **16C**.

Figure 6.24  $^{19}\text{F}$  NMR spectrum of complex **16C**Figure 6.25 IR spectrum of complex **16C**.

#### 6.4 LINEAR OPTICAL STUDY

The electronic spectra of the ligands (**L<sub>4</sub>-L<sub>8</sub>**) and complexes (**12C-16C**) are shown in Figure 6.26 to 6.35. Spectra of complexes are dominated by one main absorption band in the region 400 nm. From the spectra it confirms that main absorption band of complexes is red shifted compared to the free ligands (330 nm).

Figure 6.26 UV-visible spectrum of ligand L<sub>4</sub>Figure 6.27 UV-visible spectrum of ligand L<sub>5</sub>

Figure 6.28 UV-visible spectrum of ligand L<sub>6</sub>Figure 6.29 UV-visible spectrum of ligand L<sub>7</sub>

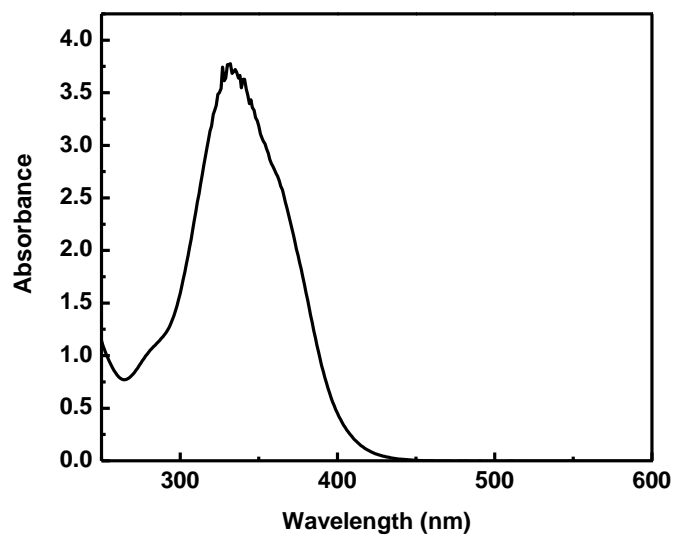
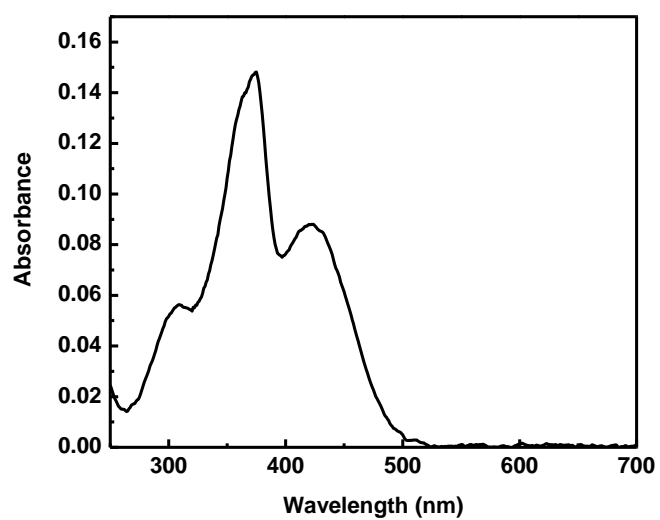
Figure 6.30 UV-visible spectrum of ligand L<sub>8</sub>

Figure 6.31 UV-visible spectrum of complex 12C

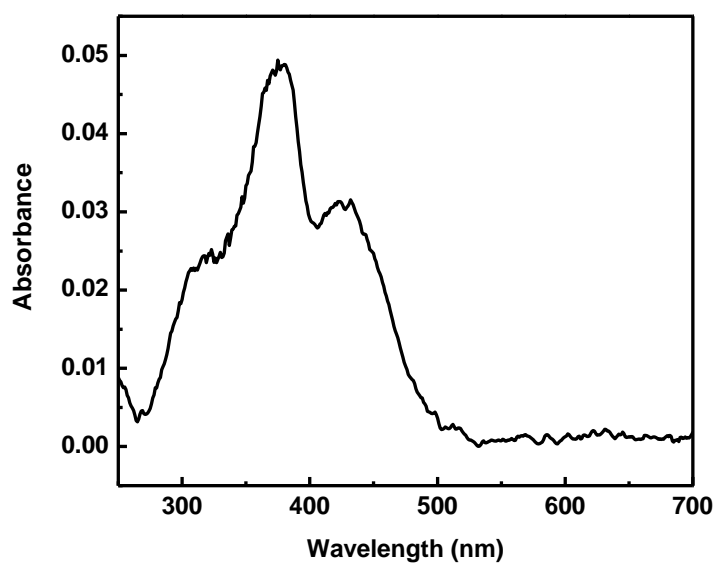


Figure 6.32 UV-visible spectrum of complex 13C

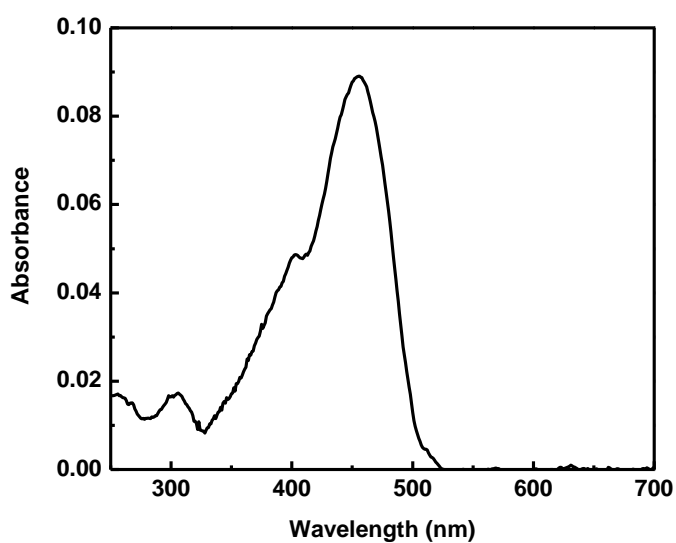


Figure 6.33 UV-visible spectrum of complex 14C

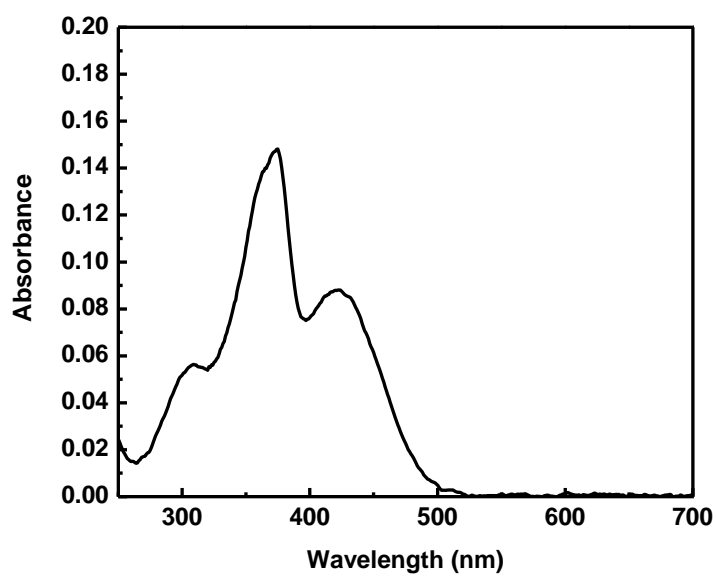


Figure 6.34 UV-visible spectrum of complex 15C

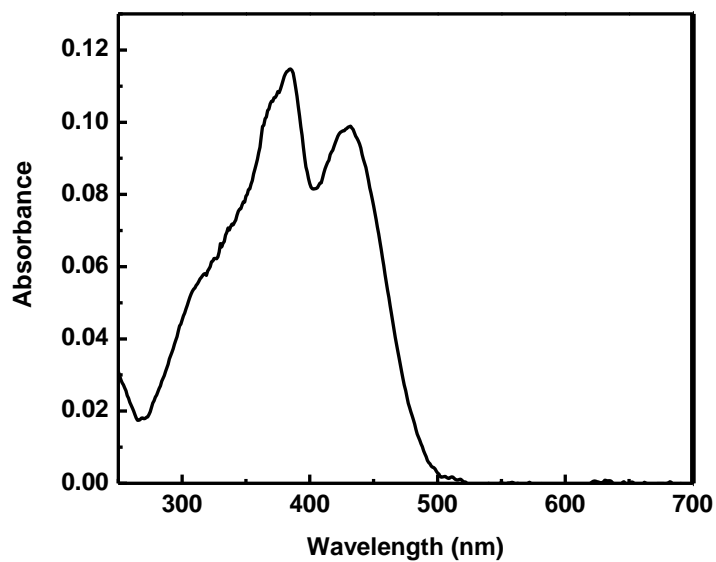


Figure 6.35 UV-visible spectrum of complex 16C

## 6.5 RESULTS AND DISCUSSION

### 6.5.1 Spectral analysis

The difluoroboronates (**12C-16C**) were synthesized by reaction of hydroxyl chalcones (**L<sub>4</sub>-L<sub>8</sub>**) with and trifluoride etherate in dry benzene. The existence of the oxygen boron coordination bond in compounds **12C-16C** was established by IR spectroscopy, which shows 15-20 cm<sup>-1</sup> shift of the carbonyl band in the boron complexes (1615-1620 cm<sup>-1</sup>) with respect to the 2'-hydroxychalcones **L<sub>4</sub>-L<sub>8</sub>** (~1640 cm<sup>-1</sup>), due to the coordination of the boron atom to oxygen (Horacio Reyes et al. 2006). Formation of the complexes increases delocalization as evidenced by the fact that the hydroxyl chalcones are yellow crystals while the complexes are orange coloured. The UV spectra confirm this fact and provide insight into the NLO properties. Comparison of the absorption values for the hydroxyl chalcones (**L<sub>4</sub>-L<sub>8</sub>**) with those of the boron complexes shows a red shift and an increase in intensity which evidences their potential as NLO materials. <sup>1</sup>H NMR data for hydroxyl chalcones **L<sub>4</sub>-L<sub>8</sub>** and corresponding boron complexes **12C-16C** shows that upon complexation chemical shifts values are slightly shifted to higher frequencies. The absence of peak for the hydroxyl proton in the complexes shows that participation of phenolic oxygen atom in the complexes. In the complexes (**12C-16C**) the <sup>19</sup>F NMR chemical shifts were in the range of 141.8 to 145.3 which agree well with the literature values (Horacio Reyes et al. 2006).

### 6.5.2 Nonlinear optical studies

The open aperture z-scan curves of complexes (**12C-16C**) are given in Figures 6.36-Figure 6.40. These curves show an increase in absorption when the sample is nearing the beam focus. Since the residual absorption of the samples at the excitation wavelength is in the vicinity of 50%, the nonlinearity can be expected to arise from a two-step or three-step excitation process involving real excited states, which essentially amounts to reverse saturable absorption (RSA). Genuine two-photon (2PA) and three-photon (3PA) absorption involving virtual states also can take place in the system, but these will be relatively weak compared to the RSA process. However, an excitation where two photons are involved will numerically fit to a two-photon absorption equation irrespective of whether real or virtual states are involved. Similarly, if three photons are involved, it will fit to a three-photon absorption

equation. Therefore we tried to fit our data to two-photon and three-photon equations, and the best fit was obtained to the two-photon process described by the nonlinear transmission equation (Sutherland 1996),

$$T = \left( \frac{(1-R)^2 \exp(-\alpha L)}{\sqrt{\pi q_0}} \right) \int_{-\infty}^{\infty} \ln \left[ \sqrt{1 + q_0 \exp(-t^2)} \right] dt \quad (6.1)$$

where  $T$  is the actual  $z$ -dependent sample transmission (product of linear transmission and normalized transmittance), and  $L$  and  $R$  are the length and surface reflectivity of the sample respectively.  $\alpha$  is the linear absorption coefficient.  $q_0$  is given by  $\beta(1-R)I_0L_{eff}$ , where  $\beta$  is the two-photon absorption coefficient, and  $I_0$  is the on-axis peak intensity.  $L_{eff}$  is given by  $1 - \exp^{-\alpha l}/\alpha$ . The quantity  $\beta$  here is the *effective* 2PA coefficient, as it is a lumped coefficient for the effects of RSA as well as genuine 2PA. The  $\beta$  values of complexes were shown in Table 6.1. In all these materials strong excited state absorption was found to happen concurrently with genuine 2PA, since the samples used had some residual absorption at the excitation wavelength of 532 nm.

The Open aperture Z-scan (i.e. without aperture in front of the detector) was performed to measure the nonlinear absorption in the sample, which is related to imaginary part of third-order optical susceptibility  $\chi^{(3)}$ . Figures 6.36-6.40 shows the open aperture Z-scan curve of the complexes which are symmetric with respect to the focus indicating intensity dependent absorption. The absorption may be due to two photon absorption (TPA), excited state absorption (ESA), reverse saturable absorption (RSA), etc. Nonlinear absorption of nano second pulses can be understood using the five level model (Feng et al. 2005 and Unnikrishnan et al. 2002) shown in Figure. 3.25. The relevant energy levels are the singlet levels  $S_0$ ,  $S_1$ , and  $S_2$  and the triplet levels are  $T_1$  and  $T_2$ . Each of these states contains number of vibrational levels. When the molecule is excited by the laser pulse, electrons are initially excited from lowest vibrational level of  $S_0$  to upper vibrational levels of  $S_1$ , where they relax in picoseconds by nonradiative decay. In nanosecond time scale, singlet transition does not deplete the population of  $S_1$  level appreciably, since atoms excited to  $S_2$  decay to  $S_1$  itself within picoseconds. From  $S_1$ , electrons are transferred to  $T_1$  via intersystem

crossing (ISC), from where transitions to  $T_2$  occur. The two processes ( $S_1 \rightarrow S_2$ ) and ( $T_1 \rightarrow T_2$ ) are known as ESA (Excited state absorption) and if the excited state absorption cross-sections ( $\sigma_s$ ) are larger than that of the ground state ( $\sigma_G$ ) the process is called RSA (reverse saturable absorption). With excitation of laser pulses on the nanosecond scale, which is true in our case, triplet-triplet transitions are expected to make significant contribution to nonlinear absorption.

Table 6.1 The values of the two-photon absorption (2PA) coefficients  $\beta$  of the complexes 12C-16C.

Complex	Z-scan result $\beta$ (m/W)
12C	$2.5 \times 10^{-11}$
13C	$1.8 \times 10^{-11}$
14C	$2.4 \times 10^{-11}$
15C	$6.4 \times 10^{-11}$
16C	$7.7 \times 10^{-11}$

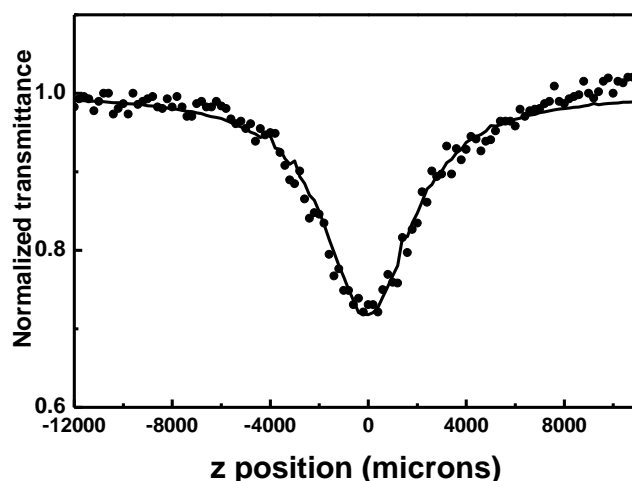


Figure 6.36 Open aperture z-scan traces for complex **12C**. The filled circles are measured data points and solid curve is the numerically calculated fit for a two-photon absorption process using Equation 6.1.

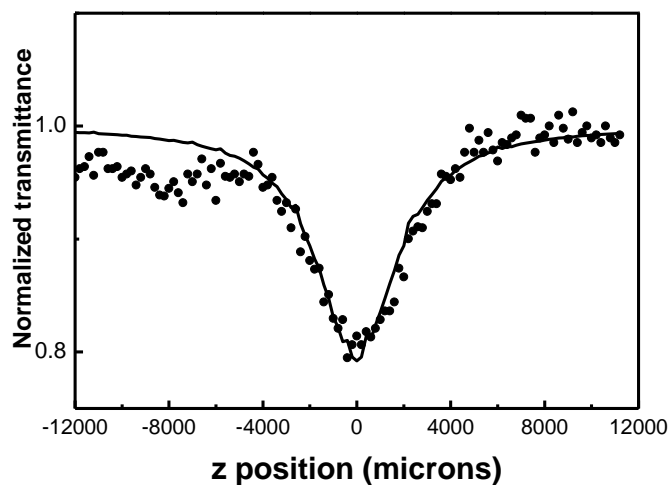


Figure 6.37 Open aperture z-scan traces for complex **13C**. The filled circles are measured data points and solid curve is the numerically calculated fit for a two-photon absorption process using Equation 6.1.

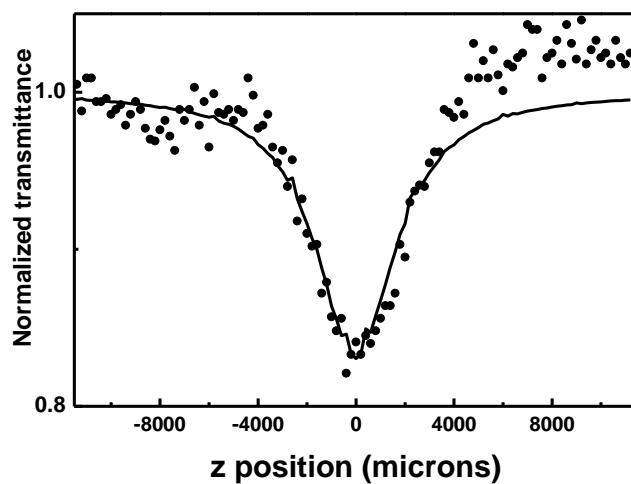


Figure 6.38 Open aperture z-scan traces for complex **14C**. The filled circles are measured data points and solid curve is the numerically calculated fit for a two-photon absorption process using Equation 6.1.

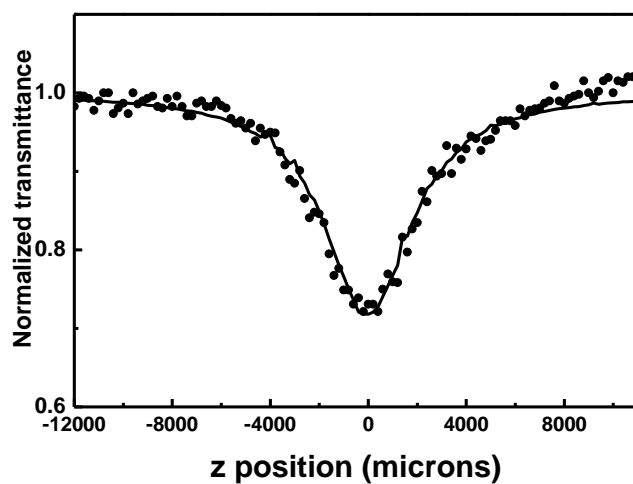


Figure 6.39 Open aperture z-scan traces for complex **15C**. The filled circles are measured data points and solid curve is the numerically calculated fit for a two-photon absorption process using Equation 6.1.

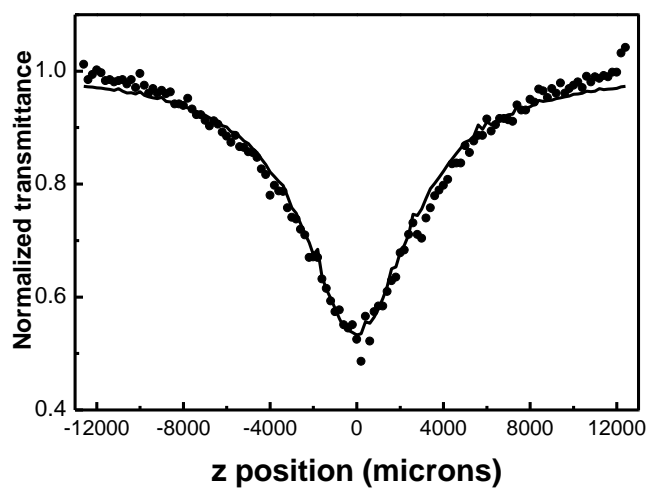


Figure 6.40 Open aperture z-scan traces for complex **16C**. The filled circles are measured data points and solid curve is the numerically calculated fit for a two-photon absorption process using Equation 6.1.

## CHAPTER 7

### SYNTHESIS, CHARACTERIZATION AND THIRD-ORDER NONLINEAR OPTICAL STUDIES OF BORON SCHIFF BASE COMPLEXES

#### *Abstract*

*In this chapter, three substituted ligands  $N,N'$ - $p$ -phenylene bis (salicylideneimine) ( $L_9$ - $L_{11}$ ) as well as their coordinatively saturated boron complexes  $17C$ - $19C$  were synthesized and characterized. From the analytical and spectral studies, the formation of the complexes was confirmed. Nonlinear optical properties of the complexes are investigated at 532 nm using single beam Z-scan technique employing nanosecond laser pulses. The complexes show optical limiting behaviour due to “effective” two-photon absorption. The values of the effective two-photon absorption (2PA) coefficients ( $\beta$ ) are calculated. Strong donor-acceptor mechanism (“push-pull” system), is the responsible factors for this observed third-order nonlinear optical response.*

#### 7.1 INTRODUCTION

Recently much effort has been devoted to the design and synthesis of boron-containing compounds for their potential applications in functional materials, including organic light-emitting devices (OLEDs) (Liu et al. 2002 and Zhang et al 2006), nonlinear optics (Liu et al. 2002), fluorescent and fluoride ion sensors (Shigehiro et al. 2002 and Sole and Gabba 2004), and bio-molecular probes (Yang et al. 2001 and Killoran et al. 2002). Wang and co-workers have systematically reported the synthesis, structures, and photoluminescent (PL) and electroluminescent (EL) properties of boron containing compounds (Wu et al. 1999, Liu et al 2002 and Liu et al 2005). In view of the important potential applications of boron-containing compounds in OLEDs, our interest focused on the possibility of Schiff base boron complexes utilized as nonlinear optical materials. Boron is strongly electrophilic by virtue of its tendency to fill the vacant p-orbital and completes the octet, so in contrast to organometallic compounds, organoboron compounds are in general more stable owing to the increased covalency of B–O and B–N bonds. Thus, boron complexes may provide extra stability to counteract the instability of C=N bonds in Schiff base.

In this chapter, three substituted ligands N,N'-*p*-phenylenebis(salicylideneimine) (**L<sub>9</sub>**-**L<sub>11</sub>**) as well as their coordinatively saturated boron complexes **17C**-**19C** were synthesized and characterized. The non-linear optical properties of complexes were investigated for the potential optoelectronic applications.

## **7.2 EXPERIMENTAL**

### **7.2.1 Materials**

All the chemicals used were of analytical grade. Solvents were purified and dried according to standard procedure (Vogel 1989). *p*-phenylenediamine, salicylaldehyde derivatives and borontrifluoride etherate were purchased from Sigma Aldrich.

### **7.2.2 Analysis and measurements**

The <sup>1</sup>H and <sup>19</sup>F spectra were recorded using Bruker AV 400 spectrometer operating at the frequency of 400 MHz. The spectra were recorded in solution with DMSO as internal lock. Electronic spectra were measured on a Cintra 101 (GBC) UV-Vis double beam spectrophotometer with 0.6 nm resolution in DMSO solution of the complexes in the 200 – 800 nm range. FT - IR spectra were recorded on a Thermo Nicolet Avatar FTIR-ATR spectrometer with 4 cm<sup>-1</sup> resolution in the frequency range 400 – 4000 cm<sup>-1</sup>. The C, H and N contents were determined by Thermoflash EA1112 series elemental analyzer.

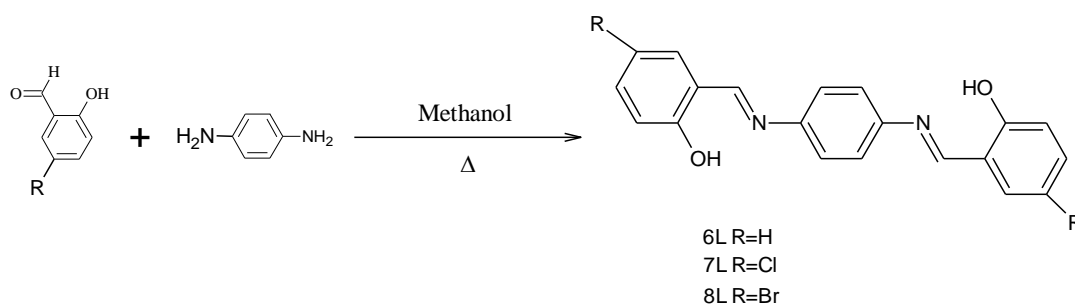
### **7.2.3 Z-scan measurement**

Open-aperture Z-scan measurements were performed to determine the nonlinear transmission of laser light through the samples. The Z-scan is a widely used technique developed by Sheik Bahae et al. (1990) to measure optical nonlinearity of materials, and the open aperture Z-scan gives information about the nonlinear absorption coefficient. Here a laser beam is focused using a lens and passed through the sample. The beam's propagation direction is taken as the z-axis, and the focal point is taken as z = 0. The beam will have maximum energy density at the focus, which will symmetrically reduce towards either side for the positive and negative values of z. The experiment is done by placing the sample in the beam at different positions with respect to the focus (different values of z), and measuring the corresponding light transmission. The graph plotted between the sample position z

and the normalized transmittance of the sample  $T$  (norm) (transmission normalized to the linear transmission of the sample) is known as the  $z$ -scan curve. The nonlinear absorption coefficient of the sample can be numerically calculated from the  $z$ -scan curve. In our experiment, DMF solutions of the samples taken in 1 mm cuvettes were irradiated by plane polarized 5 ns laser pulses at 532 nm obtained from the second harmonic output of a Q-switched Nd:YAG laser (MiniLite, Continuum). The laser pulse energy was 100 micro Joules and the beam focal spot radius ( $\omega_0$ ) was 18 microns. These values yield a Rayleigh range ( $z_0$ ) of 1.9 mm, and on-axis peak intensity ( $I_0$ ) of  $6.29 \times 10^9 \text{ W/cm}^2$ , for a spatially Gaussian beam. The laser was run in the single shot mode using a data acquisition programme, with an approximate interval of 3 to 4 seconds between each pulse. This low repetition rate prevents sample damage and cumulative thermal effects in the medium.

#### 7.2.4 General procedure for synthesis of ligands ( $L_9$ - $L_{11}$ )

*p*-Phenylenediamine and derivatives of salicylaldehyde were dissolved in anhydrous methanol, and the reaction mixture was heated to reflux for 3 h. After cooled to room temperature, a bright yellow precipitate separated from the reaction solution. The solid product was collected by filtration and purified by recrystallization to give a yellow powder of corresponding Schiff base (**Scheme 7.1**).



Scheme 7.1 Synthesis of ligands  $L_9$ - $L_{11}$

##### 7.2.4.1 Synthesis of *N,N'*-*p*-phenylene bis (salicylideneimine) ( $L_9$ )

*O*-phenylenediamine (1.0 g, 9.24mmol) and salicylaldehyde (2.25g, 18.49 mmol) were dissolved in 20 ml of anhydrous methanol, and the reaction mixture was heated to reflux for 3 h. After cooled to room temperature, a bright yellow precipitate separated from the reaction solution. The solid product was collected by filtration and purified by recrystallization to give a yellow powder, yield 80%.  $^1\text{H}$  NMR (400 MHz, DMSO):  $\delta$ : ppm: 13.10 (2H, s), 9.3 (2H, s), 7.69-7.65 (2H, m), 7.55 (4H, s), 7.45-7.39

(2H, m) and 7.02-6.95 (4m) (Figure 7.1). IR ( $\text{cm}^{-1}$ ): 1602.8, 1275.2 (Figure 7.2). Anal calcd for  $\text{C}_{20}\text{H}_{16}\text{N}_2\text{O}_2$ , C 75.92%, H 5.05%, N 8.85%. Found C 75.83 %, H 5.00 %. N 8.66%. UV-vis:  $\lambda_{\text{max}}$ /nm (DMSO) 372.9 (Figure 7.12).

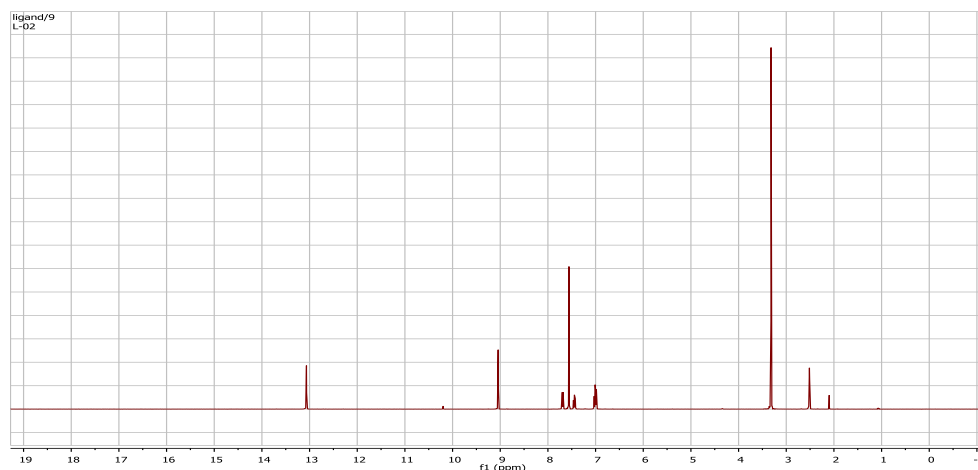


Figure 7.1  $^1\text{H}$  NMR spectrum of ligand  $\text{L}_9$

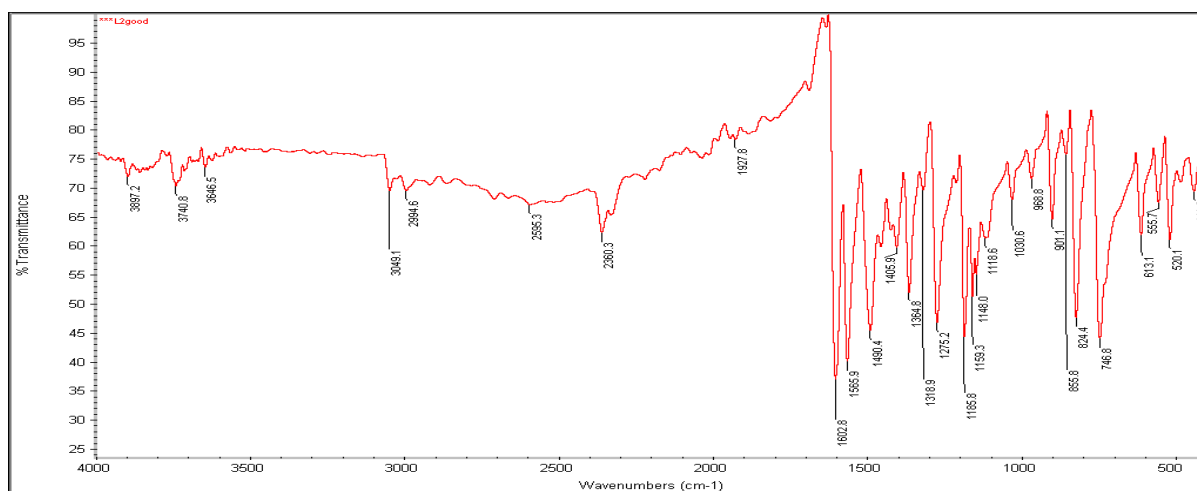
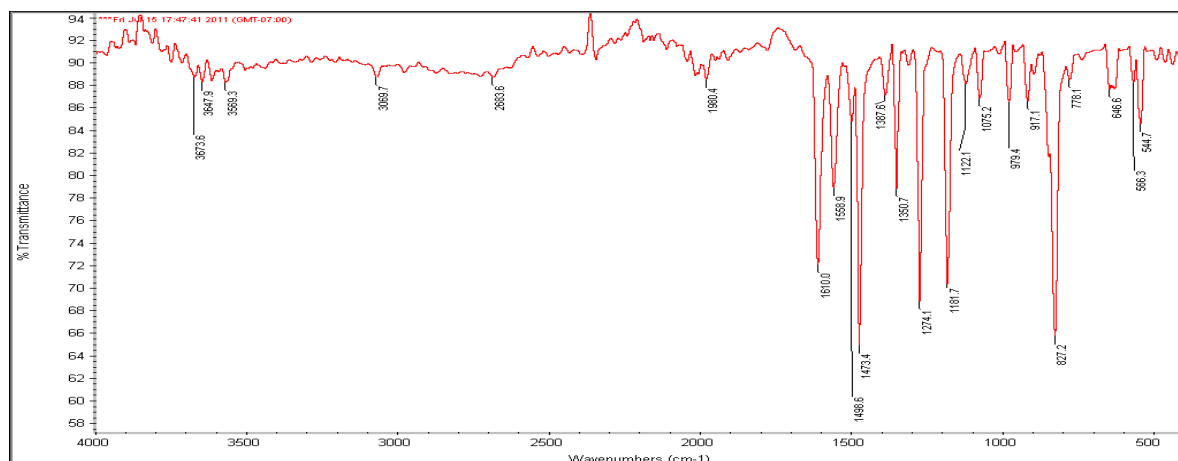


Figure 7.2 IR spectrum of ligand  $\text{L}_9$

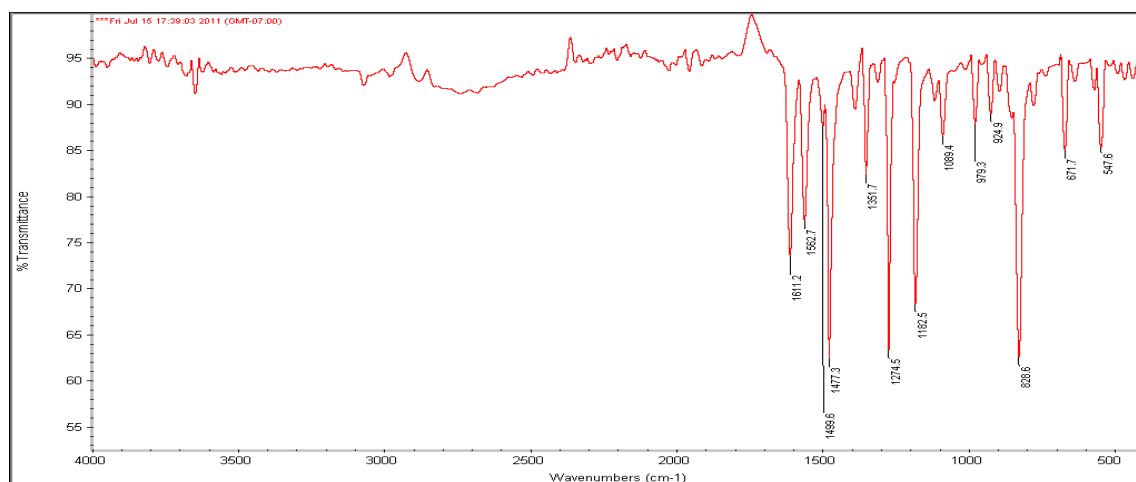
#### 7.2.4.2 Synthesis of *N,N'*-*p*-phenylenebis (chloro-salicylideneimine) ( $\text{L}_{10}$ )

Following similar procedure as used for  $\text{L}_9$ , reaction of *p*-phenylenediamine (1.00 g, 9.24mmol) and 5-chloro-salicylaldehyde (2.89, 18.14mmol) gave a light yellow solid of  $\text{L}_{10}$ , yield 88%. IR ( $\text{cm}^{-1}$ ): 1610.0., 1274.1 (Figure 7.3). Anal calc for  $\text{C}_{20}\text{H}_{14}\text{Cl}_2\text{N}_2\text{O}_2$ , C 62.35%, H 3.63%, N 7.26%. Found C 62.25%, H 3.43%, N 7.18%. UV-vis:  $\lambda_{\text{max}}$ /nm (DMSO) 381.5(Figure 7.13).

Figure 7.3 IR spectrum of ligand  $L_{10}$ 

#### 7.2.4.3 Synthesis of *N,N'*-*p*-phenylenebis (bromo-salicylideneimine) ( $L_{11}$ )

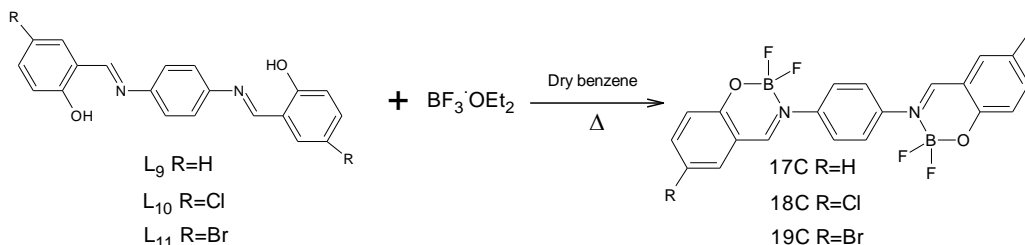
Following similar procedure as used for  $L_9$ , reaction of *p*-phenylenediamine (1.00 g, 9.24mmol) and 5-bromo-salicylaldehyde (3.71g, 18.49mmol) gave a light yellow solid of  $L_{11}$ . yield 88%. IR ( $\text{cm}^{-1}$ ): 1611.2, 1274.5 (Figure 7.4). Anal calcd for  $\text{C}_{20}\text{H}_{14}\text{Br}_2\text{N}_2\text{O}_2$ , C 50.66%, H 2.95%, N 5.90%. Found C 50.25%, H 2.43%, N 5.50%. UV-vis:  $\lambda_{\text{max}}$ /nm (DMSO) 382.3 (Figure 7.14).

Figure 7.4 IR spectrum of ligand  $L_{11}$ 

#### 7.2.5 General procedure for synthesis of Boron Schiff base complexes (17C-19C)

Borontrifluoride etherate and corresponding Schiff base ligands were dissolved in anhydrous benzene. After the reaction mixture was heated to reflux under nitrogen for half an hour, triethylamine was added to the reaction solution and the mixture was heated to reflux for 9 h. A light green–yellow solid precipitated from the

solution (Scheme 7.2). The solid product was collected by filtration and purified by recrystallization and sublimation.



Scheme 7.2 Synthesis of complexes **17C-19C**

### 7.2.5.1 Synthesis of the boron complex **17C**

Borontrifluoride diethyletherate (0.32g, 2.53 mmol) and **L<sub>9</sub>** (0.61 g, 2 mmol) were dissolved in 30 ml of anhydrous benzene. After the reaction mixture was heated to reflux under nitrogen for half an hour, triethylamine (0.3 ml) was added to the reaction solution and the mixture was heated to reflux for 9 h. A light green–yellow solid precipitated from the solution. The solid product was collected by filtration and purified by recrystallization and yield was found to be 70%. <sup>1</sup>H NMR (400 MHz, DMSO): δ: ppm: 9.28 (2H, s), 7.85 (4H, s), 7.84-7.82 (2H, m), 7.79-7.75 (2H, m), 7.17-7.12 (4H, m) (Figure 7.5). <sup>19</sup>F NMR (400MHz, CDCl<sub>3</sub>), [δ, ppm]: 141.43 (Figure 7.6). IR (cm<sup>-1</sup>): 1620.3, 1210.6 (Figure 7.7). Anal calcd for C<sub>20</sub>H<sub>14</sub>B<sub>2</sub>F<sub>4</sub>N<sub>2</sub>O<sub>2</sub>: C:58.30%, H:3.39%, N:6.79%. Found C:58.12 %, H:3.20 %. N:6.66%. UV-vis: λ<sub>max</sub>/nm (DMSO) 319.0 and 374.3 (Figure 7.15).

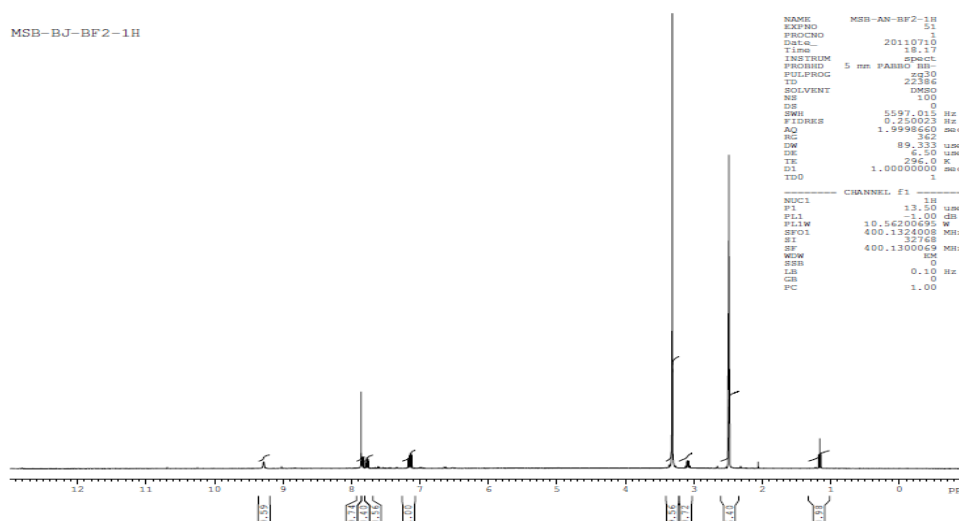
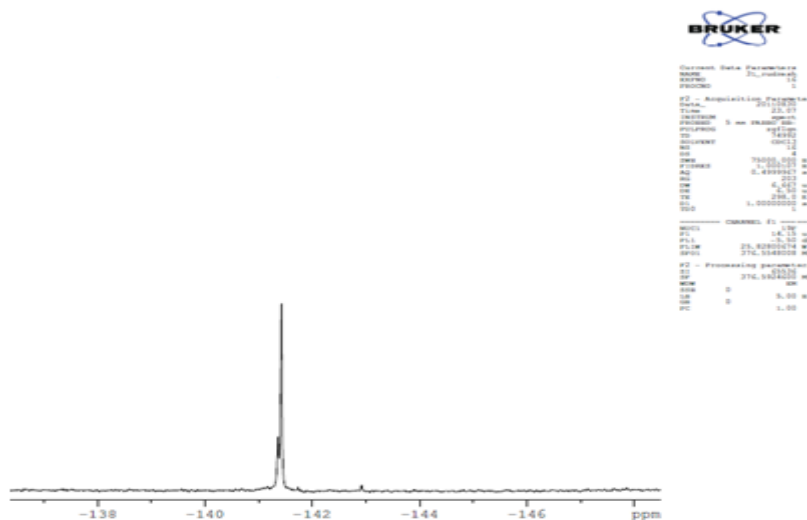
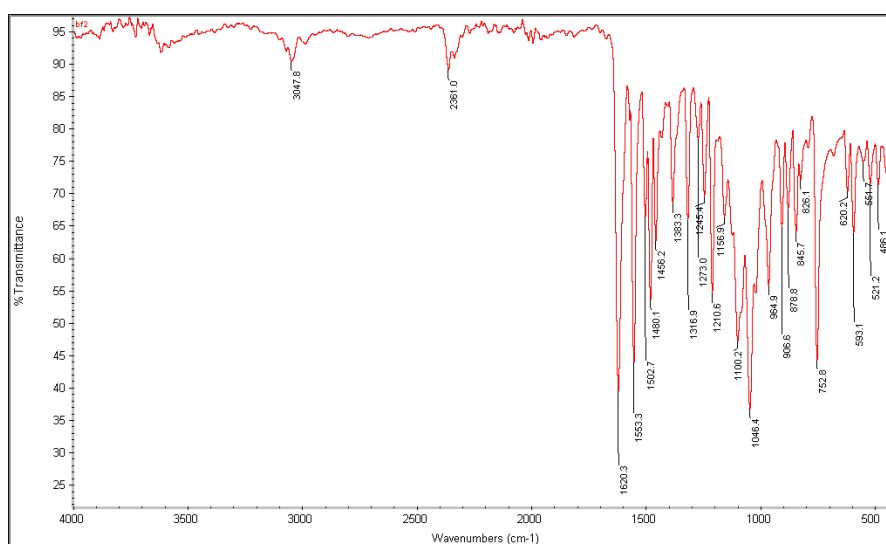
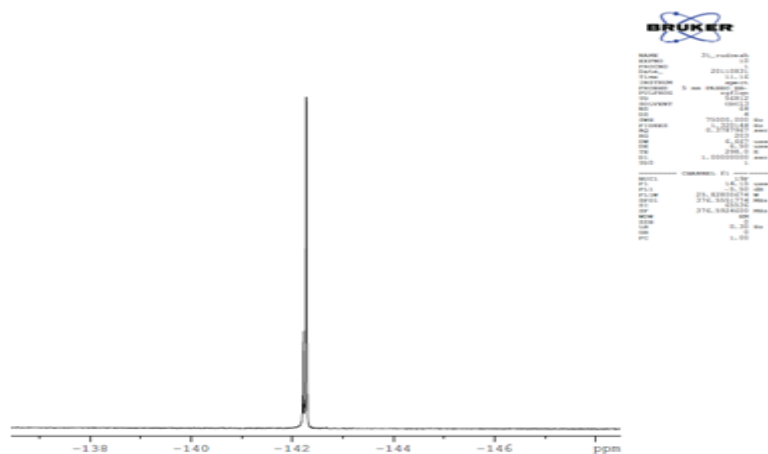
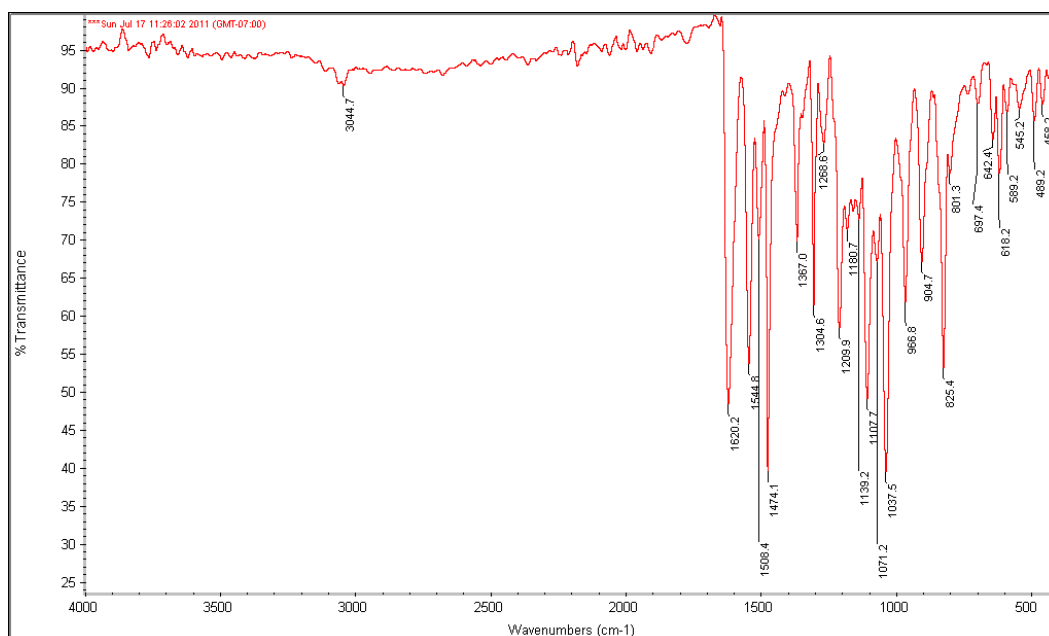


Figure 7.5 <sup>1</sup>H NMR spectrum of complex **17C**

Figure 7.6  $^{19}\text{F}$  NMR spectrum of complex **17C**Figure 7.7 IR spectrum of complex **17C**.

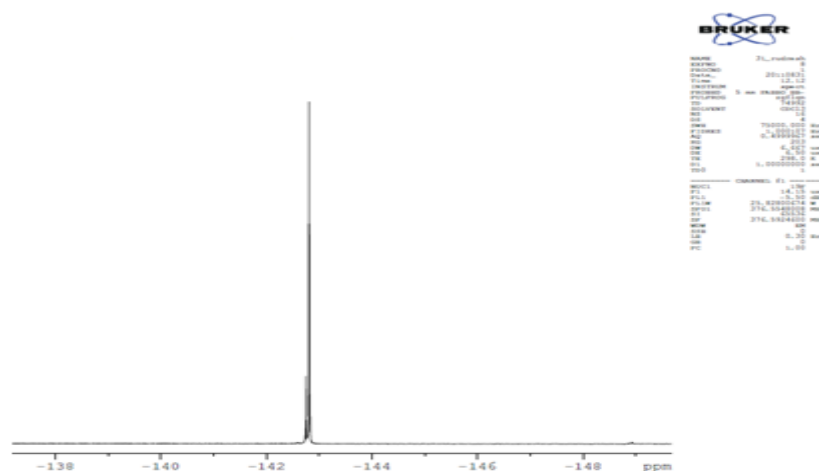
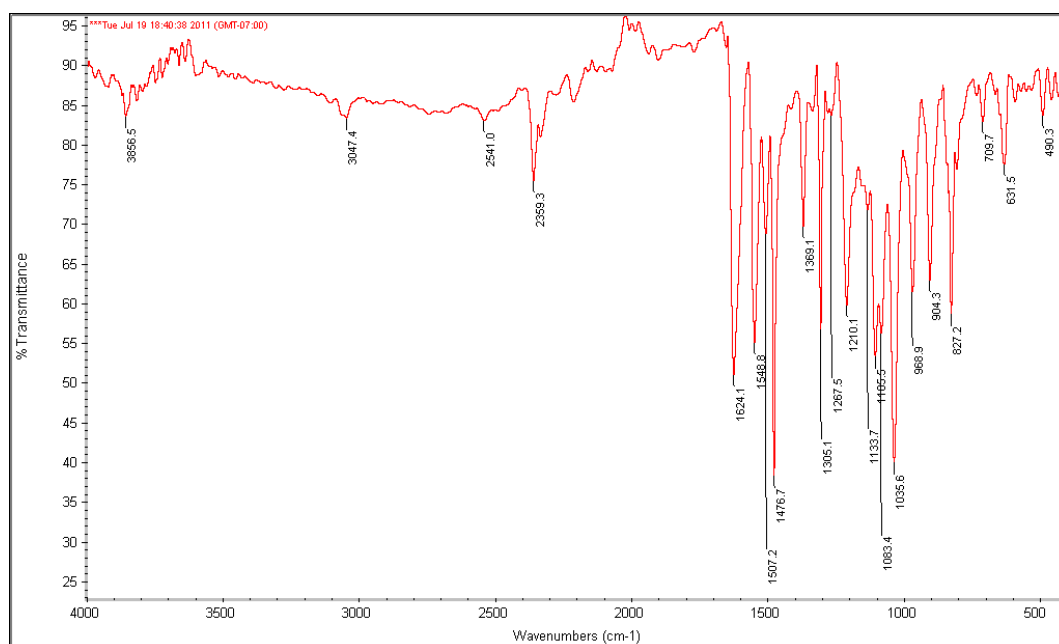
#### 7.2.5.2 Synthesis of the boron complex **18C**

The compound **18C** was prepared following the same procedure used for **17C**. Reaction of **L<sub>10</sub>** (0.2 g, 0.591 mmol), Boron trifluoride diethyletherate (0.29 g, 2.07mmol) and triethylamine (0.3 ml) in 40 ml anhydrous benzene gave **18C** as a light green-yellow solid purified by recrystallization. Yield: 75%.  $^{19}\text{F}$  NMR (400MHz,  $\text{CDCl}_3$ ), [ $\delta$ , ppm]: 142.28 (Figure 7.8). IR ( $\text{cm}^{-1}$ ): 1620.2, 1209.9 (Figure 7.9). Anal calcd for  $\text{C}_{20}\text{H}_{12}\text{B}_2\text{Cl}_2\text{F}_4\text{N}_2\text{O}_2$ , C 49.95 %, H 2.49 %.N 5.82%. Found C 49.34 %, H 2.38 %. N 5.43%.UV-vis:  $\lambda_{\text{max}}$ /nm (DMSO) 335.2 and 395.0 (Figure 7.16).

Figure 7.8  $^{19}\text{F}$  NMR spectrum of complex **18C**Figure 7.9 IR spectrum of complex **18C**

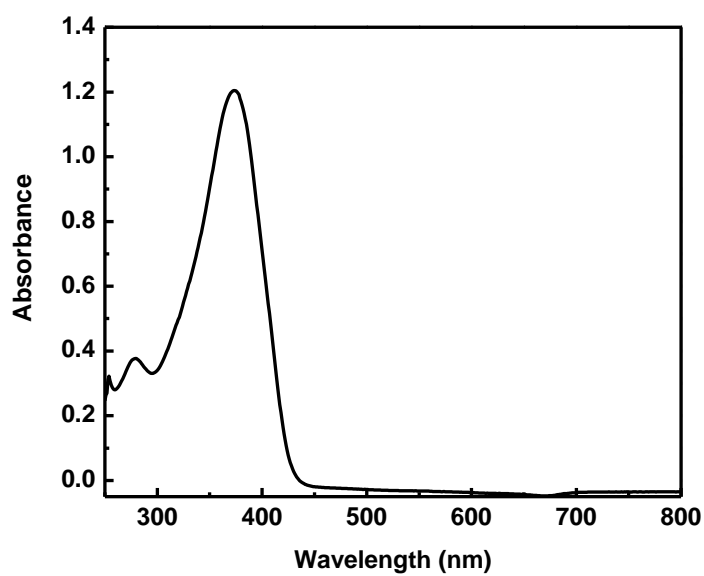
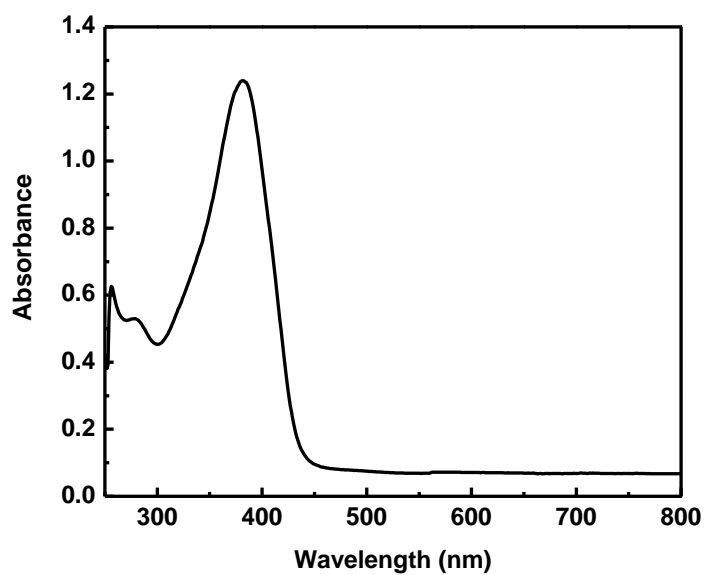
### 7.2.5.3 Synthesis of the boron complex **19C**

The compound **19C** was prepared following the same procedure used for **17C**. Reaction of **L11** (0.2 g, 0.42 mmol), Boron trifluoride diethyletherate (0.23 g, 1.68mmol) and triethylamine (0.3 ml) in 40 ml anhydrous benzene gave **8C** as a light green-yellow solid purified by recrystallization. Yield: 75%.  $^{19}\text{F}$  NMR (400MHz,  $\text{CDCl}_3$ ), [ $\delta$ , ppm]: 142.81 (Figure 7.10). IR (KBr,  $\text{cm}^{-1}$ ): 1624.1, 1210.1 (Figure 7.11). Anal calcd for  $\text{C}_{20}\text{H}_{14}\text{B}_2\text{Br}_2\text{F}_4\text{N}_2\text{O}_2$ , C 42.15%, H 2.1%, N 4.91%. Found C 42.12 %, H 2.00 %. N 4.66%. UV-vis:  $\lambda_{\text{max}}$ /nm (DMSO) 331.6 and 394.20 (Figure 7.17).

Figure 7.10  $^{19}\text{F}$  NMR spectrum of complex **19C**Figure 7.11 IR spectrum of complex **19C**

### 7.2.6 Linear optical study

The electronic spectra of the ligands ( $L_9$ - $L_{11}$ ) and complexes (**17C**-**19C**) are shown in Figures 7.12-7.14 and 7.15-7.17 respectively. Spectrum of complexes are dominated by one main absorption band in the region 375-295 nm and a shoulder near 330 nm which are ascribed to the  $\pi$  to  $\pi^*$  transitions. From the spectra it confirms that main absorption band of complexes are red shifted compared to the free ligands.

Figure 7.12 UV-visible spectrum of ligand L<sub>9</sub>Figure 7.13 UV-visible spectrum of ligand L<sub>10</sub>

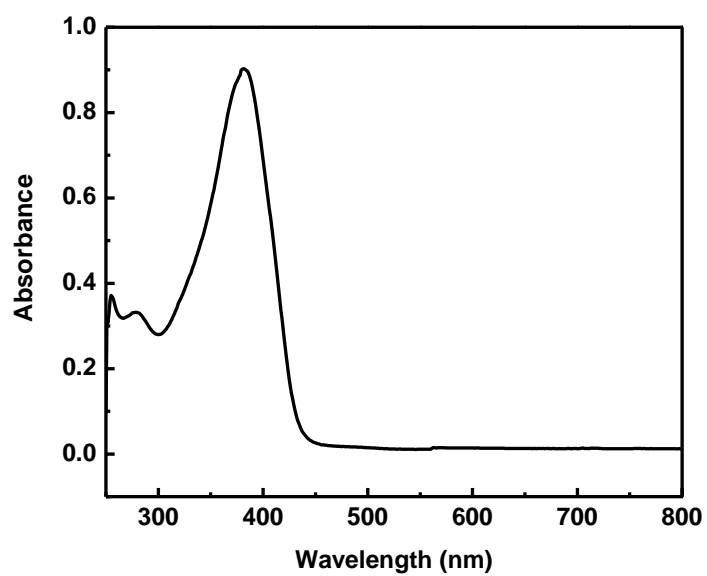
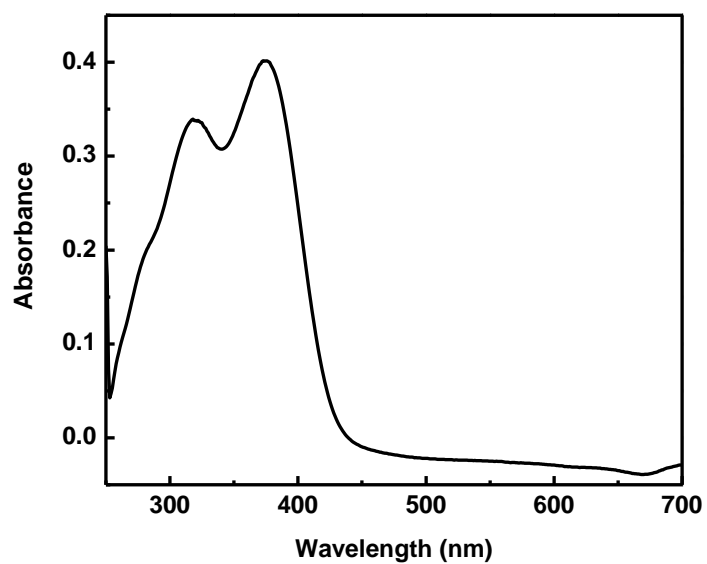
Figure 7.14 UV-visible spectrum of ligand L<sub>11</sub>

Figure 7.15 UV-visible spectrum of complex 17C

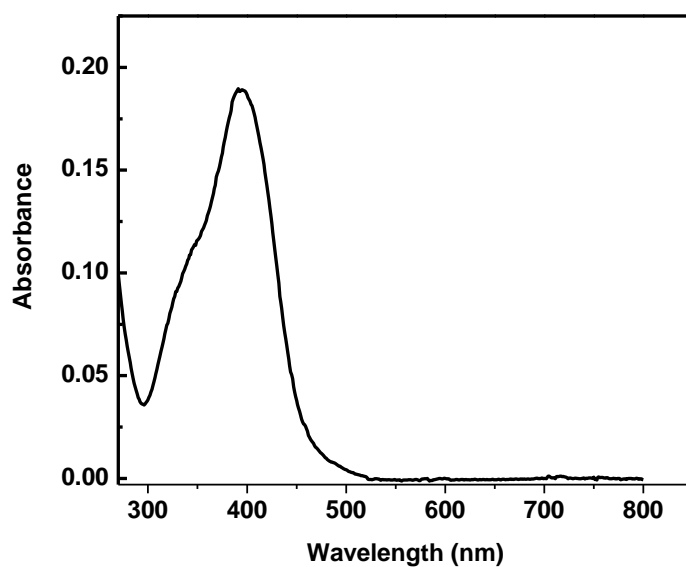


Figure 7.16 UV-visible spectrum of complex 18C

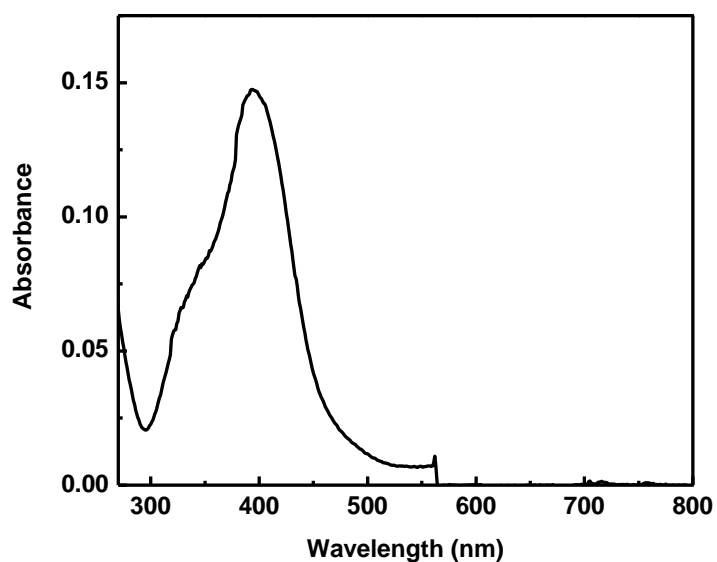


Figure 7.17 UV-visible spectrum of complex 19C.

## 7.3 RESULTS AND DISCUSSION

### 7.3.1 Spectral analysis

The bis-salicylaldiminato Schiff-bases **L<sub>9</sub>**-**L<sub>11</sub>** were synthesized from refluxing the corresponding amines with salicylaldehyde derivatives and then their boron

complexes were prepared using a method slightly modified from that reported by QiufeiHou et al. 2007. The resulting boron compounds were characterized with  $^1\text{H}$  NMR,  $^{19}\text{F}$  NMR, IR, UV-visible spectroscopy and elemental analysis.  $^1\text{H}$  NMR spectra of complex 6C shows  $\delta$  values for the proton higher shifted upon complexation from that of free ligands. Further absence of peak for the hydroxyl proton in the spectrum shows participation of phenolic oxygen atom in the complex. The IR spectra of complexes show absorption bands at  $\sim 1620\text{ cm}^{-1}$  assigned to the C=N stretching of ligands coordinated to the metal through the nitrogen atoms (Blanca et al. 2008). These bands are shifted to the higher wave number compared with free ligands ( $\sim 1610\text{ cm}^{-1}$ ). UV- visible spectrum of complexes are dominated by one main absorption band in the region 375-295 nm and a shoulder near 330 nm which are ascribed to the  $\pi$  to  $\pi^*$  transitions. From the spectra it confirms that main absorption band of complexes are red shifted compared to the free ligands.

### 7.3.2 Nonlinear optical studies

The open aperture z-scan curves of complexes **17C-19C** are shown in Figures 7.18-7.20. All these curves show an increase in absorption when the sample is nearing the beam focus. Since the residual absorption of the samples at the excitation wavelength is in the vicinity of 50%, the nonlinearity can be expected to arise from a two-step or three-step excitation process involving real excited states, which essentially amounts to reverse saturable absorption (RSA). Genuine two-photon (2PA) and three-photon (3PA) absorption involving virtual states also can take place in the system, but these will be relatively weak compared to the RSA process. However, an excitation where two photons are involved will numerically fit to a two-photon absorption equation irrespective of whether real or virtual states are involved. Similarly, if three photons are involved, it will fit to a three-photon absorption equation. Therefore we tried to fit our data to two-photon and three-photon equations, and the best fit was obtained to the two-photon process described by the nonlinear transmission equation (Sutherland 1996)

$$T = \left( \frac{(1-R)^2 \exp(-\alpha L)}{\sqrt{\pi q_0}} \right) \int_{-\infty}^{\infty} \ln \left[ \sqrt{1 + q_0 \exp(-t^2)} \right] dt \quad (7.1)$$

where  $T$  is the actual  $z$ -dependent sample transmission (product of linear transmission and normalized transmittance), and  $L$  and  $R$  are the length and surface reflectivity of the sample respectively.  $\alpha$  is the linear absorption coefficient.  $q_0$  is given by  $\beta(1 - R)I_0L_{eff}$ , where  $\beta$  is the two-photon absorption coefficient, and  $I_0$  is the on-axis peak intensity.  $L_{eff}$  is given by  $1 - \exp^{-\alpha l}/\alpha$ . The quantity  $\beta$  here is the *effective* 2PA coefficient, as it is a lumped coefficient for the effects of RSA as well as genuine 2PA. The  $\beta$  values of complexes are summarized in Table 7.1. In all the complexes strong excited state absorption was found to happen concurrently with genuine 2PA, since the samples used had some residual absorption at the excitation wavelength of 532 nm.

The Open aperture  $Z$ -scan (i.e. without aperture in front of the detector) was performed to measure the nonlinear absorption in the sample, which is related to imaginary part of third-order optical susceptibility  $\chi^{(3)}$ . Figures 7.18-7.20 show the open aperture  $Z$ -scan curves of the complexes which are symmetric with respect to the focus indicating intensity dependent absorption. The absorption may be due to two photon absorption (TPA), excited state absorption (ESA), reverse saturable absorption (RSA), etc. Nonlinear absorption of nanosecond pulses can be understood using the five level model (Feng et al. 2005 and Unnikrishnan et al. 2002) shown in Figure. 3.25. The relevant energy levels are the singlet levels  $S_0$ ,  $S_1$ , and  $S_2$  and the triplet levels are  $T_1$  and  $T_2$ . Each of these states contains number of vibrational levels. When the molecule is excited by the laser pulse, electrons are initially excited from lowest vibrational level of  $S_0$  to upper vibrational levels of  $S_1$ , where they relax in picoseconds by nonradiative decay. In nanosecond time scale, singlet transition does not deplete the population of  $S_1$  level appreciably, since atoms excited to  $S_2$  decay to  $S_1$  itself within picoseconds. From  $S_1$ , electrons are transferred to  $T_1$  via intersystem crossing (ISC), from where transitions to  $T_2$  occur. The process ( $S_0 \rightarrow S_1$ ) is known as ground state absorption. The two process ( $S_1 \rightarrow S_2$ ) and ( $T_1 \rightarrow T_2$ ) are known as ESA (Excited state absorption) and if the excited state absorption cross-sections ( $\sigma_s$ ) are larger than that of the ground state ( $\sigma_G$ ) the process is called RSA (reverse saturable absorption). With excitation of laser pulses on the nanosecond scale, which

is true in our case, triplet-triplet transitions are expected to make significant contribution to nonlinear absorption.

Table 7.1 The values of the two-photon absorption (2PA) coefficients  $\beta$  of the complexes 17C-19C

Complex	Z-scan result $\beta$ (m/W)
17C	$2.99 \times 10^{-11}$
18C	$2.42 \times 10^{-11}$
19C	$0.93 \times 10^{-11}$

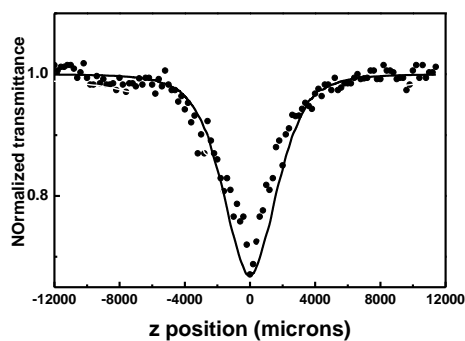


Figure 7.18 Open aperture z-scan traces for complex **17C**. The filled circles are measured data points and solid curve is the numerically calculated fit for a two-photon absorption process using Equation 7.1.

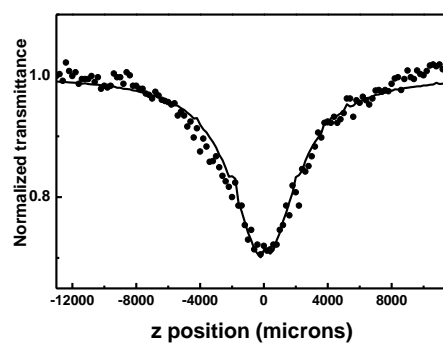


Figure 17.19 Open aperture z-scan traces for complex **18C**. The filled circles are measured data points and solid curve is the numerically calculated fit for a two-photon absorption process using Equation 7.1.

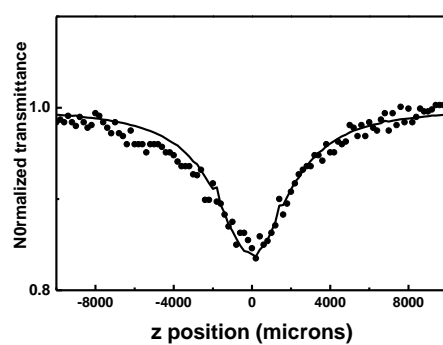


Figure 7.20 Open aperture z-scan traces for complex **19C**. The filled circles are measured data points and solid curve is the numerically calculated fit for a two-photon absorption process using Equation 7.1.

## CHAPTER 8

### SUMMARY AND CONCLUSIONS

#### *Abstract*

*This chapter provides the summary of the work presented in this thesis along with the conclusions.*

The work presented in this thesis has been broadly divided into seven chapters with several sections in each chapter. The First Chapter titled 'Introduction' outlines the brief introduction about nonlinear optics and subsequent sections give general introduction to nonlinear optical process, experimental techniques for the determination of NLO properties, nonlinear optical materials and coordination complexes as NLO materials. The Second Chapter titled 'A brief overview of the previous work' outlines the literature survey concerning coordination complexes as NLO materials and at the end objectives and scope of the present work was described. The following observations were drawn from the results presented in different chapters. Chapter 3 provides a detailed synthetic procedure of six metal complexes. From the analytical and spectral studies, tetrahedral structure has been assigned to the complexes. Third-order nonlinear optical properties of these novel complexes was investigated using the nano second single beam Z-scan technique. Z-scan results indicate that the complexes exhibit self-defocusing effect. The operating nonlinear mechanism leading to optical power limiting was found to be reverse saturable absorption. Strong dipolar interactions between metal ions (Zn(II), Cd(II) and Hg(II)) and ligands are the responsible factors for this observed third-order nonlinear optical response. The high thermal stability and large optical nonlinearity of these complexes offer them potential candidate as a NLO applications. Chapter 4 describes the third-order optical nonlinearity of the composite film of coordination complexes [CoL<sub>2</sub>PPh<sub>3</sub>Cl] (7C) and [PdL<sub>2</sub>PPh<sub>3</sub>] (8C) (L<sub>2</sub>=N-(2-pyridyl)-N'-(salicylidene) hydrazine, PPh<sub>3</sub> = triphenylphosphine) with PMMA have been investigated by using Differential Optical Kerr Gate (DOKG) and open aperture Z-scan measurements. The ultrafast third-order nonlinearity of composite film of coordination complexes and

PMMA were estimated to be as large as  $10^{-10}$  esu. by femto second optical Kerr gate technique. The single beam Z-scan technique was used to investigate the nonlinear absorption property of the composite near 800 nm. Open aperture Z-scan measurement, showed that the complexes exhibit saturable absorption. The nonlinear absorption coefficient of complexes 7C and 8C are found to be  $-3.2 \times 10^{-11}$  m/W  $-2.3 \times 10^{-11}$  m/W respectively. The NLO studies on a series of metal complexes derived from these reported complexes will help us to understand metal–ligand charge transfer and identify ways to enhance the nonlinear absorption cross sections in these complexes. Having large value of  $\chi^{(3)}$  and ultrafast response time makes these complexes as a potential optical materials in ultrafast photonic devices. Chapter 5 deals with the synthesis, characterization and third-order nonlinear optical studies of copper (I) complexes  $[\text{Cu}(\text{Cl})(\text{N},\text{N}'\text{-C}_{12}\text{H}_6\text{N}_2\text{O}_2)(\text{PPh}_3)]$ ,  $[\text{Cu}(\text{Br})(\text{N},\text{N}'\text{-C}_{12}\text{H}_6\text{N}_2\text{O}_2)(\text{PPh}_3)]$  and  $[\text{Cu}(\text{I})(\text{N},\text{N}'\text{-C}_{12}\text{H}_6\text{N}_2\text{O}_2)(\text{PPh}_3)]$ . Nonlinear optical properties of the complexes are investigated at 532 nm using single beam Z-scan technique employing nanosecond laser pulses. From analytical and spectral studies, a distorted tetrahedral structure has been assigned to the complexes. Being a polarizable molecular system with  $\pi$ -conjugated pathways having an asymmetric charge distribution, strong intra molecular charge transfer excitations exist in these compounds. These contribute substantially to the observed nonlinearity. Chapter 6 describes the synthesis, characterization and third-order nonlinear optical studies of boron 2-hydroxychalcone complexes. From the analytical and spectral studies, the formation and tetrahedral geometry of the complexes was confirmed. Nonlinear optical properties of the complexes are investigated at 532 nm using single beam Z-scan technique employing nanosecond laser pulses. Z-scan studies show that all investigated complexes exhibit large optical third-order nonlinearity. Strong donor-acceptor mechanism (“push-pull” system), is the responsible factors for this observed third-order nonlinear optical response. The complexes show optical limiting behaviour due to “effective” two-photon absorption. Chapter 7 represents synthesis of substituted ligands N,N'-p-phenylene bis(salicylideneimine) as well as their coordinatively saturated binuclear boron complexes were synthesized and characterized. From the analytical and spectral studies, the formation of the complexes and their tetrahedral coordination geometry was confirmed. Nonlinear optical properties of the complexes are investigated at 532

nm using single beam Z-scan technique employing nanosecond laser pulses. Observed nonlinearity in these binuclear complexes is because of highly electron withdrawing boron atoms attached to the  $\pi$ -bridge. This makes the complexes highly polarizable. The complexes show optical limiting behaviour due to “effective” two-photon absorption.

Formation and structure of the ligands and complexes were confirmed from various analytical and spectroscopic techniques. Being a polarizable molecular system with  $\pi$ -conjugated pathways having an asymmetric charge distribution, strong intra molecular charge transfer excitations exists in these compounds. These contribute substantially to the observed nonlinearity. Observed effective TPA coefficients ( $\beta$ ) of all complexes found to be large in the order of  $10^{-11}$ . The high thermal stability and large optical nonlinearity of these complexes make them potential candidates for photonic applications such as frequency up conversion lasing, three-dimensional fluorescence imaging and multi photon microscopy etc.



**REFERENCES**

Afanasev A.V., Zinoviev A.P., Antipov O.L., Bushuk B.A., Bushuk S.B., Rubinov A.N., Yu. Fominih J., Klapshina L.G., Domrachev G.A and Douglas W.E. (2002). "Picosecond z-scan measurements of nonlinear optical susceptibility of films and solutions of novel organometallic polymers." *Opt. Commun.* 201, 207-215.

Akrivos P.D., Hadjikakou S.K., Karagiannidis P., Mentzafos D and Terzis A. (1993). "Study of the geometric preferences of copper(I) halide coordination compounds with triarylphosphines. Crystal structure of  $[\text{Cu}_2\text{I}_2\{\text{P}(\text{m-tolyl})_3\}_3]$ ." *Inorg.Chim.Acta.*, 206, 163-168.

Albota M., Beljonne D., Bredas J.L., Ehrlich J.E., Fu J.Y, Heikal A.A., Hess S.E., Kogej T., Levin M.D., Marder S.R., McCord-Maughon D., Perry J.W., Rockel H., Rumi M., Subramaniam G., Webb W.W., Wu X.L and Xu C. (1998). "Design of Organic Molecules with Large Two-Photon Absorption Cross Sections." *Science* 281, 1653-1656.

Aslanidis P., Cox P.J., Karagiannidis P., Hadjikakou S.K and Antoniadis C.D. (2002). "Copper(I) Halide Complexes with Triphenylphosphane and Heterocyclic Thione Ligands: The Crystal Structures of  $[\text{Bis}(\text{Triphenylphosphane})(\text{Benzimidazole-2-Thione})\text{Copper(I) Iodide}]$ ,  $[\text{Bis}(\text{Triphenylphosphane})(\text{Benzothiazole-2-Thione})\text{Copper(I) Iodide}]$ , and  $\text{Bis}[\mu\text{-5-(Benzimidazole-2-Thione)}(\text{Triphenylphosphane})\text{Copper(I) Chloride}]$ ." *Eur. J. Inorg. Chem.*, 2216-2222.

Aslanidis P., Hadjikakou S.K., Karagiannidis P., Kojic-Prodic B and Luic M. (1994). "Preparation and spectral studies of dinuclear mixed-ligand copper(I) complexes. The crystal structure of  $\text{bis}[\mu\text{-s}(\text{pyridine-2-thione})(\text{tntp}) \text{copper(I) bromide}]$ ." *Polyhedron*, 13, 3119-3125.

Bartholomew G.P., Rumi M., Pond S.J.K., Perry J.W., Tretiak S., Bazan G.C. (2004). "Two-Photon Absorption in Three-Dimensional Chromophores Based on [2.2]-Paracyclophane." *J. Am. Chem. Soc.* 126, 11529-11542.

Benning R. G. (1995). "Chromophores for second-order non-linear optic materials." *J. Mater. Chem.*, 5, 365-378.

Bernard R., Cornu D., Baldeck P.L., Caslavsky J., Letoffe J.M., Scharff J.P and Miele P. (2005). "Synthesis, characterization and optical properties of  $\pi$ -conjugated systems incorporating *closo*-dodecaborate clusters: new potential candidates for two-photon absorption processes." *Dalton Trans.* 3065–3071.

Bhawalkar J.D., He G.S and Prasad P.N. (1996). "Nonlinear multiphoton processes in organic and polymeric materials." *Rep. Prog. Phys.* 59, 1041.

Bhawalkar J.D., He G.S., Park C.K., Zhao C.F., Ruland G and Prasad P.N. (1996). "Efficient, two-photon pumped green upconverted cavity lasing in a new dye." *Opt. Commun.* 124, 33-37.

Bhawalkar J.D., Kumar N.D., Zhao C.F and Prasad P.N. (1997). "Two-photon photodynamic therapy." *J. Clin. Laser Med. Surg.* 15, 201-204.

Bing Gu., Yue-Hua Wang., Xian-Chu Peng., Jian-Ping Ding., Jing-Liang He., Hui-Tian Wang. (2004). "Giant optical nonlinearity of a  $\text{Bi}_2\text{Nd}_2\text{Ti}_3\text{O}_{12}$  ferroelectric thin film." *Appl. Phys. Lett.* 85, 3687-3689.

Biradar N.S., Patil B.R and Kulkarni, V.H. (1976). "Tin(IV) complexes with 2-methoxy-2'-hydroxy chalcones." *Inorg.Chim.Acta.* 20, 183-185.

Birdar N. S., Patel B.R and Kulkarni V.H. (1975). "Complexes of nickel(II) with o,o'-dihydroxy chalcones." *Inorg.Chim.Acta.* 15, 33-38.

Blanca M. Munoz, Rosa Santillan, Mario Rodriguez, Jose Manuel Mendez, Margarita Romero, Norberto Farfan, Pascal G. Lacroix, Keitaro Nakatani, Gabriel Ramos-Ortiz, Jose Luis Maldonado. (2008). "Synthesis, crystal structure and non-linear optical properties of boronates derivatives of salicylideneiminophenols." *J. Organomet. Chem.* 693, 1321–1334.

Bourgault, M., Mountassir, C., Le Bozec, H., Ledoux, I., Pucetti, G and Zyss, J. (1993). "synthesis and second-order Nonlinear Optical properties of New Bipyridyl Metal Complexes." *J.Chem.Soc.,Chem.Commun.*, 1623-1624.

- Bredas J.L., Meyers F., Pierce B.M. and Zyss J. (1992). "On the second-order polarizability of conjugated  $\pi$ -electron molecules with octupolar symmetry: the case of triaminotrinitrobenzene." *J. Am. Chem. Soc.* 114, 4928-4929.
- Burland D.M. (1994). "Optical Nonlinearities In Chemistry: Introduction." *Chem. Rev.* 94, 1-2.
- Catharina Hiort., Per Lincoln and Bengt Norden. (1993). "DNA binding of  $\Delta$ - and  $\Lambda$ -[Ru(phen)<sub>2</sub>DPPZ]<sup>2+</sup>." *J. Am. Chem. Soc.* 115, 3448-3454.
- Chao H., Li R.H., Ye B.H., Li H., Feng X.L., Cai J.W., Zhou J.Y and Ji L.N. (1999). "Syntheses, characterization and third order non-linear optical properties of the ruthenium(II) complexes containing 2-phenylimidazo[4,5-f][1,10]phenanthroline derivatives." *J. Chem. Soc. Dalton Trans.* 3711-3717.
- Chemla D.S., Oudar J.L and Jerphagnon J. (1975). "Origin of the second-order optical susceptibilities of crystalline substituted benzene." *Phys. Rev. B*, 12, 4534-4546.
- Cheng L.T., Tam W and Eaton D.F. (1990). "Quadratic hyperpolarizabilities of Group 6A metal carbonyl complexes." *Organometallics*, 9, 2856-2857.
- Cho B.C., Son K.H., Lee S.H., Song Y.S., Lee Y.K., Jeon S.J., Choi J.H., Lee H and Cho M. (2001). "Two Photon Absorption Properties of 1,3,5-Tricyano-2,4,6-tris(styryl)benzene Derivatives." *J. Am. Chem. Soc.* 123, 10039-10045.
- Cho B.R., Piao M.J., Son K.H., Lee S.H., Yoon S.J., Jeon S.J and Cho M. (2002). "Nonlinear Optical and Two-Photon Absorption Properties of 1,3,5-Tricyano-2,4,6-tris(styryl)benzene-Containing Octupolar Oligomers." *Chem. Eur. J.* 8, 3907-3916.
- Chuang-Tian Chen and Guangzhao Liu. (1986). "Recent advances in nonlinear optical and electro-optical materials." *Ann. Rev. Mater. Sci.*, 16, 203-243.
- Chuluo Yang., Jingui Qui., Jiang Zhao., Jiahai Si., Fengzhong Dong., Yougui Wang and Peixian Ye and Cheng Ye (2001). "Synthesis and third order optical nonlinearity of some salts comprising planar complex cation and anion." *synthetic metals*, 120, 789-790.

Chung S.J., Kim K.S., Lin T.C., He G.S., Swiatkiewicz J and Prasad P.N. (1999). "Cooperative Enhancement of Two-Photon Absorption in Multi-branched Structures." *J. Phys. Chem. B* 103, 10741-10745.

Coe, B.J., Harris, J.A., Harrington, L.J., Jeffery, J.C., Rees, L.H., Houbrechts, S and Persoons, A. (1998). "Enhancement of Molecular Quadratic Hyperpolarizabilities in Ruthenium(II) 4,4'-Bipyridinium Complexes by N-Phenylation." *Inorg.chem.*, 37, 3391-3399.

Cui Y., Li F., Lu Z.H and Wang S. (2007). "Three-coordinate organoboron with a B=N bond: substituent effects, luminescence/electroluminescence and reactions with fluoride." *Dalton Trans.* 2634–2643.

Cumpston B.H., Ananthavel S.P., Barlow S., Dyer D.L., Erskine J.E., Oin A.A.J., Rockel H., Rumi M., Wu X.L., Marder S.R and Perry J.W. (1999). "Two-photon polymerization initiators for three-dimensional optical data storage and microfabrication." *Nature*, 398, 51-54.

Dalton, L. R., Harper A. W., Ghosn R., Steier W. H., Ziari M., Fetterman H., Shi Y., Mustacich R. V., Jen K. Y and Shea K. J. (1995). Synthesis and Processing of Improved Organic Second-Order Nonlinear Optical Materials for Applications in Photonics." *Chem. Mater.*, 7, 1060-1081.

Das S., Jana A., Ramanathan V, Chakraborty T., Ghosh S., Das P.K and Bharadwaj P.K. (2006). "Design and synthesis of 1,10-phenanthroline based Zn(II) complexes bearing 1D push-pull NLO-phores for tunable quadratic nonlinear optical properties." *J. Organomet. Chem.* 691, 2512-2516.

Das S., Nag A., Goswami D and Bharadwaj P.K. (2006). "Zinc(II)- and Copper(I)-Mediated Large Two-Photon Absorption Cross Sections in a Bis-cinnamaldiminato Schiff Base." *J. Am. Chem. Soc.* 128, 402-403.

Debattista N. B and Pappano N. B. (1997). "Complexant efficiency of 2'-hydroxy-4-R-chalcones for Aluminium (III) and substituent's effect." *Talanta*. 44, 1967-1971.

- Dhenaut, C., Ledoux, I., Samuel, I.D.W., Zyss, J., Bourgault, M and Le Bolzec, H. (1995). "Chiral metal complexes with large octupolar optical nonlinearities." *Nature*, 374, 339-342.
- Dileep Ramakrishna, BadekaiRamachandraBhat. (2010). "Palladium–Schiff base–triphenylphosphinecatalyzed oxidation of alcohols." *Appl. Organomet. Chem.* 24, 663-666.
- Dileep R and RamachandraBhat B.2010. "Cobalt complexes in [EMIM]Cl – A catalyst for oxidation of alcohols to carbonyls." *Inorg. Chem. Commun.*, 13, 195-198.
- Dixon I.M., Collin J.P J.-P.Sauvage J.P and Flamigni L. (2001). "Porphyrinic Dyads and Triads Assembled around Iridium(III) Bis-terpyridine:Photoinduced Electron Transfer Processes." *Inorg. Chem.*, 40, 5507-5517.
- Ehrlich J.E., Wu X.L., Lee I.Y.S., Hu Z.Y., Roedel H., Marder S.R and Perry J.W. (1997). "Two-photon absorption and broadband optical limiting with bis-donor stilbenes." *Opt. Lett.* 22, 1843-1845.
- Elbing M and Bazan G.C. (2008). "A New Design Strategy for Organic Optoelectronic Materials by Lateral Boryl Substitution." *Angew. Chem. Int. Ed.* 47, 834–838.
- Entwistle C.D and Marder.T.B. (2002). "Boron Chemistry Lights the Way: Optical Properties of Molecular and Polymeric Systems." *Angew.Chem. Int. Ed.* 41, 2927–2931.
- Evans O.R and Lin W. (2002). "Crystal Engineering of NLO Materials Based on Metal–Organic Coordination Networks." *Acc. Chem. Res.* 35, 511-522.
- Feng W., Yi W., Wu H., Ozaki M., and Yoshino K. (2005). "Enhancement of third-order optical nonlinearities by conjugated polymer-bonded carbon nanotubes." *J. Appl. Phys.*, 98, 034301-034307.
- Fleitz P.A., Sutherland R.A., Stroghendl F.P., Larson F.P and Dalton L.R. (1998). "Nonlinear measurements on AF-50." *SPIE Proc.* 3472, 91.

- Franken, P.A., Hill, A.E., Peters, C.W and Weinreivh (1961). "Generation of Optical Harmonics." *Phys.Rev.Lett.*,7, 118-119.
- Frazier C.C and Harvey M.A. (1986). "Second-harmonic generation in transition-metal-organic compounds." *J. Phys. Chem.*, 90, 5703-5706.
- Green M.L.H., Marder S.R., Thompson M.E., Bandy J.A., Bloor D., Kolinsky and Jones R.J. (1997). "Synthesis and structure of (cis)-[1-ferrocenyl-2-(4-nitrophenyl)ethylene], an organotransition metal compound with a large second-order optical nonlinearity." *Nature*, 330, 360-362.
- Hadjikakou S.K., Akrivos P.D., Karagiannidis P., Mentzafos D and Terzis A. (1993). "Study of the geometric preferences of copper(I) halide coordination compounds with triarylphosphines. Crystal structures of  $[\text{CuCl}\{\text{P}(o\text{-tolyl})_3\}]_2$  and  $[\text{CuBr}\{\text{P}(o\text{-tolyl})_3\}]_2$  ." *Inorg.Chim.Acta.*, 210, 27-31.
- Hadjikakou S.K., Antoniadis C.D., Aslanidis P., Cox P.J and Tsipis A.C. (2005). "An Exploration of the Structural and Bonding Variability in Mixed-Ligand Benzimidazole-2-thione(bromo)(triarylphosphane)dicopper(I) Complexes with Diamond-Shaped  $\text{Cu}_2(\mu\text{-X})_2$  Core Structures." *Eur. J. Inorg. Chem.*, 1442-1452.
- Haglund, R.F., Yang, L., Magruder III, R.H., Wittig, J.E., Becker, K and Zuhr, R.A. (1993). "Picosecond nonlinear optical response of a Cu:silicananocluster composite." *Optics Letters*, 18, 373-375.
- Halvorson C., Hays A., Kraabel B., Wu R., Wudl F and Heeger A.J. (1994). "A 160-Femtosecond Optical Image Processor Based on a Conjugated Polymer." *Science*, 265, 1215-1216.
- Hawthorne M. F and Lee M. W. (2003). "A critical assessment of boron target compounds for boron neutron capture therapy." *J. Neurooncol.* 62, 33-45.
- He G.S., Bhawalkar J.D., Zhao C.F and Prasad P.N. (1995). "Optical limiting effect in a two-photon absorption dye doped solid matrix." *Appl. Phys. Lett.* 67, 2433.

He G.S., Zhao C.F., Bhawalkar J.D and Prasad P.N. (1995). "Two-photon pumped cavity lasing in novel dye doped bulk matrix rods." *Appl. Phys.Lett.*67, 3703.

Hongliang, Yang.,Xinqiang, Wang., Quan, Ren., Guanghui, Zhang., Xiangbing, Sun., Lin, Feng., Shufeng, Wang and Zhenwei, Wang (2005). "Study on the third-order nonlinear optical properties of bis(tetrabutylammonium)bis(1,3-dithiole-2-thione-4,5-dithiolato)cadium." *Opt. Commu.* 256, 256-260.

Horacio Reyes, Ma. Concepcion Garcia, Blanca M. Flores, Hector Lopez-Rebolledo, Rosa Santillan and Norberto Farfan. (2006). "Synthesis, NMR and X-Ray Diffraction Analysis of Boron Complexes Derived from Hydroxychalcones." *J. Mex. Chem. Soc.*, 50(3),106-113.

Horst Kunkely and ArndVogler. (2002). "Electronic spectra of  $\pi$ -cyclopentadienyl(triethyl phosphine) copper(I). Ligand-to-ligand charge transfer." *Inorg. Chem. Commu.*, 5, 112–114.

Hurst S.K., Humphrey M.G., Isoshima T., Wostyn K., Asselberghs I., Clays K., Persoons A., Samoc M. and Luther-Davices B. (2002). "Organometallic Complexes for Nonlinear Optics.28.<sup>1</sup> Dimensional Evolution of Quadratic and Cubic Optical Nonlinearities in Stilbenylethynylruthenium Complexes." *Organometallics* 21, 2024-2026.

Jiang Y. B., Wang X. J and Lin L. (1994). "Fluorescent Probing of the Restriction by Aqueous Micelles of the Formation of the PhotoinducedBiradical State P\* of 4-(Dimethylamino)chalcone." *J. Phys. Chem.* 98, 12367-12372.

Jingui Qin., Daoyu Liu., Chaoyang Dai., Chuangtian Chen., Baichang Wu., Chuluo Yang and Caimao Zhan (1999). "Influence of the molecular configuration on second-order nonlinear optical properties of coordination compounds." *Coord. Chem. Rev.*, 188, 23–34.

Jinhai, Si.,Qiguang, Yang., Yougui, Wang., Peixian, Ye., Shoubai, Wang., Jingui, Qin and Daoyu Liu (1996). "Excited-state enhancement of the third-order optical nonlinearity of a square planar complex." *Opt. Commu.*, 132, 311-315.

John Kiran A., Ashok Mithun., ShivaramaHolla B., Shashikala H.D., Umesh G., and Chandrasekharan K. (2007). "Nonlinear optical studies of 1-3-diaryl-propenones containing 4-methylthiophenyl moieties." *Opt. Commun.* 269, 235-240.

John Kiran A., Udayakumar D., Chandrasekharan K., Ahdikari A.V., Shashikala H.D and Reji Philip.(2007). "Nonlinear optical studies of a newly synthesized copolymer containing oxadiazole and substituted thiophenes." *Opt. Commun.* 271, 236.

Joseph, P., Morrall, Gulliver, T., Dalton, Mark G., Humphrey, and Mark, Samo (2008). "Organotransition Metal Complexes for Nonlinear Optics." *Advances in Organometallic Chemistry*, 55.

Karagiannidis P., Hadjikakou S.K., Aslanidis P and Huntas A. (1990). "Synthesis and photochemical study of Cu(I) complexes with tri-*p*-tolylphosphine and heterocyclic thiones. The crystal structure of  $[\text{CuCl}(\text{pymtH})(\text{p-CH}_3\text{C}_6\text{H}_4)_3\text{P}]_2$  ." *Inorg.Chim.Acta.*, 178, 27-34.

Karthikeyan B., Anija M, Suchandsandeep C.S., Muhammad Nadeer T.M and Reji Philip.(2008). "Optical and nonlinear optical properties of copper nanocomposite glasses annealed near the glass softening temperature." *Opt. Commun.*, 281, 2933-2937.

Kawata S., Sun H.B., Tanaka T and Takada K. (2001). "Finer features for functional microdevices." *Nature*, 412, 697-698.

Killoran J., Allen L., Gallagher J.F., Gallagher W.M and Oshea D.F, (2002). "Synthesis of BF<sub>2</sub> chelates of tetraarylazadipyrromethenes and evidence for their photodynamic therapeutic behaviour." *Chem. Commun.* 17, 1862-3.

Kiran A.J., Lee H.W., Sampath Kumar H.C., Rudresha B.J., Bhat B.R., D-IYeom., Kim K and Rotermund F. (2010). "The ultrafast nonlinear optical response and multi-photon absorption of a new metal complex in the near-infrared spectral range." *J. Opt. A* 12, 035211.

- Kogej T., Beljonne D., Meyers F., Perry J.W., Marder S.R and Bredas J.L. (1998). "Mechanisms for enhancement of two-photon absorption in donor-acceptor conjugated chromophores." *Chem. Phys. Lett.* 298, 1-6.
- Kubicki M., Hadjikakou S.K and Xanthopoulou M.N. (2001). "Synthesis, characterisation and study of mercury(II) bromide complexes with triphenylphosphine and heterocyclic thiones. The crystal structures of [bis(triphenylphosphine) dibromomercury(II)] and [dibromo (pyrimidine-2-thionato) (triphenylphosphine) mercury(II)]. Extended intra-molecular linkages via N---H...Br and C---H...Br interactions." *Polyhedron*, 20, 2179-2185.
- Kurian P.A., Vijayan C., Sathiyamoorthy K., SuchandSandeep C.S and Reji Philip.(2007). "Excitonic Transitions and Off-resonant Optical Limiting in CdS Quantum Dots Stabilized in a Synthetic Glue Matrix." *Nano. Res. Lett.* 2, 561-568.
- Kurtz S. K. (1972). "Nonlinear Optical Materials, -Laser Hand-book." Vol. 1, Ed. F. T. Arecchi, E. O. Schults-DuBois, North-Holland, Amsterdam, 923.
- Lambert C., Stadler S., Bourhill G and Brauchle C. (1996). Polarized  $\pi$ -Electron Systems in a Chemically Generated Electric Field: Second-Order Nonlinear Optical Properties of Ammonium/Borate Zwitterions." *Angew. Chem. Int. Ed. Engl.* 35, 644-646.
- Ledoux I., Zyss J., Siegel J and Lehn J.M. (1990). "Second-harmonic generation from non-dipolar non-centrosymmetric aromatic charge-transfer molecules." *Chem. Phys. Lett.* 172, 440-444.
- Lee H.W., Anthony J.K., Nguyen H.D., Mho S.I., Kim K., Lim H., Lee J and Rotermund F. (2009). "Enhancedultrafastopticalnonlinearity of porousanodizedaluminum oxide nanostructures." *Optics Express*,17, 19093.
- Lesley M. J. G., Woogward A., Taylor N. J., Marder T. B., Cazenobe I., Ledoux I., Zyss, J., Thornton A., Bruce D. W and Kakkar A. K. (1998). "Lewis Acidic Borane Adducts of Pyridines and Stilbazoles for Nonlinear Optics." *Chem. Mater.* 10, 1355-1365.

Li R., Kenyon G. L., Cohen F.E., Chen X., Gong B., Domínguez J. N., Davidson E., Kurzban G., Miller R.E., Nuzum E. O., Rosenthal P. J and McKerrow J. H. (1995). "In Vitro Antimalarial Activity of Chalcones and Their Derivatives." *J. Med. Chem.* 38, 5031-5037.

Lin C. N., Hsieh H. K., Ko H. H., Hsu M. F., Lin H. C., Chang Y. L., Chung M. I., Kang J. J., Wang J. P and Teng C. M. (2001). "chalcones as potent antiplatelet agents and calcium channel blockers." *Drug Develop. Res.* 53, 9-14.

Liu Q.D., Mudadu M.S., Schmider H., Thummel R., Tao Y and Wang S.N. (2002). Tuning the Luminescence and Electroluminescence of Diphenylboron Complexes of 5-Substituted 2-(2'-Pyridyl)indoles." *Organometallics*, 21, 4743-4749.

Liu Q.D., Mudadu M.S., Thummel R., Tao Y and Wang S.N. (2005). "From Blue to Red: Syntheses, Structures, Electronic and Electroluminescent Properties of Tunable Luminescent N,N Chelate Boron Complexes." *Adv. Funct. Mater.* 15, 143-154.

Liu Z., Fang Q., Wang D and Xu G. (2004). "Triaryl Boron-Based A- $\pi$ -A vs Triaryl Nitrogen-Based D- $\pi$ -D Quadrupolar Compounds for Single- and Two-Photon Excited Fluorescence." *OrgLett.* 6, 2933-2936.

Long N.J. (1995). "Organometallic Compounds for Nonlinear Optics—The Search for En-light-enment." *Angew Chem. Int. Ed. Engl.* 34, 21-28.

Lorimer S. D and Perry N. B. (1994). "Antifungal Hydroxy-acetophenones from the New Zealand Liverwort, *Plagiochila fasciculata*." *Planta Med.* 60, 386- 387.

Maimann, T.H (1960). "Stimulated Optical Radiation in Ruby." *Nature*, 187, 493-494.

Makita H., Tanaka T., Fujitsuka H., Tatematsu N., Satoh K., Hara A and Mori H. (1996). "Chemoprevention of 4-Nitroquinoline 1-Oxide-induced Rat Oral Carcinogenesis by the Dietary Flavonoids Chalcone, 2-Hydroxychalcone, and Quercetin." *Cancer Res.* 56, 4904-4909.

---

Marder S.R. (1992). in: D.W. Bruce, D. O'Hare (Eds.) "Inorganic Materials." Wiley, New York, p. 116.

Marder S.R., Torruellas W.E., Blanchard-Desce M., Ricci V., Stegeman G.I., Gilmour S., Bredas T., Jun Li., Bublitz G.U and Boxer S.G. (1997). "Large Molecular Third-Order Optical Nonlinearities in Polarized Carotenoids." *Science*, 276, 1233-1236.

Maria Konstantaki, Emmanuel Koudoumas, Stelios Couris, Philippe Laine, Edmond Amouyal and Sydney Leach.(2001). "Substantial non-linear optical response of new polyads based on Ru and Os complexes of modified terpyridines." *J. Phys. Chem. B* 105, 10797-10804.

Mario Rodriguez, Rigoberto Castro-Beltran, Gabriel Ramos-Ortiz, Jose Luis Maldonado, Norberto Farfan, Oscar Dominguez, Jesus Rodriguez, Rosa Santillan, Marco Antonio Meneses-Nava, Oracio Barbosa-Garcia and Jorge Peon (2009). "Synthesis and third-order nonlinear optical studies of a novel four-coordinated organoboron derivative and a bidentate ligand The effect of the N→B coordinative bond." *Syn. Met.* 159, 1281–1287.

Maruo S., Nakamura O., and Kawata S. (1997). "Three-dimensional microfabrication with two-photon-absorbed photopolymerization." *Opt. Lett.* 22, 132-134.

Mata J.A., Peris E., Uriel S., Llusar R., Asselberghs I and Persoons A. (2001). "Preparation and properties of new ferrocenylheterobimetallic complexes with counterion dependent NLO responses." *Polyhedron* 20, 2083-2088.

Mathews, S.J., Chaitanya, Kumar S., Giribabu, L and Venugopal, Rao S. (2007). "Large third-order optical nonlinearity and optical limiting in symmetric and unsymmetrical phthalocyanines studied using Z-scan." *Opt. Commun.*, 280, 206-212.

Minoshima K., Taiji M and Kobayashi T. (1991). "Femtosecond time-resolved interferometry for the determination of complex nonlinear susceptibility." *Opt. Lett.* 16, 1683-1685.

Moayad Hossaini Sadr., Jaber Jahanbin Sardroodi., Davood Zare., Neil R. Brooks William Clegg and Yinglin Song (2003). "Nonlinear optical properties and crystal

---

structure determination of a pentanuclearcopper(I) cluster  $(\text{NEt}_4)_2[\text{MoS}_4(\text{CuBp})_4]$  ( $\text{Bp} = \text{H}_2\text{B}(\text{pyrazolyl})_2$ )." *Polyhedron*, 25, 3285–3288.

Montana M. P., Pappano N. B and Debattista N. B. (1998). "New analytical reagents for europium(III)." *Talanta*. 47, 729-733.

Munoz B.M., Santillan R., Rodriguez M., Mendez J.M., Romero M., Farfan N., Lacroix P.G., Nakatani K., Ramos-Ortiz G and Maldonado J.L. (2008). "Synthesis, crystal structure and non-linear optical properties of boronates derivatives of salicylideniminophenols." *J. Organomet. Chem.* 693, 1321–1334.

Nalwa H.S and Miyata S. (1997). "Nonlinear Optics of Organic Molecules and Polymers." CRC Press, Boca Raton, FL.

Nalwa H.S. (1991). "Organometallic materials for nonlinear optics." *Appl. Organomet. Chem.*, 5, 349-377.

Naseema K., VSujith K., Manjunatha K.B., BalakrishnaKalluraya., Umesh G and Vijayalakshmi Rao G. (2010). *Optic Laser &Tech.* 42, 741.

Painelli A., Del Freato L and Terenziani F. (2001). "Vibronic contributions to resonant NLO responses: two-photon absorption in push–pull chromophores." *Chem. Phys. Lett.* 346, 470-478.

Palaniandavar M and Natarajan, C. (1980). "Cobalt(II), nickel(II) and copper(II) complexes of some 2'-hydroxychalcones." *Aust. J. Chem.* 33, 737-745.

Pati S.K., Marks T.J and Ratner M.A. (2001). "Conformationally Tuned Large Two-Photon Absorption Cross Sections in Simple Molecular Chromophores." *J. Am. Chem. Soc.*, 123, 7287-7291.

Peticolas W.L. (1967). "Multiphoton spectroscopy." *Annu. Rev. Phys. Chem.* 18, 233-260.

Pizzotti M., Ugo R., Roberto D., Bruni S., Fantucci P and Rovizzi C. (2002). "Organometallic Counterparts of Push–Pull Aromatic Chromophores for Nonlinear

Optics: Push–Pull Heteronuclear Bimetallic Complexes with Pyrazine and *trans*-1,2-Bis(4-pyridyl)ethylene as Linkers.” *Organometallics*, 21, 5830-5840.

Pond S.J.K., Tsutsumi O., Rumi M., Kwon O., Zojer E., Bredas J.L., Marder S.R and J.W. Perry J.W. (2004). “Metal-Ion Sensing Fluorophores with Large Two-Photon Absorption Cross Sections: Aza-Crown Ether Substituted Donor–Acceptor–Donor Distyrylbenzenes.” *J. Am. Chem. Soc.* 126, 9291-9306.

Poornesh P., Pramod K. Hegde, Umesh G., Manjunatha M.G., Manjunatha K.B and Adhikari A.V. (2010). “Nonlinear optical and optical power limiting studies on a new thiophene-based conjugated polymer in solution and solid PMMA matrix.” *Optic Laser & Tech.* 42, 230-236.

Poornesh P., SeetharamShettigar., Umesh G., Manjunatha K.B., PrakashKamath K., Sarojini B.K and Narayana B. (2009). “Nonlinear optical studies on 1,3-disubstituent chalcones doped polymer films.” *Opt. Mater*, 31, 854-85.

Poornima S, Liyanage, Rohini de Silva M and Nalin de Silva K.M. (2003). “Nonlinear optical (NLO) properties of novel organometallic complexes: high accuracy density functional theory (DFT) calculations.” *J. Mol. Struct. (Theochem)*, 639, 195-201.

Prasad P.N and Williams D.J. (1991). “Introduction to Nonlinear Optical Effects in Molecules and Polymers.” Wiley Interscience: New York: 300–302.

Qiufei H., Liyan Z., Hongyu Z., Yue W and Shimei J. (2007). “Synthesis and luminescent properties of two Schiff-base boron complexes.” *Journal of Lumin.* 126, 447–451.

Qiyang Chen, Kuang Li, Sargent E.H and ZhiYuang Wang.(2003). “Ultrafast nonresonant third-order optical nonlinearity of fullerene-containing polyurethane films at telecommunication wavelengths.” *Appl. Phys. Lett.*, 83, 2115-2117.

Raghava Naidu R. (1975). “2'-hydroxychalcone as an analytical reagent for beryllium.” *Talanta*. 22, 614-616.

Rangel-Rojo, R., Kimura, K., Matsuda, H., Mendez-Rojas, M.A and Watson, W.H. (2003). "Dispersion of the third-order nonlinearity of a metallo-organic compound." *Opt. Commun.*, 228, 181-186.

Rei Okamura, TetsuakiFujihara, Tohru Wada, Koji Tanaka. (2006). "Comparison of Basicity of the Diimine and Quinoid Group of 1,10-Phenanthroline-5,6-dione Ligated on Pt(II)" *Bull. Chem. Soc. Jpn.*, 79, 106-112.

Reinhardt B., Brott L.L., Clarson S.J., Dillard A.G., Bhatt J.C., Kannan R., Yuan L., He G.S and Prasad P.N. (1998). "Highly Active Two-Photon Dyes: Design, Synthesis, and Characterization toward Application." *Chem. Mater.* 10, 1863-1874.

Ren, Q., Sun, X.B., Wang, X. Q., Zhang, G.H., Yang, X.D., Zhang, F.J., Yang, H.L., Chow, Y.T and Xu D. (2008). "Short pulse Z-scan investigations of optical nonlinearities of a novel organometallic complex:  $[(C_2H_5)_4N]_2[Cu(dmit)_2]$  at 532 and 1064nm" *Appl. Phys.*, A 90, 685–688.

Ren, Q., Wang, X.Q., Yang, H.L., Zhang, G.H., Sun, X.B., Guo, W.F., Zhang, F.J., Zhang, X., Chow, Y.T., and Xu, D. (2007). "Third order optical nonlinearity of a novel material:  $[(C_4H_9)_4N][Co(dmit)_2]$ ." *Laser physics*, 17 (8), 1058-1061.

Reyes H., Munoz B.M., Farfan N., Santillan R., Rojas-Lima S., Lacroix P and Nakatani K. (2002). "Synthesis, crystal structures, and quadratic nonlinear optical properties in a series of push–pull boronate derivatives." *J. Mater. Chem.* 12, 2898–2903.

Robert W. Boyd (1992). "Nonlinear optics." Academic Press, INC. Harcourt Brace Jovanovich, Publishers Boston, San Diego, New York, London, Sydney, Tokyo, and Toronto.

Rudzinski W.E., Aminabhavi T.M., Biradar N.S and Patil, C.S. (1983). "Tellurium complexes with substituted chalcones." *Inorg.Chim.Acta.* 70, 175-178.

Sampath Kumar H.C., RamachandraBhat B, Rudresha B.J., Ravindra R and Reji Philip., (2010). "Synthesis, Characterization and Non-linear optical studies of N, N'-

bis(2-hydroxynaphthalidene)phenylene-1,2-diamine) of M (M= Ni(II), Zn(II) and Fe (II)) Schiff-Base Complexes.” *Chem. Phys. Lett.*, 494, 95-99.

Sanjib Das., Atanu Jana., Ramanathan V., Tapas Chakraborty., Sampa Ghosh., Pushpendu K. Das and Parimal K. Bharadwaj (2006). “Design and synthesis of 1, 10-phenanthroline based Zn (II) Complexes bearing 1D push-pull NLO-phores for tunable Quadratic nonlinear optical properties.” *J. Organomet Chem.*, 691, 2512-2516.

Seetharam Shettigar, Umesh G., Chandrasekharan K., Sarojini B.K and Narayana B. (2008). “Studies on third-order nonlinear optical properties of chalcone derivatives in polymer host.” *Opt. Mater.* 30, 1297-1303.

Sheik-Bahae M., Said A.A., Wei T-H., Hagan D.J and Van Stryland E.W. (1990) “Sensitive measurement of optical nonlinearities using a single beam.” *IEEE J. Quantum Electron.*, 26, 760-769.

Shigehiro Y., Toshiaki S., Seiji A and Kohei T. (2002). “Dibenzoborole-Containing  $\pi$ -Electron Systems: Remarkable Fluorescence Change Based on the “On/Off” Control of the  $p_{\pi}-\pi^*$  Conjugation.” *J. Am. Chem. Soc.* 124, 8816.

Sivaramakrishnan S., Muthukumar V.S, Sivasankara Sai S., Venkataramanaiah K., Reppert J., Rao A.M., Anija M., Philip R and Kuthirummal N. (2007). “Nonlinear optical scattering and absorption in bismuth nanorod suspensions.” *Appl. Phys. Lett.*, 91, 093104.

Slepkov A.P., Hegmann F.A., Yuming Zhao., Rik R tykwinski and Kenji Kamada. (2002). “Ultrafast Optical Kerr Effect Measurements of Third-Order Nonlinearities in Cross-Conjugated iso-Polydiacetylene Oligomers.” *J. Chem. Phys.* 116, 3834-3840.

Sole S and Gabba F.P. (2004). “A bidentate borane as colorimetric fluoride ion sensor.” *Chem. Commun.* 11, 1284-1285.

Su Z.M., Wang X.J., Huang Z.H., Wang R.S., Feng J.K and Sun J.Z. (2001). “Nonlinear optical properties for pyridines and stilbazoles adducted by borane.” *Syn. Met.* 119, 583-584.

Suginome M., Uehlin L., Yamamoto A and Murakami M. (2004). "A New Look at Boron Enolate Chemistry: Aminative C–C Bond Formation Using Diaminoboron Enolate with Aldehyde." *Org. Lett.* 6, 1167-1169.

Sun, Xiang-Bang., Ren, Quan., Wang, Xin-Qiang., Zhang, Guang-Hui., Yang, Hong-Liang., Feng, Lin., Xu, Dong and Lin, Zhi-Bo (2008). "Nonlinear optical properties of  $[(\text{CH}_3)_4\text{N}]\text{Au}(\text{dmit})_2$  using Z-scan technique." *Chinese physics*, 15(11), 2618-2622.

Sutherland R.L., Handbook of Nonlinear Optics, Marcel Dekker (New York) 1996.

Twieg R. J and Jain K. (1983). "In: Nonlinear Optical Properties of Organic Molecules and Polymeric Materials." D. J. Williams Ed. ACS Symposium series 233. American Chemical Society. Washington, D. C.

Udayakumar D., John Kiran A., VasudevaAdhikari A., Chandrasekharan K., Umesh G and Shashikala H.D. (2006). "Third-order nonlinear optical studies of newly synthesized polyoxadiazoles containing 3,4-dialkoxythiophenes." *Chem. Phys.* 331, 125-130.

Unikrishnan K.P., Thomas J., Nampoore V.P.N., and Vallabhan C.P.G. (2002). "Third order nonlinear optical studies in europium naphthalocyanine using degenerate four wave mixing and Z-scan." *Opt. Commun.*, 204, 385.

Vance F.W and Hupp J.T. (1999). "Probing the Symmetry of the Nonlinear Optic Chromophore  $\text{Ru}(\text{trans-4,4'-diethylaminostyryl-2,2'-bipyridine})_3^{2+}$ : Insight from Polarized Hyper-Rayleigh Scattering and Electroabsorption (Stark) Spectroscopy." *J. Am. Chem. Soc.* 121, 4047-4053.

Ventelon L., Charier S., Moreaux L., Mertz J and Blanchard- Desce M. (2001). "Nanoscale Push–Push Dihydrophenanthrene Derivatives as Novel Fluorophores for Two-Photon-Excited Fluorescence." *Angew. Chem.* 113, 2156-2159.

Verbiest T., Houbrechts S., Kauranen M., Clays K and Persoons A. (1997). "Second-order nonlinear optical materials: recent advances in chromophore design." *J. Mater. Chem.* 7, 2175-2189.

- Vogel, A. I. (1989). "Textbook of Practical Organic Chemistry." 5<sup>th</sup> ed., Longman, London.
- Vogler A and Kunkely H. (1997). "Inorganic Chromophores: Optical Charge Transfer in Coordination Compounds." *Comments Inorg. Chem.*, 19, 283-306.
- Vogler A and Kunkely H., (1990)., "Optical Ligand to Ligand Charge Transfer of Metal Complexes Including Ligand-Based Mixed-Valence Systems." *Comments Inorg. Chem.*, 9, 201-220.
- Voigt-Martin I.G., Li G., Yakimanski A., Schulz G and Wolff J.J. (1996). "The Origin of Nonlinear Optical Activity of 1,3,5-Triamino-2,4,6-trinitrobenzene in the Solid State: The Crystal Structure of a Non-Centrosymmetric Polymorph as Determined by Electron Diffraction." *J. Am. Chem. Soc.* 118, 12830-12831.
- Wang X.Q., Ren Q., Zhang F.J., Guo W.F., Sun X.B., Sun J., Yang H.L., Zhang G.H., Hou X.Q and Xua D. (2008). "Preparation, characterization, thermal and third-order nonlinear optical properties of bis(tetraethylammonium)bis(2-thioxo-1,3-dithiole-4,5-dithiolato)cuprate(II)." *Mater. Res. Bull.* 43, 2342-2353.
- Wenfang, Sun., Thomas, H.Patton., Laura, K.Stultz., Juan, Pablo Claude (2003). "Resonant third-order nonlinearities of tetrakis(2,2'-dipyridyl)diruthenium complexes." *Opt. Commun.*, 218, 189-194.
- Wu Q.G., Esteghamatian M., Hu N.X., Popovic Z., Enright G., Breeze S.R and Wang S.N. (1999). "Isomerism and Blue Electroluminescence of a Novel Organoboron Compound: BIII<sub>2</sub>(O)(7-azain)<sub>2</sub>Ph<sub>2</sub>." *Angew.Chem. Int. Ed.* 38, 985.
- Xiao-Zeng You (1997). "Chemical studies on the nonlinear optics of coordination compounds." *Journal of photochemistry and photobiology A: chemistry*, 106, 85-90.
- Yang W., He H and Drueckhammer D.G. (2001). "Computer-Guided Design in Molecular Recognition: Design and Synthesis of a Glucopyranose Receptor." *Angew.Chem. Int. Ed.* 40, 1714.

Yanghui Lin, Ruifang Cai, Yu Chen, Zu-en Huang, Yinghua Zhou, Guohong Ma. (1999). "Synthesis of transition-metal based nonlinear optical organometallic fullerene derivatives  $C_{60}M_2$  ( $M = Pd, Pt$ ).” *J. Mater. Sci. Lett.* 18, 1383-1385.

Yan-Ling Wang, Dong Xu, Wen-Tao Yu, Xiang-Bing Sun, QuanRen, Guang-Hui Zhang, Yun-Qiao Ding, Xin-Qiang Wang, Wen-FengGuo, Hong-Yu Chen and Lin Feng. (2008). "Synthesis, crystal structure and saturable absorption in the near-IR regions of a new copper complex of dmit: hexadecyltrimethylammoniumbis(2-thioxo-1,3-dithiole-4,5-dithiolato)-copper.” *J. Coord. Chem.* 61, 768-775.

Yong, Li., Zhao-Xia, Zhang., Ke-Chang, Li., Wen-Dong, Song and Qui-Shun, Li (2007). "A novel 3D double helix cobalt (II) coordination polymer: Synthesis, crystal structures and third-order non-linear optical properties.” *Inorg. Chem. Commun.*, 10, 1557-1560.

Yuang Z., Taylor N. J., Marder T. B., Williams I. D., Kurtz S. K and Cheng L.T. (1990). "Three coordinate phosphorus and boron as  $\pi$ -donor and  $\pi$ -acceptor moieties respectively, in conjugated organic molecules for nonlinear optics: crystal and molecular structures of  $E$ -Ph-CH=CH-B(mes)<sub>2</sub>,  $E$ -4-MeO-C<sub>6</sub>H<sub>4</sub>-CH=CH-B(mes)<sub>2</sub>, and  $E$ -Ph<sub>2</sub>P-CH=CH-B(mes)<sub>2</sub>[mes = 2,4,6-Me<sub>3</sub>C<sub>6</sub>H<sub>2</sub>].” *J. Chem. Soc. Chem. Commun.*, 1489-1492.

Yu-Peng, Tian., Wen-Tao, Yu., Cun-Yuan, Zhao., Min-Hua, Jiang., Zhi-Gang, Cai and Hoong Kun, Fun (2002). "Structural characterization and second-order nonlinear optical properties of zinc halide thiosemicarbazone complexes.” *Polyhedron* 21, 1217-1222.

Yu-Peng, Tian., Ming-Liang, Zhang., Zhang-Jun, Hu., Han-Mei, Hu., Jie-Ying, Wu., Xuan-Jun, Zhang., Sheng-Yi, Zhang., Xu-Tang, Tao., Min-Hua, Jiang., He-Ping, Chen., SuchadaChantrapromma and Hoong-Kun, Fun (2005). "Synthesis, crystal structure and NLO properties of a novel ruthenium(II) complex with unusual coordination mode.” *Transition Metal Chemistry*, 30,778–785.

Zhang H., Huo C., Ye K.Q., Zhang P., Tian W.J and Wang Y. (2006). "Synthesis, Structures, and Luminescent Properties of Phenol–Pyridyl Boron Complexes." *Inorg.Chem.* 45, 2788.

Zhang X.B., Feng J.K., Ren A.M and Sun C.C. (2005). "Theoretical study of two-photon absorption properties of a series of tetra-paracyclophane derivatives." *J. Mol. Struct. (THEOCHEM)* 756, 133-141.

Zhao C.F., He G.S., Bhawalkar J.D., Park C.K and Prasad P.N. (1995). "Newly Synthesized Dyes and Their Polymer/Glass Composites for One- and Two-Photon Pumped Solid-State Cavity Lasing." *Chem. Mater.* 1979-1983.

Zheng Q., He G.S and Prasad P.N.J. (2005). "Novel two-photon-absorbing, 1,10-phenanthroline-containing  $\pi$ -conjugated chromophores and their nickel(II) chelated complexes with quenched emissions." *J. Mater. Chem.* 15, 579-587.

Zhou G., Ho C.L., Wong W.Y., Wang Q., Ma D., Wang L., Lin Z., Marder T.B and Beeby A. (2008). "Manipulating Charge-Transfer Character with Electron-Withdrawing Main-Group Moieties for the Color Tuning of Iridium Electrophosphors." *Adv. Funct. Mater.* 18, 499–511.

Zhou X., Feng J.K and Ren A.M. (2005). "One- and two-photon absorption properties of octupolar molecules with tetrahedral structure." *Chem. Phys. Lett.* 403 (2005) 7-15.

Zyss, J. (1994). "Molecular Nonlinear Optics." Academic Press, New York.



---

**LIST OF JOURNAL PUBLICATIONS**

1. **Rudresha B.J**, Badekai Ramachandra Bhat, Dileep Ramakrishna, John Kiran Anthony, Fabian Rotermund. (2010). "Third-order optical nonlinear studies of Cobalt (II) Schiff base complex bearing triphenylphosphine using Differential Optical Kerr Gate and Z-scan studies." *Synthetic Metals*, 160, 1584-1586.
2. **Rudresha B.J.**, Ramachandra Bhat B., Sampath Kumar H.C., Shiva Kumar K.I., Safakath K and Reji Philip. (2011). "Synthesis, characterization and third-order nonlinear optical studies of copper complexes containing 1,10-phenanthroline-5,6-dione and triphenylphosphine ligands." *Synthetic Metals*. 161, 535-539.
3. **Rudresha B.J**, Badekai Ramachandra Bhat, Dileep Ramakrishna, John Kiran Anthony , Lee H.W and Rotermund F. (2012). "Large and ultrafast nonlinear optical study of palladium Schiff base complex using femtosecond differential optical Kerr gate and Z- scan techniques." *Optics & Laser Technology*, 44, 1180–1183.
4. **Rudresha B. J**, Ramachandra Bhat B, Manjunatha K. B and G. Umesh. (2011). "Synthesis, Characterization And Third Order Nonlinear Optical Studies Of Diimine Based Zn(II), Cd(II) and Hg(II) Complexes." *Optics: phenomena, Materials, Devices and characterization, AIP Conf. Proc.* 1391, 697-699.
5. **Rudresha B.J.**, K.B. Manjunatha, G. Umesh and Ramachandra Bhat B. (2012). "Octupolar metal complexes for third order nonlinear optical studies." *Chem. Phys. Lett.* 542, 159-163.
6. **Rudresha B.J.**, Sampath Kumar H.C., Reji Philip and Ramachandra Bhat B (2012). "Synthesis, characterization and third-order nonlinear optical studies of boron chalcone complexes." Communicated to *J. Organomet. Chem.*
7. **Rudresha B.J.**, Sampath Kumar H.C., Reji Philip and Ramachandra Bhat B. (2012). "Synthesis, characterization and third-order nonlinear optical studies of binuclear boron Schiff base complexes." Communicated to *Chem. Phys. Lett.*

**INTERNATIONAL/NATIONAL CONFERENCES**

1. **Rudresha B. J**, Reji Philip and Badekai Ramachandra Bhat. (2009). Presented a research paper titled “Synthesis, Characterization and Third-order nonlinear optical properties of Zn-salen and Zn-saloph complexes.” *International Conference on Emerging Trends in Chemistry*, University of Pune, Centre of advanced studies, Dept. of Chemistry, Pune.
2. **Rudresha B. J.**, Ramachandra Bhat B., Dileep R., John Kiran A., Hwang Woon Lee and Fabian Rotermund. (2010). Presented a research paper titled “The study of third-order optical nonlinearity of Cobalt (II) Schiff base complex bearing triphenylphosphine using Differential Optical Kerr Gate and Z-scan Studies.” *National Conference on Recent Trends in Chemical Research*, Dept. of Chemistry, National Institute of Technology Karnataka (NITK), Surathkal.
3. **Rudresha B. J**, Ramachandra Bhat B, Manjunatha K. B and G. Umesh. (2010). Presented a research paper titled “Synthesis characterization of 1,10-phenanthroline based Cd(II) complexes for study of third order nonlinear optical properties.” *Recent Trends in Chemical and Biological Sciences*. Dept. of chemistry, School of Chemical Sciences Kuvempu University Shankargatta, Shimoga.

## CURRICULUM VITAE

**RUDRESHA B J**

**Research Scholar**

**Department of Chemistry**

**NITK-Surathkal**

**Mangalore-575025**

**India**

**E-mail: [rudreshbj@gmail.com](mailto:rudreshbj@gmail.com)**

**Phone : +91-8105867909**

---

### Objectives

To accept challenging projects and establish myself in research and development and excel through flexible learning by adopting new technology in order to contribute towards the growth of self and organization.

### Education

1. Ph.D. Thesis: “**Synthesis Characterization and Third-order Nonlinear Optical Study of Some Transition Metal and Boron Complexes.**” Thesis submitted.  
Supervisor: Dr. B. Ramachandra Bhat
2. M.Sc. Chemistry, Kuvempu University, 67.00 %, 2005, Karnataka, India.
3. B.Sc. Chemistry, Kuvempu University, 63.50 %, 2003, Karnataka, India.

### Work Experience

Worked as project assistant at NMR Research Center (NMRRC), Indian Institute of Science (IISc), Bangalore from November 2006 to July 2008. I have been exposed to various NMR experiments like 1D and 2D. As our lab was the National Facility of our country, I also do the NMR analysis of samples received from various Industries, R&D Center, Colleges and universities across the country which include Organic and Peptide molecules.

### Synthetic Expertise & Skills

- Handled milli gram scale reactions
- Purification of products by crystallization techniques
- Analytical interpretation of organic and inorganic molecules by IR,  $^1\text{H}$ ,  $^{13}\text{C}$ ,  $^{19}\text{F}$ ,  $^{31}\text{P}$  and  $^{11}\text{B}$  NMR spectroscopic techniques.

### Instruments handled

- NMR spectrophotometers
- FT-IR spectrophotometer
- UV-Visible spectrophotometer
- Fluorescence spectrophotometer
- Radley's Parallel Synthesizer
- Buchi Rotary Evaporator

### Research publications

1. **Rudresha B.J**, Badekai Ramachandra Bhat, Dileep Ramakrishna, John Kiran Anthony, Fabian Rotermund. (2010). "Third-order optical nonlinear studies of Cobalt (II) Schiff base complex bearing triphenylphosphine using Differential Optical Kerr Gate and Z-scan studies." *Synthetic Metals*, 160, 1584-1586.
2. **Rudresha B.J.**, Ramachandra Bhat B., Sampath Kumar H.C., Shiva Kumar K.I., Safakath K and Reji Philip. (2011). "Synthesis, characterization and third-order nonlinear optical studies of copper complexes containing 1,10-phenanthroline-5,6-dione and triphenylphosphine ligands." *Synthetic Metals*. 161, 535-539.
3. **Rudresha B.J**, Badekai Ramachandra Bhat, Dileep Ramakrishna, John Kiran Anthony, Lee H.W and Rotermund F. (2012). "Large and ultrafast nonlinear optical study of palladium Schiff base complex using femtosecond differential optical Kerr gate and Z- scan techniques." *Optics & Laser Technology*, 44, 1180–1183.
4. **Rudresha B.J**, Ramachandra Bhat B, Manjunatha K. B and G. Umesh. (2011). "Synthesis, Characterization And Third Order Nonlinear Optical Studies Of Diimine Based Zn(II), Cd(II) and Hg(II) Complexes." *Optics: phenomena, Materials, Devices and characterization, AIP Conf. Proc.* 1391, 697-699.
5. **Rudresha B.J.**, K.B. Manjunatha, G. Umesh and Ramachandra Bhat B. (2012). "Octupolar metal complexes for third order nonlinear optical studies." *Chem. Phys. Lett.* 542, 159-163.

6. **Rudresha B.J.**, Sampath Kumar H.C., Reji Philip and Ramachandra Bhat B (2012). "Synthesis, characterization and third-order nonlinear optical studies of boron chalcone complexes." Communicated to *J. Organomet. Chem.*
7. **Rudresha B.J.**, Sampath Kumar H.C., Reji Philip and Ramachandra Bhat B. (2012). "Synthesis, characterization and third-order nonlinear optical studies of binuclear boron Schiff base complexes." Communicated to *Chem. Phys. Lett.*
8. Kiran A.J., Lee H.W., SampathKumar H.C., **Rudresha B.J.**, Bhat B.R., IYeom D., Kim K and Rotermund F. (2010). "The ultrafast nonlinear optical response and multi-photon absorption of a new metal complex in the near-infrared spectral range." *J. Optics A*, 035211.
9. Sampath Kumar H.C., Ramachandra Bhat B, **Rudresha B.J.**, Ravindra R and Reji Philip., (2010)., "Synthesis, Characterization and Non-linear optical studies of N, N'-bis(2-hydroxynaphthalidene)phenylene-1,2-diamine) of M (M= Ni(II), Zn(II) and Fe (II)) Schiff-Base Complexes." *Chem. Phys. Lett.*, 494, 95-99.

### Conferences attended

1. **Rudresha B. J.**, Reji Philip and Badekai Ramachandra Bhat. (2009). Presented a research paper titled "Synthesis, Characterization and Third-order nonlinear optical properties of Zn-salen and Zn-saloph complexes." *International Conference on Emerging Trends in Chemistry*, University of Pune, Centre of advanced studies, Dept. of Chemistry, Pune.
2. **Rudresha B. J.**, Ramachandra Bhat B., Dileep R., John Kiran A., Hwang Woon Lee and Fabian Rotermund. (2010). Presented a research paper titled "The study of third-order optical nonlinearity of Cobalt (II) Schiff base complex bearing triphenylphosphine using Differential Optical Kerr Gate and Z-scan Studies." *National Conference on Recent Trends in Chemical Research*, Dept. of Chemistry, National Institute of Technology Karnataka (NITK), Surathkal.
3. **Rudresha B. J.**, Ramachandra Bhat B, Manjunatha K. B and G. Umesh. (2010). Presented a research paper titled "Synthesis characterization of 1,10-

phenanthroline based Cd(II) complexes for study of third order nonlinear optical properties.” *Recent Trends in Chemical and Biological Sciences*. Dept. of chemistry, School of Chemical Sciences Kuvempu University Shankargatta, Shimoga.

### **Research experience and areas of interest**

- Optoelectronic materials
- Coordination chemistry
- Organometallic chemistry
- Catalysis
- Synthetic organic chemistry
- NMR analysis of organic and biomolecules.

### **ACHIEVEMENTS**

Qualified GATE examination during the academic year 2006- National level examination.

### **Personal details**

Address for correspondence

Rudresha B. J  
Research Scholar  
Department of Chemistry  
NITK-Surathkal  
Mangalore-575025  
India  
E-mail:[rudreshbj@gmail.com](mailto:rudreshbj@gmail.com)  
[bjrudresh@gmail.com](mailto:bjrudresh@gmail.com)

Telephone:	+91-8105867909
Date of birth:	20-06-1980
Sex:	Male
Marital status:	Single
Nationality:	Indian
Language known:	English, Kannada and Hindi

## Reference

### **Dr. B. Ramachandra Bhat**

Associate Professor

Department of Chemistry

National Institute of Technology Karnataka (NITK) Surathkal,

Srinivasnagar (PO), Mangalore Pin-575025

Karnataka, India

Ph : +91-9449553759

Fax: + 91-824-2474033

Email: [chandpoorna@yahoo.com](mailto:chandpoorna@yahoo.com)

### **Dr. A. Chittaranjan Hegde**

Professor and Head

Dept. of Chemistry

NITK-Surathkal

Mangalore-575025

Mob: +91-9980360242

Email: [hegdeac@rediffmail.com](mailto:hegdeac@rediffmail.com)